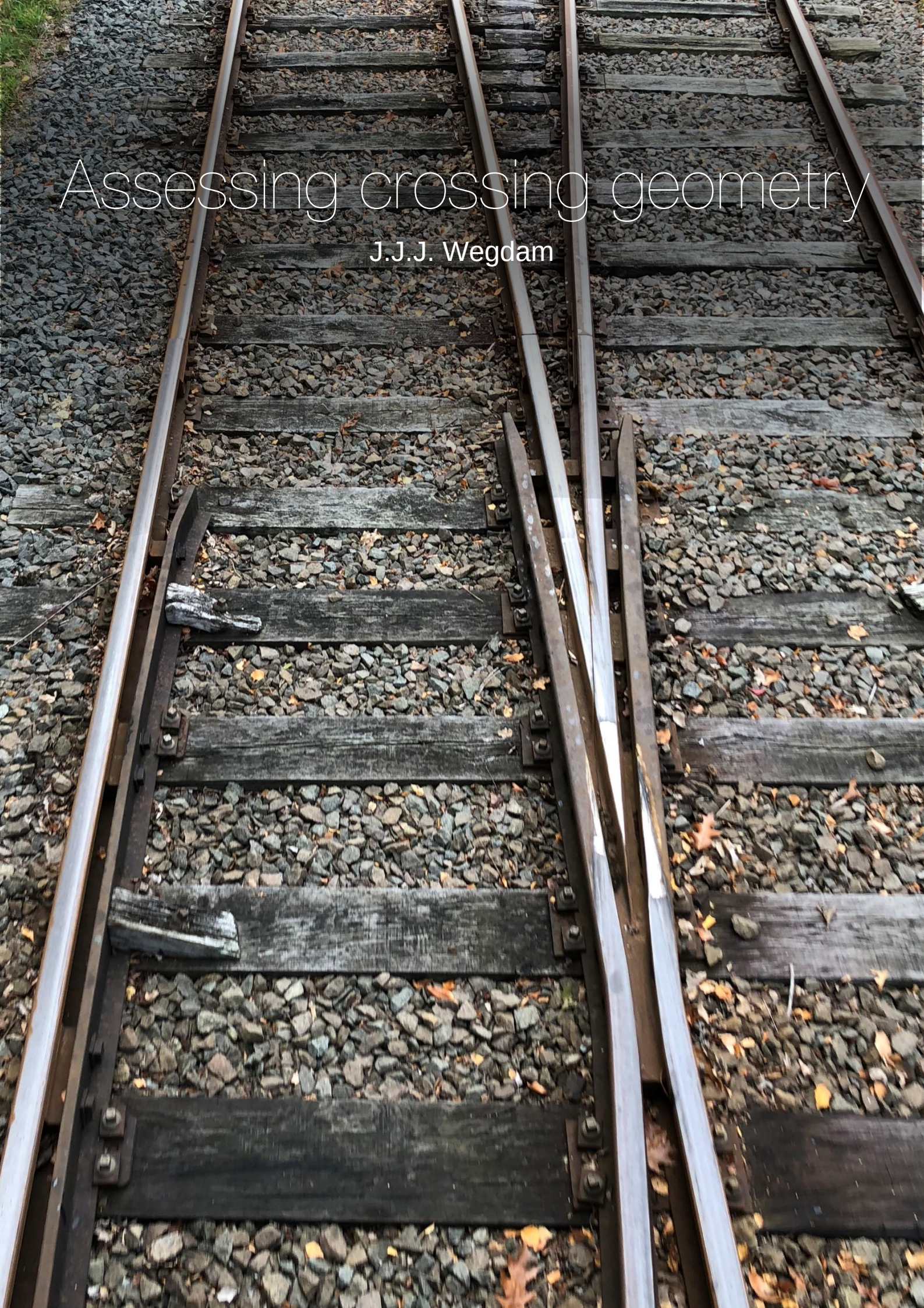

Assessing crossing geometry

J.J.J. Wegdam

Expert tool for numerical & experimental assessment of turnout crossing geometry

By

J.J.J. Wegdam

in partial fulfilment of the requirements for the degree of

Master of Science

in Civil Engineering

at the Delft University of Technology,

to be defended publicly on the 12th of December 2018 at 14:30.

Supervisor:	Dr. V.L. Markine	
Thesis committee:	Prof. dr. ir. R.P.B.J. Dollevoet,	TU Delft
	Prof. dr. A. V. Metrikine,	TU Delft
	Msc. X. Liu	TU Delft
	Dr. I.Y. Shevtsov,	ProRail

Contents

Abstract

This thesis project discusses the development of a fast assessment tool for the performance of railway turnout crossings. The assessment tool is developed in Matlab and allows the user to swiftly set up a model and assess the performance. The rail geometry input can be either design drawings or in situ measured geometry. This allows the user to compare designed, delivered and deployed crossings. Comparisons are made between several types of 1:9 crossings, by assessing the designs from various countries. The vehicle-track interaction is modelled in the commercial multi-body system (MBS) analysis package VI-Rail. The simulations indicate that the automated workflow provides insights similar to manual modelling, while being much faster. The report ends with recommendations based on the geometry comparisons and simulation results.

Acknowledgements

Valeri Markine, TU Delft

Rolf Dollevoet, TU Delft

Ivan Shevtsov, ProRail

Andrei Metrikine, TU Delft

Xiangming Liu, TU Delft

Sjors van de Vecht, WBN

Hanna Tijbosch, ProRail

Ben Ferdinande, Infrabel

Etienne Motte, Infrabel

Urs Schönholzer, SBB

David Philpott, Sheffield Hallam University

1 Introduction

The railway turnout (also known as ‘switch’ or ‘switch & crossing’) allows trains to change from one track to another. Because of this, the turnout plays an important role in keeping a railway network flexible and robust. A turnout can be divided in three panels, as shown in Figure 1. At two of these locations, it is unavoidable that the rails have variable cross-sections (geometry). This is the case at the switch and the crossing. The variable geometry is necessary to allow a wheelset to pass the turnout both in the main and the diverging directions. When railway vehicles pass the switch and crossing, the Klingel motion of their wheelsets is disturbed. The resulting vehicle behaviour makes the turnout a vulnerable spot in the railway system.

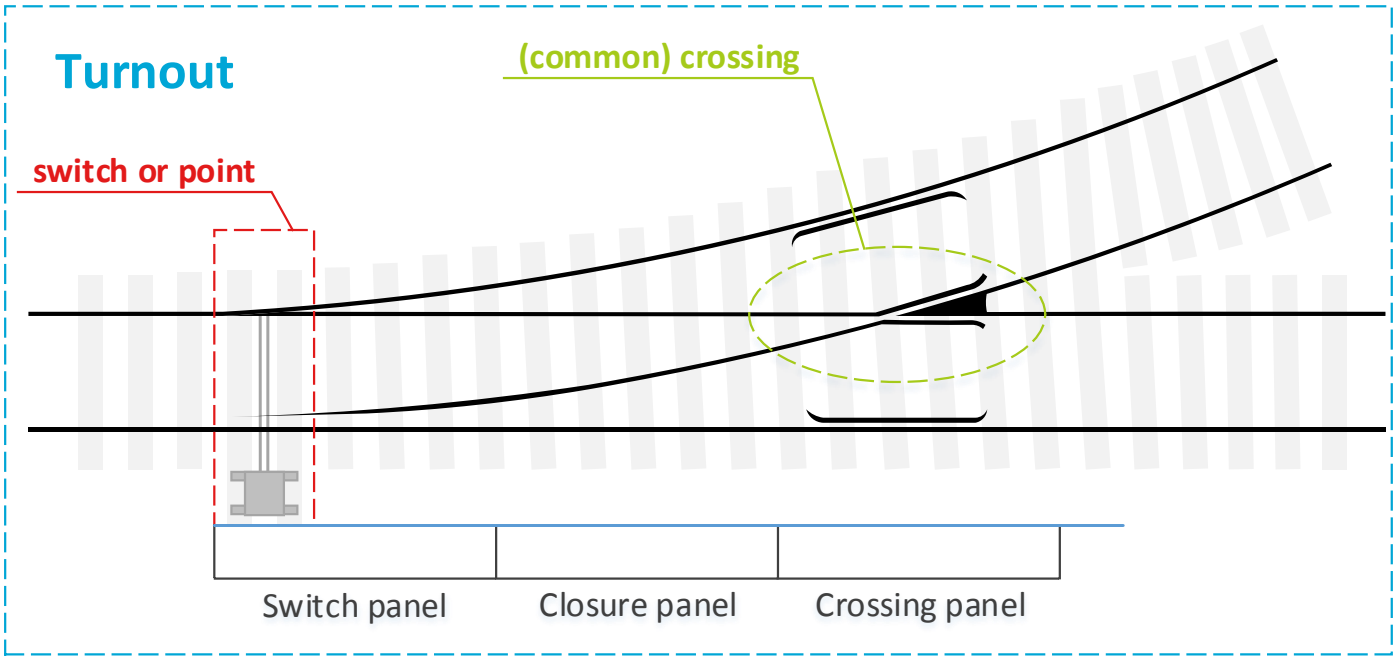

Figure 1 - Components of a turnout

Figure 2 shows the subject of this project: the crossing panel. Note how the crossing has space between the wing rails and the nose. This so-called flangeway is required to allow wheels (and especially their flanges) to pass safely through the crossing. This however leads to a discontinuity in the rail.

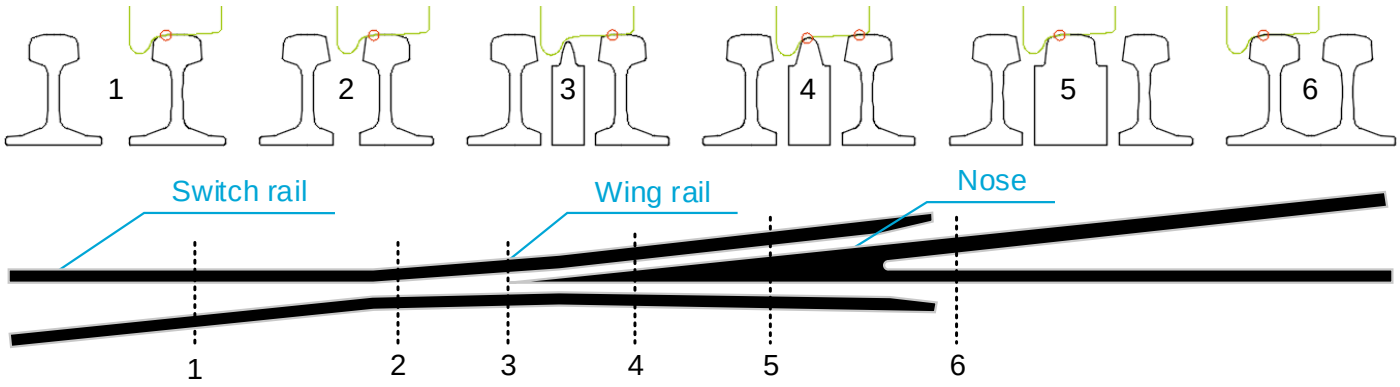

Figure 2 – Regular wheel (green) with wheel-rail contact locations (red) throughout a crossing

As Figure 2 shows, this discontinuity forces the location of the wheel-rail contact to move in the lateral direction. In addition, the cross-sections in the middle will only provide support to the wheel if the wheel is lower than it would normally be. All of this leads to vertical and lateral displacements of the wheelset which consequentially leads to adverse wheel-rail dynamics. Consequentially, crossings tend to cause a problematic amount of wear and rolling contact fatigue (RCF), like depicted in Figure 3. This problem is especially present at short crossings, where the geometry changes are present in a relatively short stretch of track.

Figure 3 - Examples of damaged crossings [1] [2]

1.1 Motivation

Present day crossing designs in the Netherlands all must be compliant with central standards, from infrastructure manager ProRail. In terms of geometry, the standards only describe requirements concerning the flangeway. The way of doing that still has close similarities with the standards from 1933 [3]. The consequence is that manufacturers can freely determine the geometry at the transition zone. Because of this, manufacturers have come up with several geometry-designs that are available to the contractors. The designs have different price tags and different performances and contractors are free to choose what design they deem most suitable for a certain location. It might be beneficial to restrict important turnouts to designs performing with a higher reliability.

While it is hard to predict the performance of a design, it can still be subjected to a full-scale field test. A good example of this is taking place while this report was written. ProRail is experimenting with a German crossing design. From preparation till the end of the one-year monitoring period, at least six years will have passed. All in all, an expensive and time-consuming procedure. There are ways to predict the performance of a new crossing without immediately doing such a field test though. This can be done by simulating

vehicle-crossing interaction through either a Multi Body System (MBS) model or a Finite Element Method (FEM) model.

MBS and FEM simulations have been conducted for Dutch crossings. As shown in [4], FEM provides more insights in stress distributions but is slower and less flexible (it is hard to adjust the model). The flexibility of MBS modelling has been utilised in [5], to run an automated optimisation of an existing design. Comparisons between various existing crossing geometries remain absent though. This absence hinders innovation.

1.2 Research goals

The clearest challenge in the current situation is the effort which is needed to compare geometries. To test a crossing, one must build the model, run the simulation and interpret the results. Doing this for only one design can already be time-consuming. This becomes a problem when doing it for many crossings. For this reason, the main goal of this project is to develop a swift and convenient comparison tool. After doing so, the project will seek to show the applicability through several topics:

- Providing an approach on the assessment of crossing geometry
- Finding geometry improvements by comparing different designs
- Providing insights in the relation between geometry and wheel-rail dynamics

1.3 Scope

A problematic case of turnout degradation can be found on Dutch crossovers. A crossover is a pair of short turnouts that connects two parallel main tracks, like in Figure 4. The most commonly used turnout in these crossovers is the regular R195 1:9 UIC54 turnout. This short turnout is the design which covers 60% of all Dutch turnouts [6]. The main tracks of the crossover are often used at 140 km/h and sometimes even up to 160 km/h. This combination of short turnouts and high speeds subjects passing vehicles to a fast change in geometry. On top of that, turnouts in main lines are exposed to much more traffic than turnouts in spurs.

This project confines itself to this type of crossing. More specific, to the main track (where turnouts are extra vulnerable due to the high vehicle speeds). In terms of running direction, only the so-called facing direction will be chosen as subject of the results assessment. This is due to time constraints of this MSc thesis project.

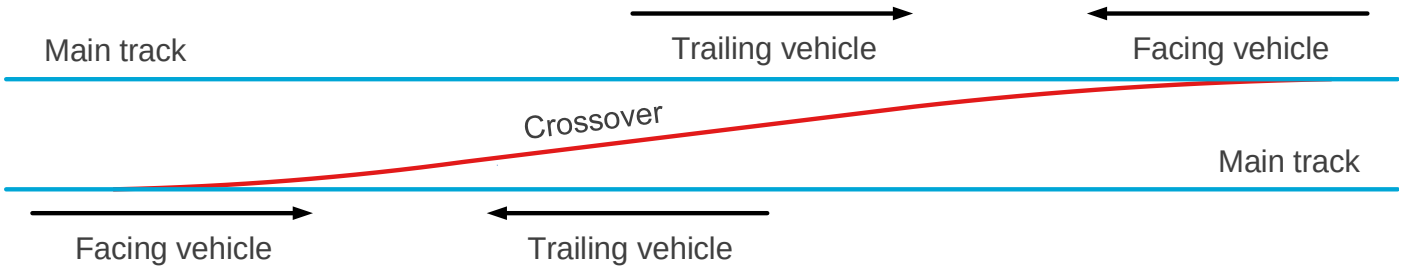

Figure 4 - Track centerlines and vehicle directions at a crossover

1.4 Project outline

The previous sections have introduced the topic and have shown the main priority of this project: making geometry comparisons simpler. In chapter 2, a tool will be introduced to make this possible. This combination of Matlab and VI-Rail will be referred to as the Assessment Tool. After the Assessment Tool itself is discussed in chapter 2, the three next chapters will focus on its branches. The input of the Assessment Tool (crossing geometry) is discussed in chapter 3. It will present the reader geometry comparisons and ends with a set of possible crossing improvements. The results themselves however, are discussed in chapter 4. The chapter focuses on answering to the last three research goals. A summary of those answers, recommendations and suggestions for future work are discussed in the last chapter: chapter 5.

2 Assessment tool

The main goal of the assessment tool is to provide maximal user-friendliness when comparing crossing geometries. The process of doing such simulations can be characterised by three parts: defining a 3D crossing shape, modelling the system and interpreting the output. Improvements to these three parts can be characterised in three challenges:

1. Optimising the pre-processing
2. Minimising the simulation time
3. Standardising the interpretation of results

This chapter discusses these challenges in its first three sections. It starts with the input, being the translation from provided geometry to a workable 3D shape. The second section discusses the interface with the simulation software (referred to as processing). The third section on 'output' discusses another translation: from the raw simulation results to convenient overviews. The chapter is concluded with an overview section.

2.1 Input

Geometry can be acquired in various phases of the life cycle of the crossing. This can be either in the **designed** crossing, right after being **delivered** from the factory or when **deployed** in the track. The assessment tool was developed compatible with all these situations. It transforms all input to 3D point clouds, which are used as input for the simulation.

In the case of *delivered* and *deployed* crossings, 3D shapes can be acquired through rail profile measurements. The creation of point clouds from these is very straight forward. The data of profile measurements also consists of point clouds, which makes the import process easy. It is simply a matter of changing the file formatting. Importing such data in to the assessment tool has been tested, as being a proof of concept. Moreover, the rail shapes from measurements have been compared to their design in section 3.2. Using the imported measurements to run a VI-Rail simulation however, remains a case for future work.

The priority of the research up till now was to deliver comparisons between *designed* crossings. Such designs are produced in CAD software and subsequently distributed as hardcopy or pdf drawings. The challenge was to reconstruct a 3D shape from a 2D drawing. As 2D drawings cannot contain dozens of cross-sections, the typical drawing contains several characteristic cross-sections. In the example of the Dutch situation, the crossing nose is defined by four cross-sections.

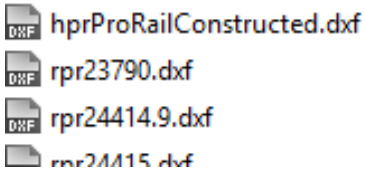

Figure 5 – CAD input example

To create a convenient way of providing such data to the assessment tool, the drawing exchange format (.dxf) has been chosen. The .dxf file format is a regular text file, which is structured in such a way that various 3D modelling software packages can work with. On one hand, this allows the user of the assessment tool to edit the input conveniently in software packages like AutoCAD. On the other hand, .dxf can be read and edited by processing software like Matlab or Python.

As shown in Figure 5, the DXF files required to run a simulation are one horizontal profile (HPR) file and one or multiple rail profiles (RPR). In this project, the horizontal profile consists of a straight line from the origin which determines the track length. Curves could be added but are out-of-scope as the project only considers the straight main track of the turnout. The RPR file also consists of lines and circle sections and is used to define the cross-sections of the rail. An example is given in Figure 6. The example shows a nose rail on the left and a wing rail on the right. Only the blue line is needed to describe the profile.

Figure 6 - An example horizontal profile; a top view from the track center line, starting in the origin

The RPR is drawn with respect to the origin, with the origin being the centre of the top the rail (in regular position). Both the HPR file and RPR files are read by Matlab, which stores the various shape characteristics from the .dxf. The usage of the term 'shape characteristics', is important. Figure 7 shows how using shape characteristics can save data usage. This is beneficial when creating a lot of cross-sections. Moreover, it protects the important property of a correct rail radius.

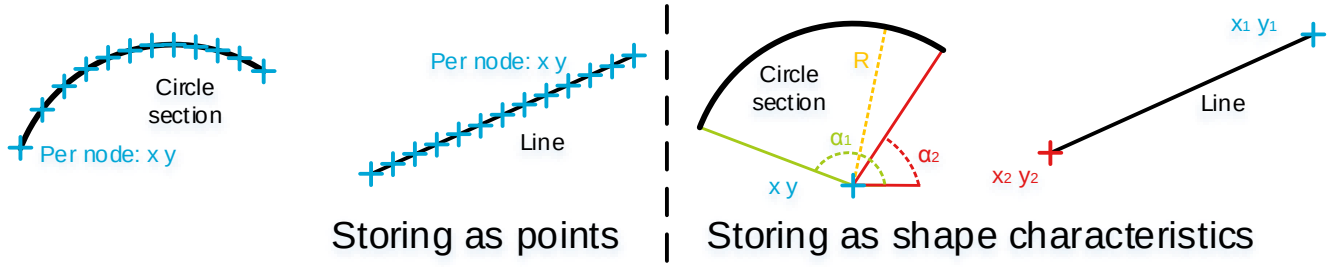

Figure 7 - Two ways to describe a shape

After the geometry is defined and stored, the geometry must be put to the test in a simulation. As discussed in section 1.1, this can be done by using either a FEM model or an MBS model. In accordance with the goal of providing a fast comparison, the MBS approach has been chosen. More specifically: the commercial software package VI-Rail is used as part of the assessment tool.

The horizontal profile and rail profiles have been described. With only these two inputs, it is possible to test geometry in VI-Rail. When not providing enough rail profiles, the model accuracy can decrease to such an extent that simulations become unreliable. This is often the case when only providing the characteristic cross-sections, from a design drawing. Between the characteristic sections, additional cross-sections should be defined to get to a valid track geometry model.

When creating intermediate cross-sections for modelling purposes, many ways are possible to do so. In [5], a method is presented where every characteristic cross-section has an equal number of nodes equally distributed along that cross-section. Between the characteristic sections, nodes are defined by interpolation of the node coordinates. While this method is very friendly to VI-Rail's variable profile algorithm, the method creates a difference between the design and the interpolated profiles.

To reduce this difference, a second method is proposed: shape-based interpolation. It uses Matlab to interpolate shape characteristics (as depicted in Figure 7) rather than node coordinates. The advantage is that it mimics the actual shape of the design closer. The difference is shown in Figure 8, for a ProRail crossing nose.

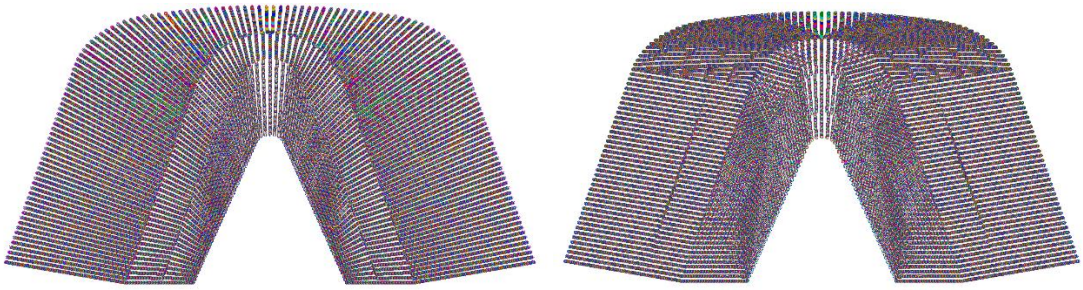

Figure 8 – Interval-based (left) and shape-based (right) interpolation for the ProRail profile

The current version however, still has two flaws:

1. Interpolating shape characteristics does not guarantee that tangent circles remain tangential (which can lead to bumps in the rail profiles)
2. The distribution of the nodes and number of nodes per cross-section varies along the nose, which disturbs the VI-Rail variable profile algorithm.

To find the effect of the interpolation errors, a set of CAD profiles has been created manually. These CAD profiles are exactly according to the design. Comparison of the real profiles and both interpolation methods should show whether improvements to the interpolation methods are worth future effort. The results from this comparison are discussed in chapter 4.

During the project, a possible improvement was found. It would make these interpolations exactly like crossings are fabricated. This can be described in three steps, as shown in Figure 9. First, define the original rail profile (like UIC54). Second, move cross-sections of milling tools along all cross-sections. Lastly, smooth the transitions between milling cuts by adding tangent circles. This method (referred to as manufacturing-based interpolation) would cover the shape more precise than interval-based or shape-based interpolation. The downside would be that it requires a more thorough analysis of the crossing design. Moreover, it would require more complex programming. To keep up with the project schedule, this third interpolation method has not yet been developed.

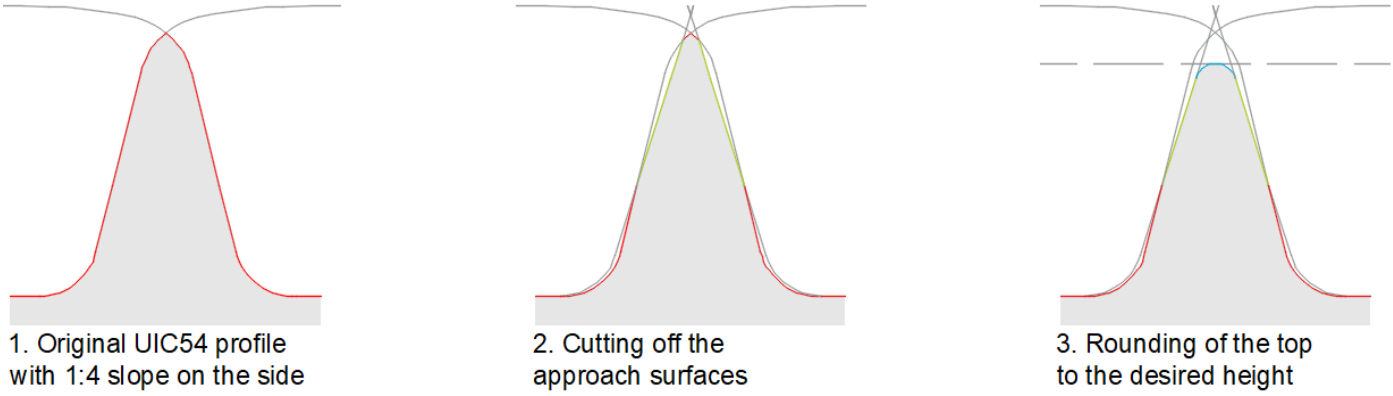

Figure 9 - Production steps during the production of a constructed crossing (all at the same cross-section)

As pointed out earlier, the profile generation is done in Matlab. Doing these steps in Matlab has the advantage of automation. The user simply places DXF files in the input folder and Matlab creates VI-Rail input files (TRK, RPR). Subsequently, the automation continues to VI-Rail. Getting familiar with VI-Rail and

all its options and building a model is quite labour intensive. To make simulations more convenient, the option has been created where the user doesn't have to open VI-Rail at all. More details on this can be found in appendix A.

The usage of VI-Rail did come with come complications, in terms of geometry delivery. Not all profiles are accepted by VI-Rail, and not all profiles are interpreted correctly by VI-Rail.

a. Nodes cannot have the same lateral coordinate. Vertical parts must be inclined slightly.
b. The sides of a profile should be pointing downwards; otherwise the contact model doesn't work.
c. A profile shouldn't contain sudden changes of slope. Use a transition curve in the flangeway.

Figure 10 shows the same situation profile as in Figure 6, but this time compatible with VI-Rail.

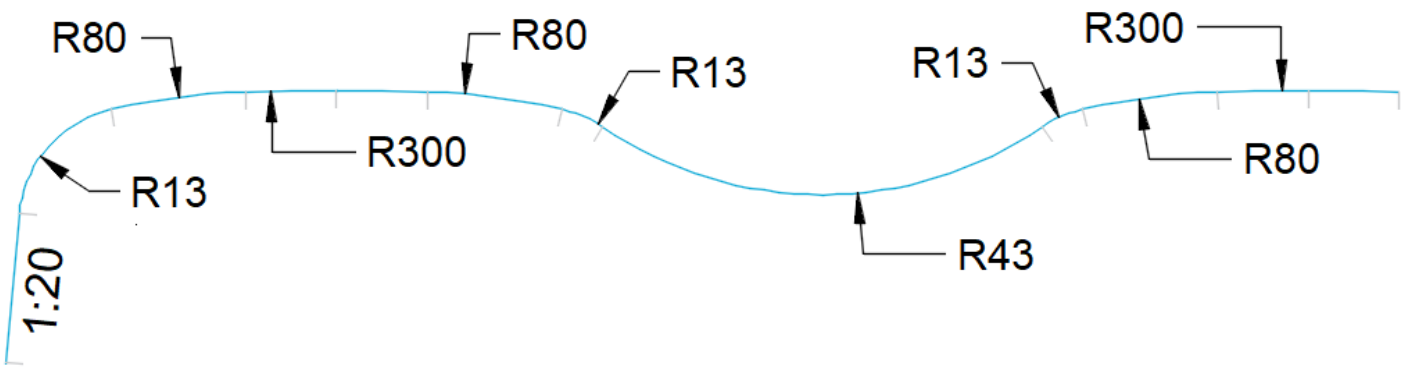

Figure 10 – A VI-Rail-compatible profile

2.2 Multi body system model

In most cases, a Multi Body System (MBS) consists of three models that interact with each other. First, the rolling stock is represented as the vehicle model. Second, a track model is defined (either stiff or flexible). Lastly, the two models are coupled by a third model: the contact model. All three models and their assumptions will be described in this chapter. For the full list of model settings, please consult the appendices.

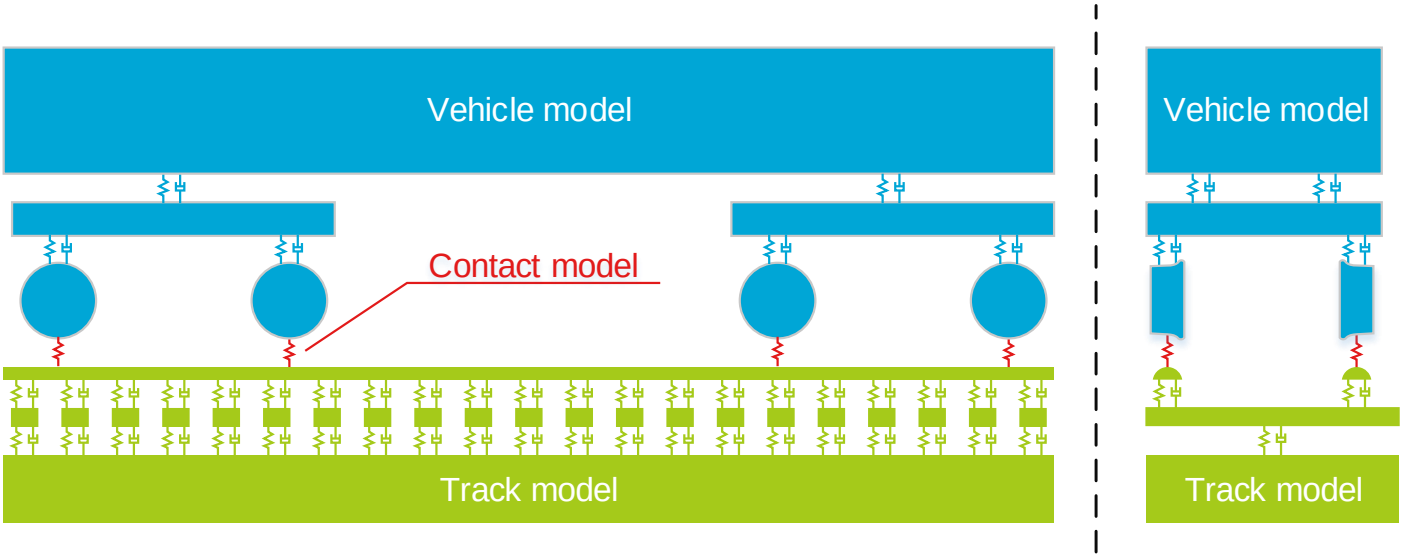

Figure 11 - MBS model setup in VI-Rail

Vehicle model

In this project, two vehicle models were used. One being a Dutch double deck passenger carriage named VIRM, the second vehicle model is the Manchester passenger carriage. Both vehicles were simulated at a speed of 140 km/h. This to comply with the case study: a vehicle running on the main track with the maximum allowed speed[1].

VIRM vehicle model

The VIRM model has been developed, by using data from the Dutch rolling stock maintainer Nedtrain. They provided characteristics such as spring stiffnesses, damping properties and masses. Geometrical properties were derived from design drawings. Further details of the VIRM model are provided in appendix C.

[1] The only exception on this can be found between the Hague and Schiphol, where international trains may run 160 km/h through a 1:9 crossing. This only happens when the HSL-Zuid track is unavailable, therefore this is not considered as relevant.

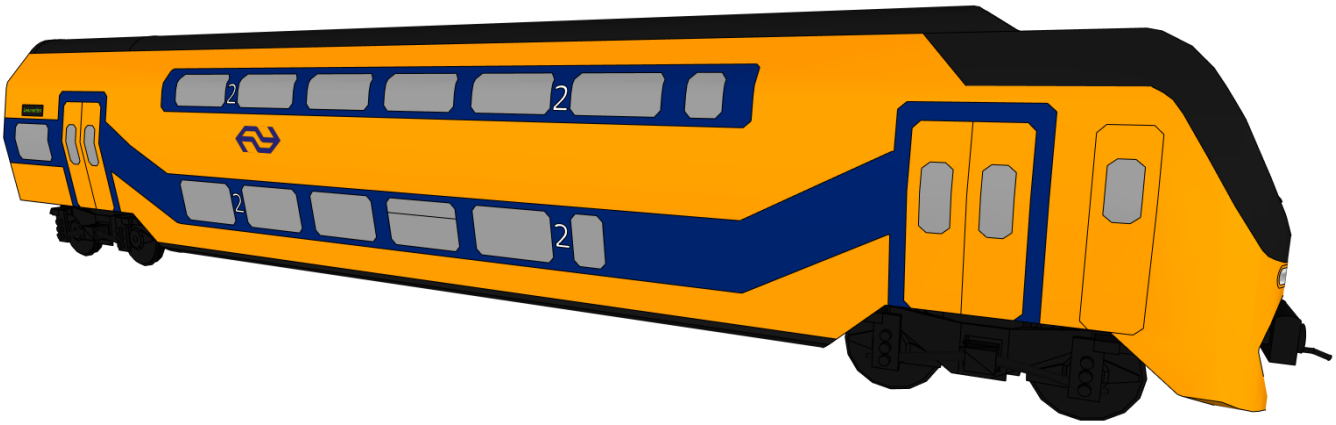

Figure 12 - Impression of the VIRM model

Manchester passenger carriage

While the VIRM model was developed in the margin this project, the second vehicle model is a well-established model. The Manchester passenger carriage [15] is regarded as standard benchmark, in dynamic rail vehicle simulation. Because of this, the latter model was used for the rail geometry comparisons. The VIRM vehicle model is only used to give an additional indication of the response by a Dutch carriage. Characteristics of the Manchester carriage are also shown in the appendix C.

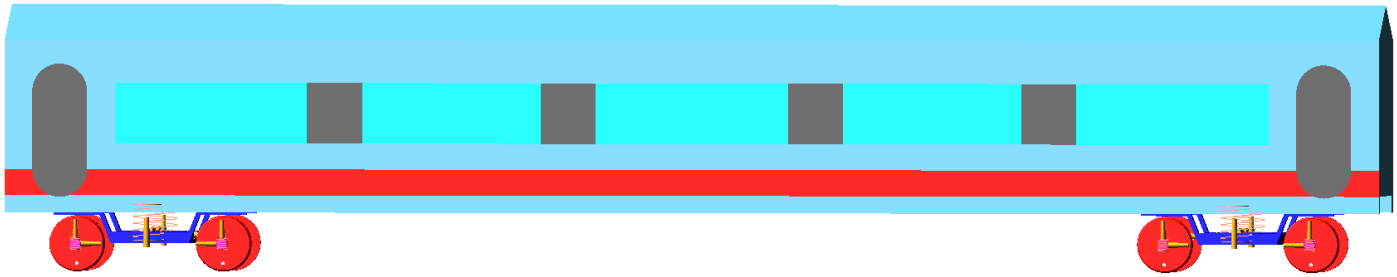

Figure 13 - Impression of the Manchester model

Contact model

VI-Rail provides three contact elements: WRTAB, WRGEN and WRQLT. The second element – WRGEN – has the longest computation time, but also is the most precise [16]. Moreover, it is the only element which is suitable for handling variable rail geometry. More details on the contact element can be found in [17]. The contact element as proposed by Kik and Piotrowski is not the only contact model. A recent study [18] compared the performance of multiple contact models, while addressing a similar problem with variable rail geometry. In the conclusions, it was proposed that all models had similar calculation times while Sichani's method [19] [20] had a high accuracy and efficiency. For now, VI-Rail's standard WRGEN model (based on Kik and Pietrowski's approach) will be used.

Track model

As the focus of this project lies at the track model, this section is split in two subsections. A part about the geometry and a part over the track properties. This creates a distinction between respectively the variable and fixed part of the track model.

Track properties

In an MBS package like VI-Rail, a lot of options are available. This is also the case for the track properties. These are split in track structure and track alignment. The track structure contains all material properties like stiffnesses and damping ratios. These properties were derived from [9] and can be found in appendix C.

After the track structure, the track alignment must be defined. Because the crossings are tested on their main track, a completely straight track of 150 m is defined. As pointed out in section 0, the vehicle speed is 140 km/h or $38.889\ m/s$.To save as much simulation time as possible, modelling time has been optimised. To reduce the modelling time, one must define the useful simulation settings. Figure 14 provides an overview of the track layout, to help understanding the location of TP in the model.

The examined wheel starts at $x = x^*$. The wheel-rail behaviour is examined in a certain area around TP (theoretical nose point). When comparing different crossing geometries, the area of variable rail profiles can be longer or shorter (depending on the design). The vehicle can be longer or shorter, depending on the choice for the Manchester model or VIRM model. After taking those factors in to account, a TP coordinate of 25 meters has been chosen.

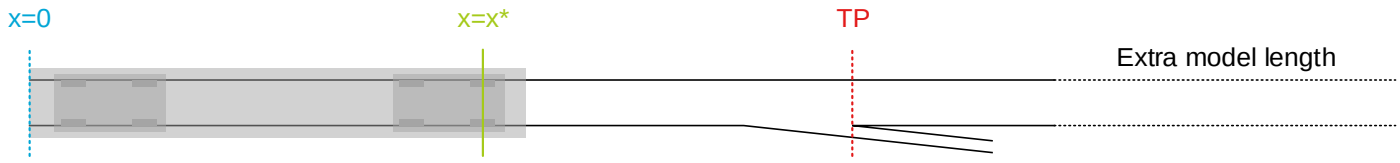

Figure 14 - Standard track layout during the modelling (top view)

After setting the coordinates, the standard simulation time has been chosen as 0.1 second. It proves to be a convenient trade-off between modelling time and simulation length (the latter being used to analyse the output). The standard simulation time can be altered in cases where the user wants to see to analyse the dampening of dynamic effects, after the crossing.

A time step of 10^{-4} second has been chosen in order to capture all relevant vibrations correctly. The timestep was chosen after trying different settings in several analyses.

These settings result in a simulation time of around 1 minute. Pre-processing and post-processing takes roughly the same amount of time. If the user wants to change the geometry step by step, the use simply won't have to worry about the simulation time. This makes the method compliant with the 'ease of comparison' goal.

Geometry

In chapter 2, a method has been proposed to import crossing geometries from various sources. These sources can be divided in designs and measurements. When importing a geometry Matlab prepares and runs a simulation always in the same files, but also stores the track in a separate backup folder. This ensures that VI-Rail and Matlab always work with the same files, while allowing the user to re-access previously simulated tracks. After the pre-processing results are stored in the right files, Matlab activates a .bat command file to run the VI-Rail simulation in the background (without needing the VI-Rail interface). More details on the workflow can be found in appendix A.

2.3 Output

After a simulation of crossing geometry (with parameters as described in Appendix C), a results file (.res) is created by VI-Rail. It contains output from all simulation variables for each time step. VI-Rail generates at least 49 different output parameters. To provide the end user fast insights, the most commonly used output parameters have been bundled in a results dashboard. The dashboard displays the wheel displacements, wear number and an indication of the contact trajectory.

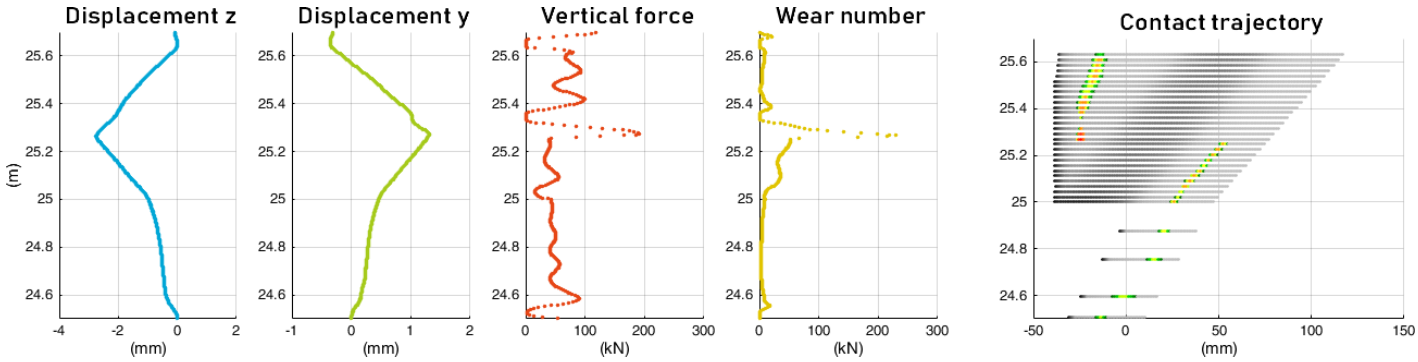

Figure 15 - Results dashboard for the ProRail cast manganese crossing

The first graph – vertical displacement – provides a signature of the wheel dip. The depth of the trajectory is a good indicator for the (lack of) support that the crossing provides to wheels that pass it. As later chapters will show, this can be solved by a higher wing rail and nose rail. Adjusting this remains a delicate matter though, because of the safety.

The displacement in the y-direction is lateral. The shape of the graph shows similarities with the vertical displacement but is not entirely the same. While it is of course a different variable, the horizontal and vertical displacement are correlated through the possible positions which a wheelset can have on the track. Locations where the shapes of the two graphs are not similar should be examined with special care.

The third graph shows the vertical contact force. This graph allows the user to see how the axle load is amplified by dynamic effects that are imposed by the crossing. Its maximum is a good indicator to compare crossing performances, because the ideal crossing amplifies the axle load as few as possible. Moreover, loss of contact ($F = 0$) is a good indicator of an incorrect geometry model (a wheel shouldn't be bouncing).

The fourth graph displays the so-called wear number, which is derived from the creepage times the creep force (summation of longitudinal and lateral). The number tells how much energy is dissipated at the wheel-rail contact and is a good indicator for wear.

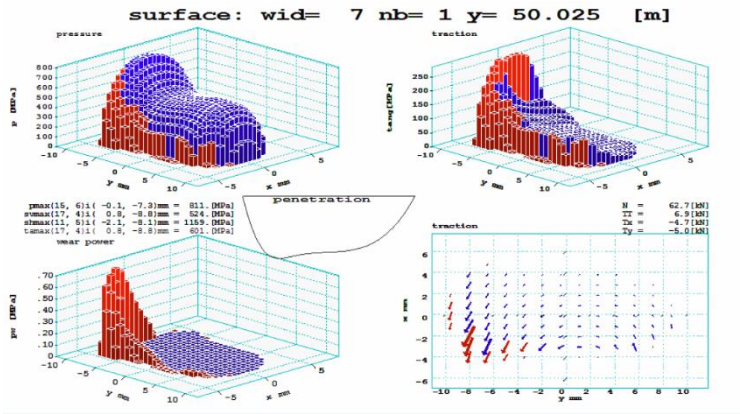

Figure 16 - Output example from VI-Rail Stress [17]

The last graph should be used with extra care. The contact indicator graph was added to compare with studies like [5], but it doesn't say anything about the distribution of stresses within the contact patch. It was made using the contact patch width and normal force. It should be used for indications only. It is advised to improve the last two graphs by output from the automatic VI-Rail stress calculation extension. This extension provides additional information on the contact patch, as indicated in Figure 16.

2.4 Overview

The previous sections have shown step-by-step how the assessment tool accelerates the process between geometry input and results output. All these steps are combined in a cloud-based workflow, as depicted in Figure 17. The user experiences it as follows:

- Creation of geometry data, in AutoCAD or from a point cloud
- Putting a copy of the geometry data in the input folder, which syncs with the simulation pc
- The input data vanishes, and the results are added to the results folder

The result is that each cycle costs roughly 3 minutes. This is in line with the goal of the project. More information on this workflow can be found in appendix A.

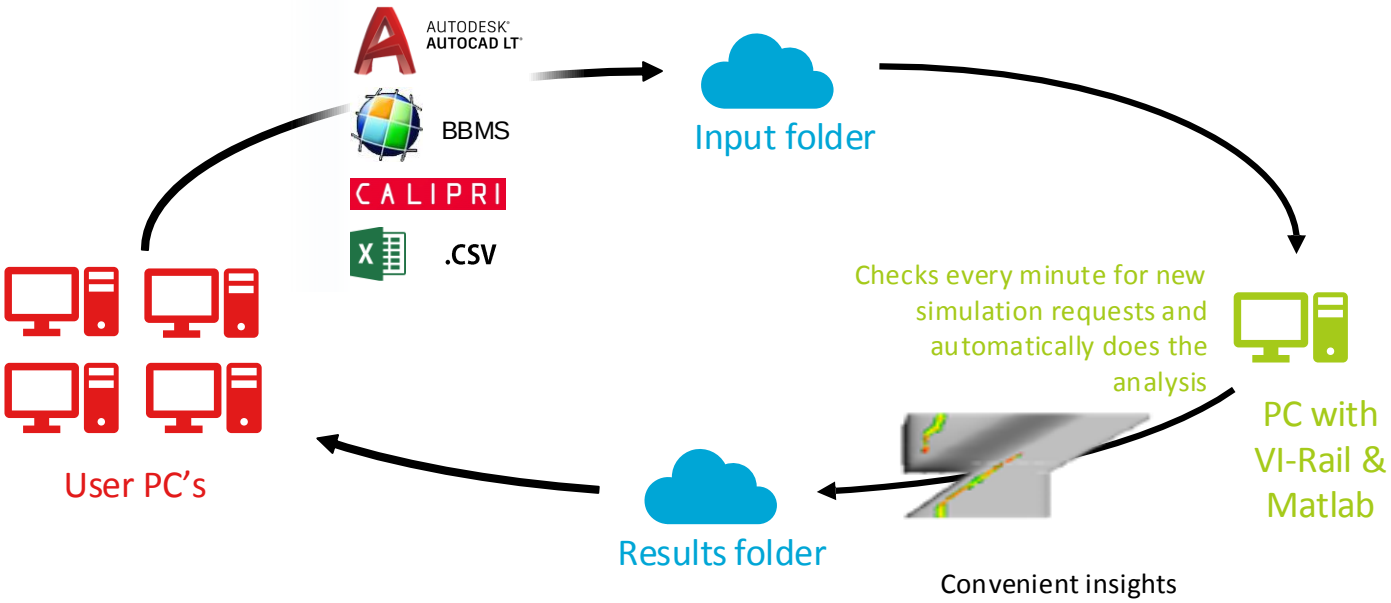

Figure 17 – Assessment tool overview

3 Comparison of crossings

As discussed in the previous chapter, the assessment of rail geometry is possible for designed, delivered and deployed crossings. This chapter compares the shape of these crossings (before simulating them) in order to learn from various design aspects, manufacturing errors and degradation processes.

In the design phase, solely design drawings are available. Old ones can be copies from hand-made drawings, but modern nowadays produced in CAD. Experience from throughout this project, showed that the original CAD files are distributed seldom. Instead, overviews are distributed in PDF format.

The shape of newly delivered products may vary from the intended design. This can be due to accuracy issues or flaws in the design specification. Because of this variation, it is important to assess this state before comparing the design with the performance in the track. The shape of these crossings can be measured at the factors; laser scanners can be used to create a point cloud which represents the crossing shape. Good indications of cross-sections can be given by hand scanners like Calipri [7]. Thorough and precise 3D data from crossings can be acquired swiftly, by using an automatic scanning rig like in Figure 18.

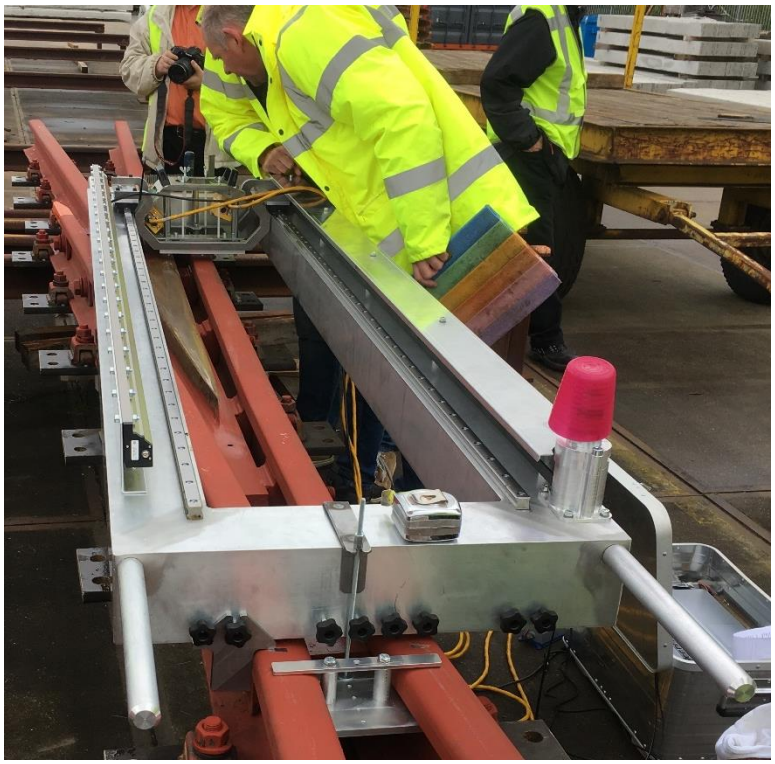

Figure 18 - Scanning rig, by De Graaf Railway Inventions

After deploying the crossing in the track, the crossing enters the last part of its service life. During this phase, access to the crossing is limited due to safety restrictions. Hand scanners and scanning rigs can be used, but only whilst the track is out of service. The crossing being in the track however, also comes with a positive effect. It can be measured by using a measurement vehicle (i.e. Eurailscout).

3.1 Comparison of designs

This chapter is concluded with a comparison of all previously mentioned geometries. This is done in two directions. The first comparison is between designs. The second part of this section will compare two crossings with their available profile measurements.

In appendix B, twelve crossing designs were compared. The crossing designs came from operators, from manufacturers and from a numerical optimisation. The designs were made between 1933 and 2017. The designs were made for three different rail profiles. The designs came from four different countries.

The disquisition of this variety of designs has shown lots of differences. This subsection seeks to categorise and visualise these differences. The categorisation has been done in the index on this page. It divided all problems in to four optimisation problems. This subsection will take the reader through two of those. The third problem is more relevant to the next subsection and the fourth problem is outside the scope of this thesis project.

I. Optimising the flangeways
   a. Approach surface angle
   b. Check rail / stock rail distance
   c. Wing / nose distance
   d. Location to start the nose
   e. End of the closure rail
   f. Start of the wing rail
   g. Wing rail side

II. Optimising the location and fixation of the transition zone(s)
   a. Wing rail elevation
   b. Height profile at the back of the nose
   c. Switch rail / wing rail transition
   d. Wing rail rounding

III. Optimising the definition of the standards
   a. Preventing multiple interpretations of the standards
   b. Defining achievable factory tolerances

IV. Non-geometrical aspects
   a. Rail material
   b. Constructed/cast/hybrid
   c. The hollow nose

Problem Ia: what is the optimal approach surface angle?

The ProRail nose design is the only design which incorporates approach surfaces with a different angle than the sides of the rail. The reason for this can be seen in Figure 19. On the left, the effect of the opposing flangeway (distance between rail and check rail) is shown. A neutral wheel (green) is free to move to the right up till the check rail, which is at about 5.6 mm from the neutral position. The middle image shows the opposing wheel, while at the tip of the crossing nose (cross sections between I and II). It can easily be seen that the approach surface and the opposing flangeway have a direct relationship with each other.

The angle of the approach surface however, is a different matter. On the right of Figure 19, a close-up is depicted. The front of the wheel flange appears to have precisely the same slope as the ProRail approach surface. It should therefore allow a large contact patch at the side of the nose, in case the nose tip must catch a wheel in extreme position. When not using the special approach surface angle, the wheel would only make contact at the top of the nose tip. This could introduce the risk of damaging it.

As the S1002 wheel is subjected to wear, the wheel flange becomes thinner. This leaves more room with respect to the nose tip: up to 2 mm before re-profiling of most of the passing wheels. From 1.5 mm wear per wheel on, the wheelset is unable to hit the approach surfaces.

Concluding: ProRail's approach surface angle is well-suited to match S1002 wheels.

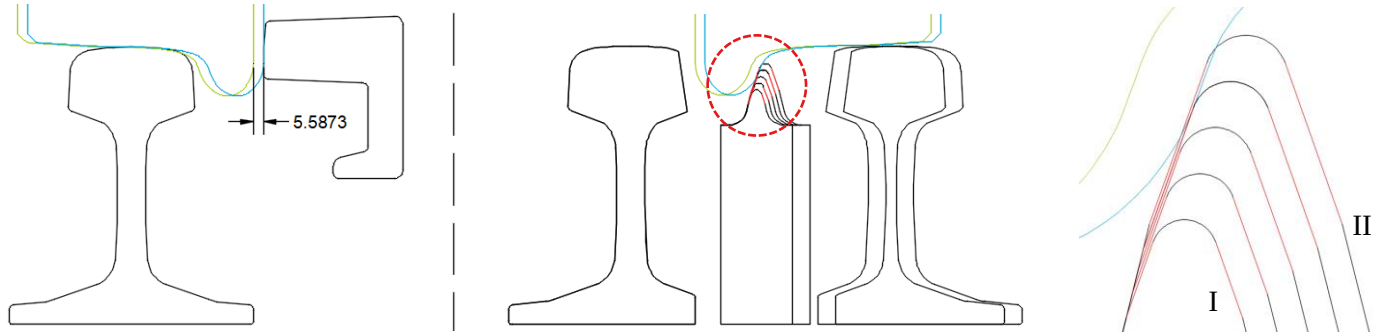

Figure 19 - The relation between check rail contact and the approach surface

Problem Ib: how close should the check rail be to the opposing rail?

The previous topic has shown the relevance of check rail tuning. The next question is how broad that flangeway should be. Table 1 shows that DB Netze uses a tighter check rail. The difference of 2 mm might seem small, but from the numbers behind Figure 19 can be derived that 1.51 mm already makes ProRail's approach surface obsolete. This because the blue wheel profile moves to the left, as a consequence of the tighter check rail. The tighter check rail thus explains the absence of an approach surface at the German crossing nose.

Design	ProRail	DB Netze	Infrabel	SBB
Check rail tuning	41 mm	39 mm	n.a.	40 mm

Table 1 - Check rail distances

When making decisions on this matter, it should not be forgotten that the check rail can be subjected to wear (which moves the blue profile to the right). Despite this, it is advisable that ProRail looks in to the tuning of the wing rail. It could make the special part of the approach surface obsolete, which would save costs.

Problem Ic: how broad should the flangeway be?

The flangeways through the crossing are a different matter than the flangeways at the check rails. As Table 2 shows: the distances are larger, and the front of the wheel can contact the crossing nose (rather than a regular rail).

Design	ProRail	DB Netze	Infrabel	SBB IV	SBB VI
Flangeway	43 mm	44 mm	45 mm	42 mm	44 mm

Table 2 - Differences in flangeway width (measured 14 mm below the rail head)

When depicting flange-back contact at both sides of the neutral position (as shown in Figure 20), the red line shows how the flangeway is wider than it could be. This is sub-optimal in terms of support that the wing rail can provide to the wheel. According to the principle of Figure 20, the crossing flangeways could be 5 mm narrower. However, this is for the ideal S1002 wheel. The current practice can be justified by wheel flange wear.

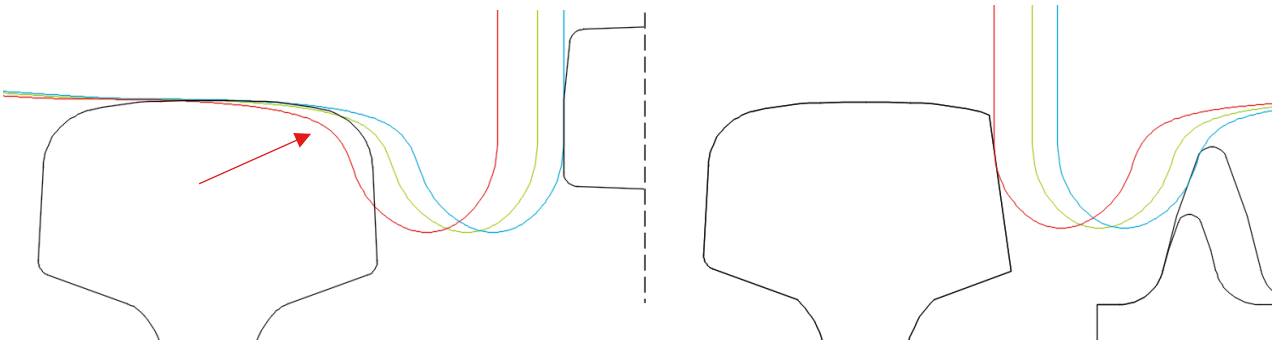

Figure 20 - The ProRail crossing flangeway (right) and its consequence at the opposing rail (left)

Problem Id: what is a safe location to start the nose?

While the ProRail nose starts at the centre of the crossing (TP), all other designs start behind it. This is because ProRail uses a two-step nose tip. While Figure 19 already shows this in front-view, Figure 21 compares this with the other designs at the side-view. It can be derived from problem Ia that the ProRail that the part between TP and TP+90 is not meant for contact at the top of the nose. It is used to counteract possible problems associated with a wide opposing flangeway.

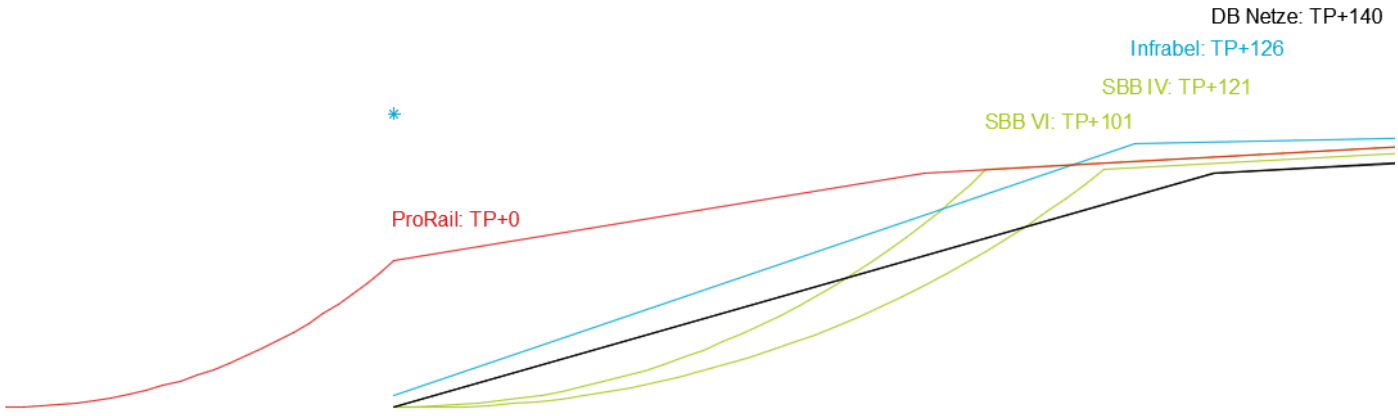

Figure 21 – The difference between ProRail's two-step nose tip and the other designs

In the case where a two-step is not needed, the comparison between nose start locations would become different. Table 3 shows where the nose starts at different crossings, in the case ProRail would not need the part between TP and TP+90. The spread of locations is smaller, but still ProRail starts the nose much earlier than DB Netze. The function of ProRail's two step nose, is to detect problems with the geometry. In the normal situation wheels should not hit the tip of the nose, but in cases of misalignment the nose tip gets brushed by the side of the wheel flange. Noses with such wear alert inspection.

The (earlier mentioned) pilot of German geometry in the Netherlands is suitable to get insight in the best location to start the nose, because it compares the two extremes from Table 3. This counts both for the location of the supporting part as well as the concept of a non-supporting nose tip for inspection purposes.

Design	WBN	Kloos	Infrabel	ProRail	SBB IV	SBB VI	DB Netze
Nose tip	(90)	(90)	126	(90)	121	101	140

Table 3 - Start locations of the nose tips in different countries (in mm from TP)

Problem Ie: how broad should the crossing throat be?

The throat of the crossing is the place where the transition between the closure rail and wing rail is located. This transition is needed because crossings incorporate intersecting flangeways. As shown in Table 4, the location of this transition is different throughout all examined countries.

Design	ProRail	DB Netze	Infrabel	SBB IV	SBB VI
Throat width	55 mm	60 mm	59 mm	58 mm	58 mm

Table 4 - The width of the crossing throat throughout different designs

In theory, this throat could be smaller, without decreasing the width of the flangeway. Figure 22 shows such a theoretical crossing, with a flangeway clearance of 43 mm. As depicted, the throat could be of roughly the same width without compromising on the flangeway clearance. This is not the case in any real design. The real designs all have crossing throats of at least 55 mm, which allows a less sharp transition between closure rail and wing rail. In other words, the transition is smoothened by bending the rail at two points instead of at one point. The importance of this is discussed at problem IIc.

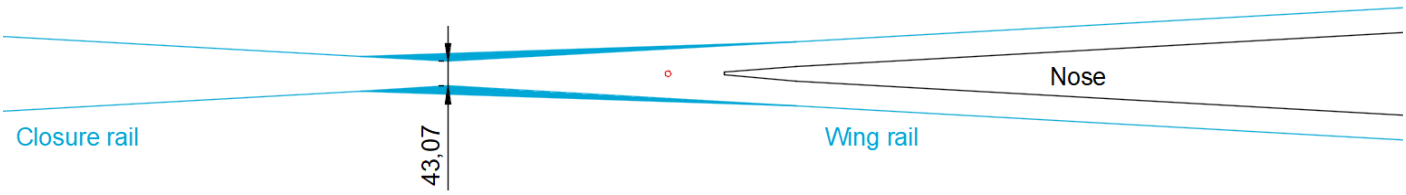

Figure 22 -Possibilities for the transition between closure rail and wing rail

Problem If: where should the wing rail start?

The other end of the closure rail / wing rail transition can be found at various locations. Figure 23 illustrates how countries choose between TP (ProRail), the start of the approach surfaces (SBB & DB Netze) and the end of the approach surfaces (Infrabel).

In terms of vehicle dynamics, the most important location is the transition between wing rail and nose rail. For this reason, it could be expected that it is beneficial to keep other geometrical transitions away from this location. ProRail's design does this the most, by using TP as location. Infrabel on the other hand, chose to end the closure/wing transition relatively far. This cannot pose a problem because the elevated wing rail

provides a constant support (as discussed in problem IIa). Simulations are advised to gain further insights in this matter.

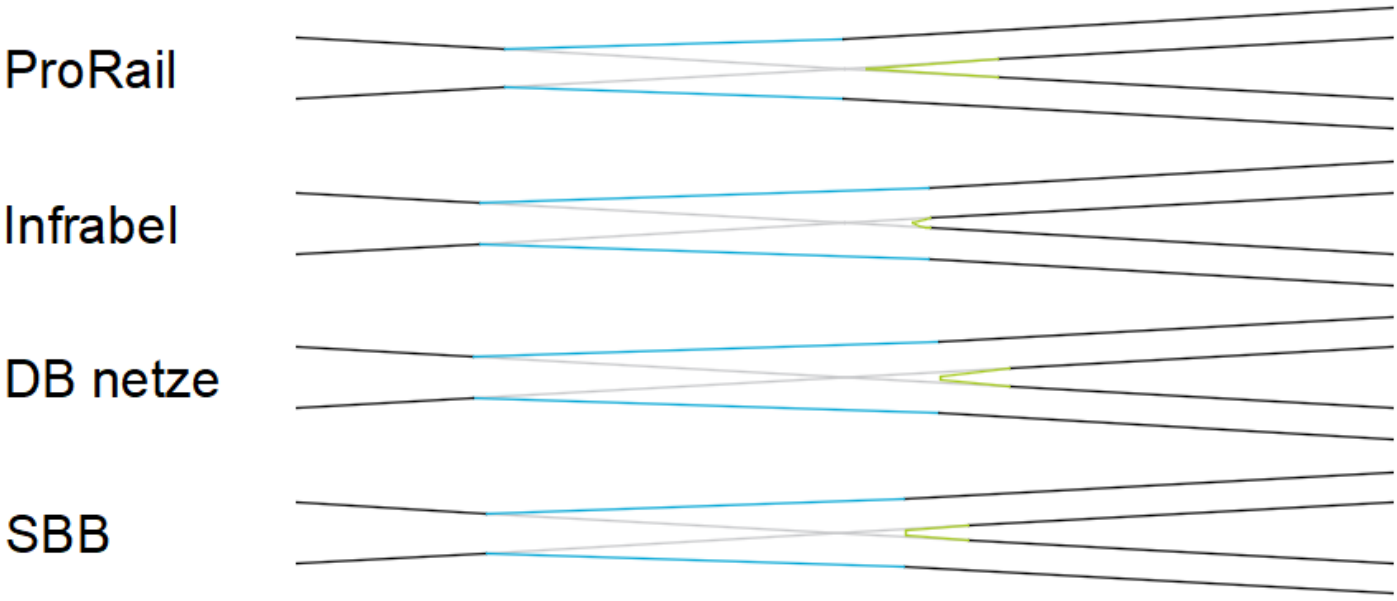

Figure 23 - Relation between the approach surfaces (green) and the wing/closure transition (blue)

Problem Ig: what is a good angle for the side of the wing rails?
The side of the wing rail is the last problem concerning the flangeways. Table 5 shows how two different concepts are available: a slope of about 1:6 or 1:7 or a vertical face.

Design	ProRail	DB Netze	Infrabel	SBB IV	SBB VI
Slope	1:7	Vertical	Vertical	1:6	1:6

Table 5 - Slopes at the side of several wing rail designs

The consequence of this, can be seen when projecting the wheel on both wing rails, like in Figure 24. It can be derived that the slope of the wing rail influences the contact location during flangeback contact. Determining the desirable location on the wheel is out-of-scope for this project.

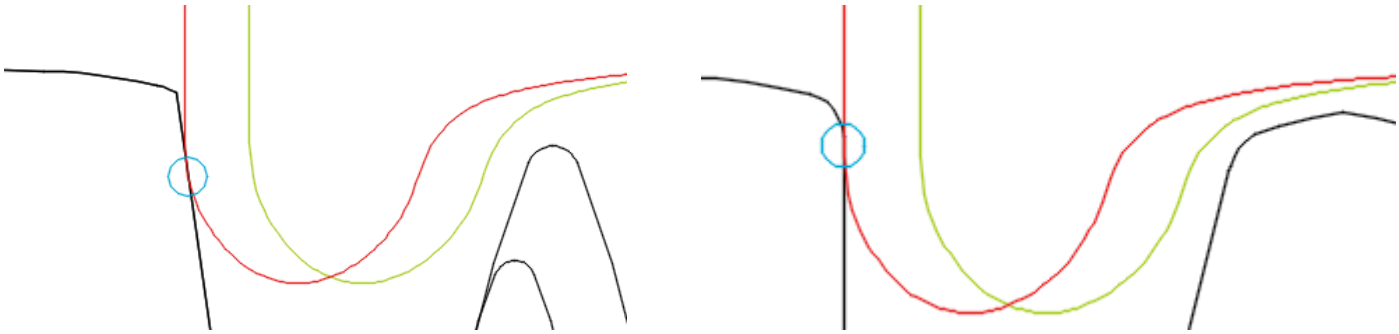

Figure 24 – Flange-back contact locations, resulting from different wing slopes

Problem Ih: can geometry be altered in a safe way, to strengthen the tip of the nose?
The tip of the nose is characterised by a limited width, due to the flangeways. This makes the nose tip a vulnerable point in the crossings. The examined designs (as discussed in appendix B) show two ways to strengthen this part of the crossing. The Swiss SBB VI crossing does this at the base of the nose, by gradually decreasing the 1:4 slope on the side of the nose. This provides more stability at the base of the crossing.
BWG claims to have improved the DB Netze nose, by adding more material at the top of the nose. The reason for this is to improve the robustness at the top of the nose tip. Both principles are depicted in Figure 25 and explained in appendix B.

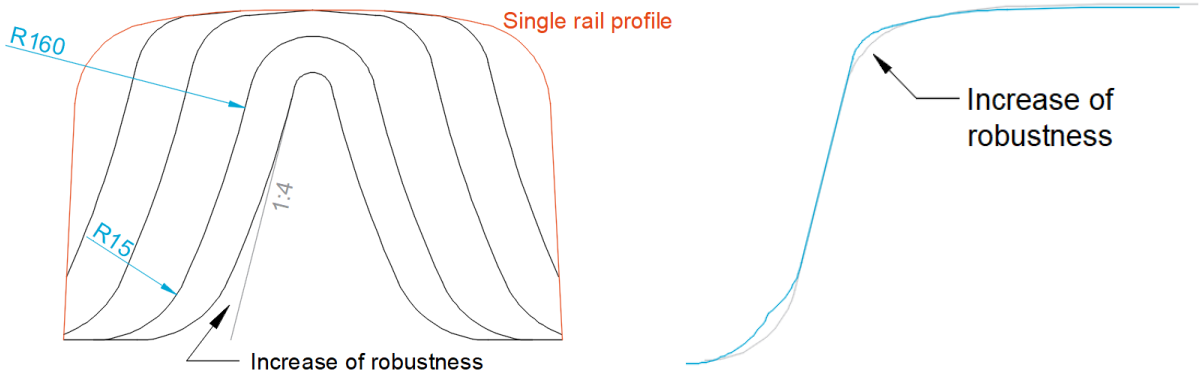

Figure 25 - Ways to increase the robustness at the base or at the top of the nose

Problem IIa: what is the ideal location and shape of the top of the wing rail?

This problem is the first problem which touches the optimisation of transition zones. Before the nose is designed, the desired wing rail should be chosen. This design order is important, because the shape of the wing rail is more constrained than the shape of the nose. To illustrate this, Figure 26 shows three different approaches of shaping the wing rail. The starting point is the ProRail design, which uses a regular constructed wing rail based on the UIC 54 profile. Altering the shape of the wing profile to a more efficient shape immediately means lowering the wing profile, which is not beneficial. Kloos surpassed this problem by elevating the wing rail. The designers used the extra space to match the wing profile with the S1002 wheel profile. Infrabel did the same in a cast crossing. Conclusion: the ideal location and shape of the top of the wing rail are constrained by the type of crossing (constructed/cast and elevated/default). When space is available to alter the rail profile, matching the rail profile with the wheel profile can be beneficial.

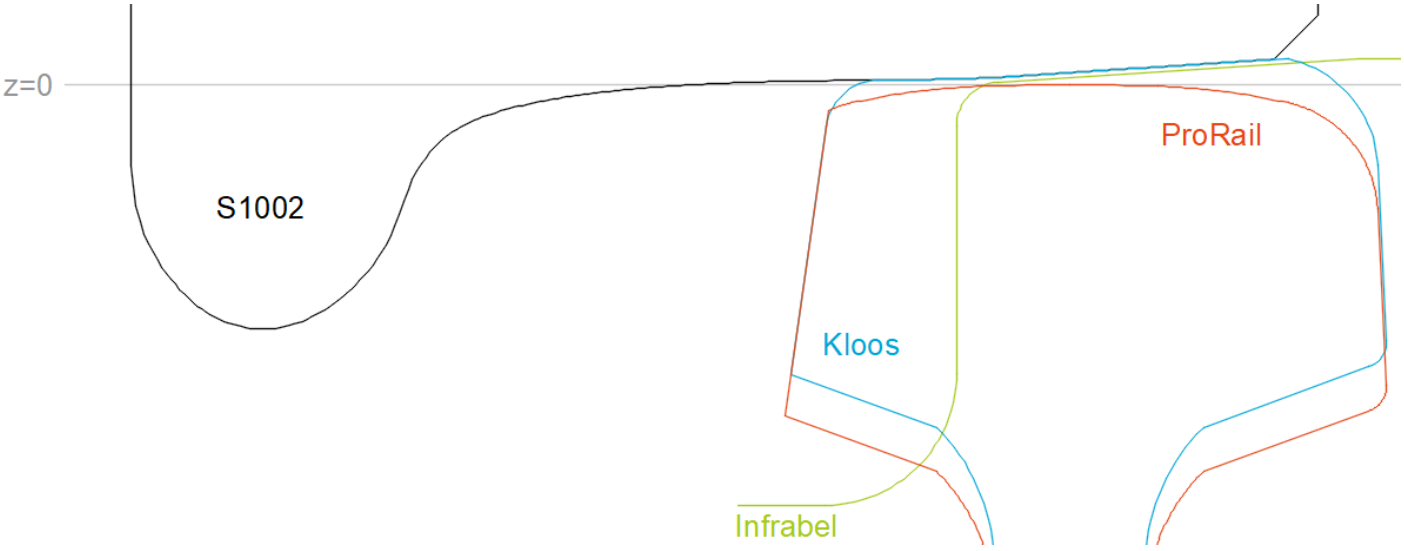

Figure 26 - Different ways to shape the wing rail

Problem IIb: what is the ideal height profile at the back of the nose?

As soon as the desired wing rail support has been determined, the wing/nose transition can be finished by determining the height of the back of the nose. This part of the crossing serves either as the departure or arrival location of the wing/nose transition. Table 6 compares this location in terms of length and slope.

The designers seem to have mixed opinions on the slope (and thus the length) of the back of the crossing. A slope which is too steep is unfavourable for facing wheels, because of the angle of impact. A slope which is too gentle is unfavourable for trailing wheels, because this moves the transition zone to the (weaker) front of the nose. Simulations should prove the best solution.

Company	WBN	Kloos	Infrabel	ProRail	SBB IV	SBB VI	DB Netze
Nose tip	(90.5)	(90)	126	(90)	121	101	140
Nose back start	181	180	288	180	222	202	240
Nose back end	497	495	496	630	656	725	1310
Nose back slope	1:50	1:50	1:74	1:54	1:58	1:66	1:117

Table 6 - Height profiles at the back of crossing noses

Problem IIc: how should the transition between closure rail and wing rail be shaped?

This problem shows why transition zones has been mentioned in plural. The transition between the wing rail and nose rail should not be regarded as the one and only transition zone in a crossing. Simulations have shown that the transition between closure rail and wing rail is also important. When this is done too abrupt, the crossing introduces dynamic amplification to the contact forces.

The difference between a good design and a 'too abrupt' transition is determined at the location of the contact patch in this area. The approximate location of an undisturbed contact patch is shown in green, in Figure 27. It can be seen how the transition between UIC54 and wing rail is much shorter at the constructed crossing. The constructed crossing moves the entire cross section to the side starting at the crossing throat. This immediately includes the sensitive part of the cross section; the location of the contact patch. This results in a sudden change of contact patch support and thus in unwanted dynamics. The cast crossing negotiates this problem by rounding off the side of the wing rail. This is discussed at the next problem.

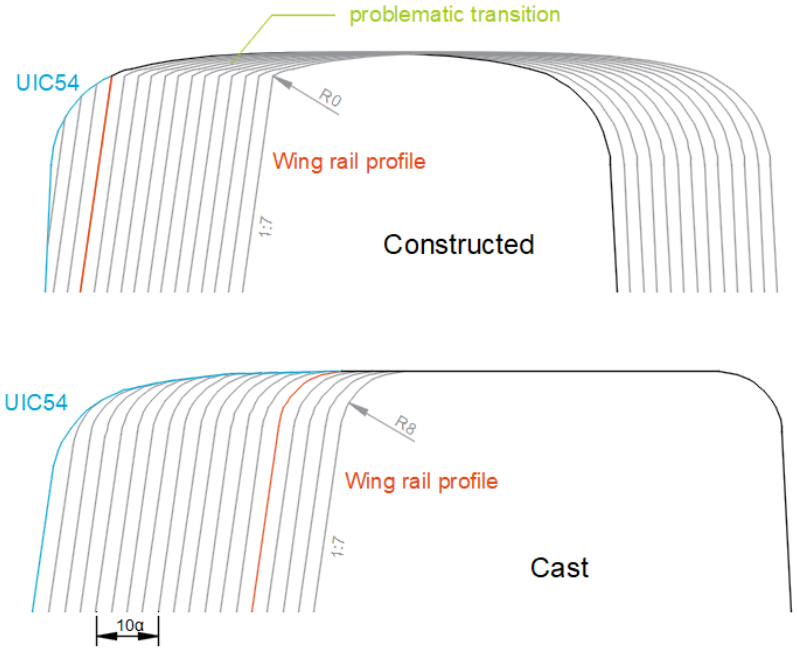

Figure 27 - Switch rail / wing rail transitions at ProRail

A possible way to reduce the problem at the constructed crossing is to bend this part of the crossing with a larger radius. The concept is shown in Figure 28. It uses the same throat width as ProRail but replaces the

kinks with a smoother transition. This would gradually start/end the lateral push of the contact patch. This concept must be investigated further before implementing it.

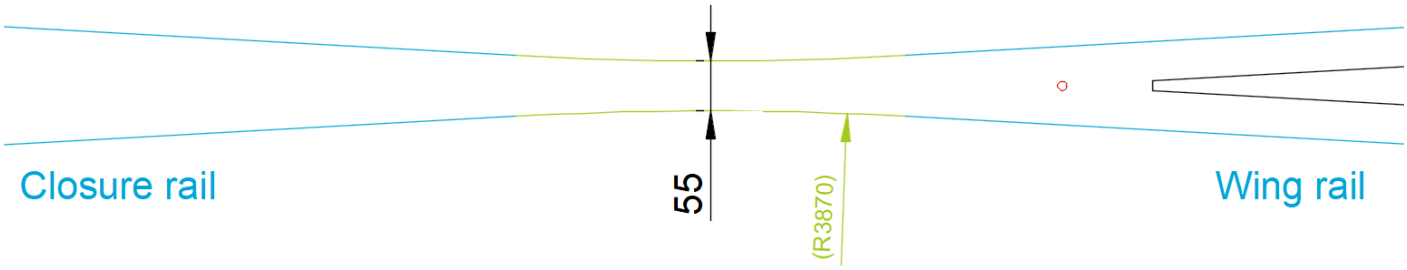

Figure 28 - Possible solution to the transition problem at constructed crossings

Problem IId: should the wing rail be rounded off at the flangeway and if so: with what radius?

At the previous problem, it was described that Manoir's cast crossings (manufactured for ProRail) has a smoother switch rail / wing rail transition because of wing rail rounding. This is due to the fact that the contact patch support is decreased less abruptly, by applying this rounding. ProRail does not require this for its constructed crossings. Despite this, Kloos still invests time (money) in improving the crossing design in this way. For this reason, Kloos joins up with the all other designs in Figure 29.

The radius at which the rounding is done varies between 5 and 10 mm. The perfect radius depends on multiple factors. Cast and constructed crossings should be treated differently, because of the limited width of the rail head at constructed crossings. Moreover, a difference is present between crossings that do or do not use an elevated wing rail.

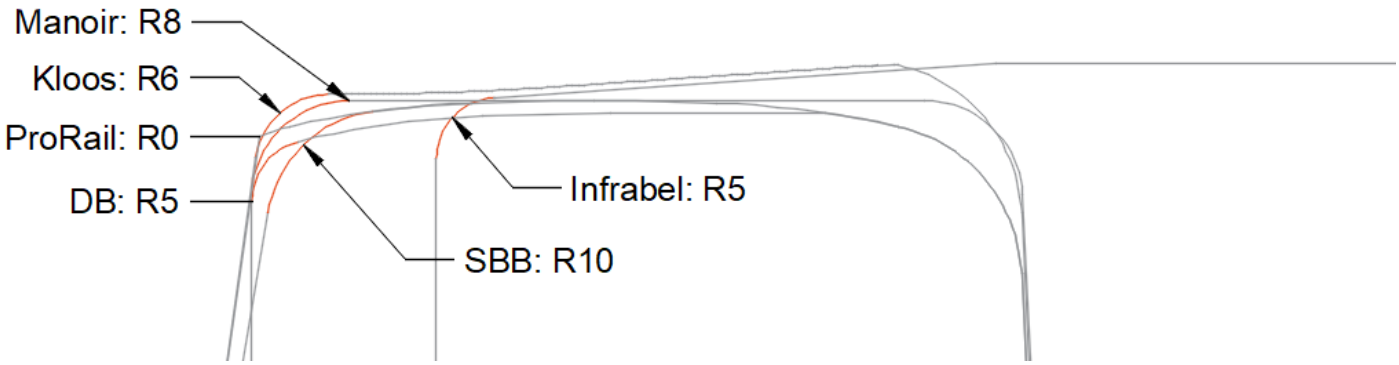

Figure 29 - Different ways to round off the wing rail

Problem IIIa: how to make sure that standards can be interpreted in just one way?

When turnout manufacturers create a design, it should comply with the standards of the customer. When defining aspects of these standards, the customer can choose to either constrain the designer or give room to the designer. Constraining the designer can be beneficial when the customer must be certain of particular aspects of the design (i.e. desired safety measures like flangeway). Giving the designer freedom can be beneficial when the customer wants to make use of innovation capacity of the manufacturers.The customer can have reasons for both choices, but the most important matter is that the customer is aware of the choice. When this is not the case, the customer is no longer in control; manufacurers may deliver a product which does not match the wishes of the customer.

When choosing to constrain the manufacturer, the customer must define a 3D shape with convenient 2D drawings. An example of different approaches can be found on the back of the crossing nose. The examined designs can be divided in three of these approaches.

ProRail and SBB leave room for interpretation to the manufacturers. Their standards define the crossing nose by providing a height profile (side view) of the top of the nose, combined with various characteristic cross-sections. The characteristic cross-sections are used to define the tip of the nose and thus serve as an insurance of safety in terms of flangeway. It is clear that ProRail and SBB (either aware or unaware) chose to leave the back of the nose undefined.

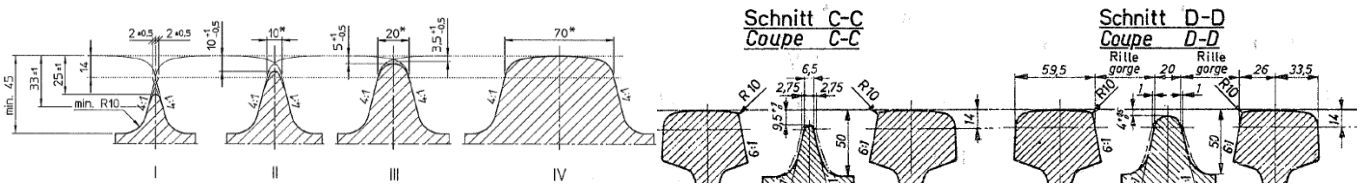

Figure 30 - ProRail standards (left) and SBB (standards)

Infrabel is clearer in its standards. When analysing the drawings, all cross-sections can be related to a profile of ideal support (as depicted in Figure 31).

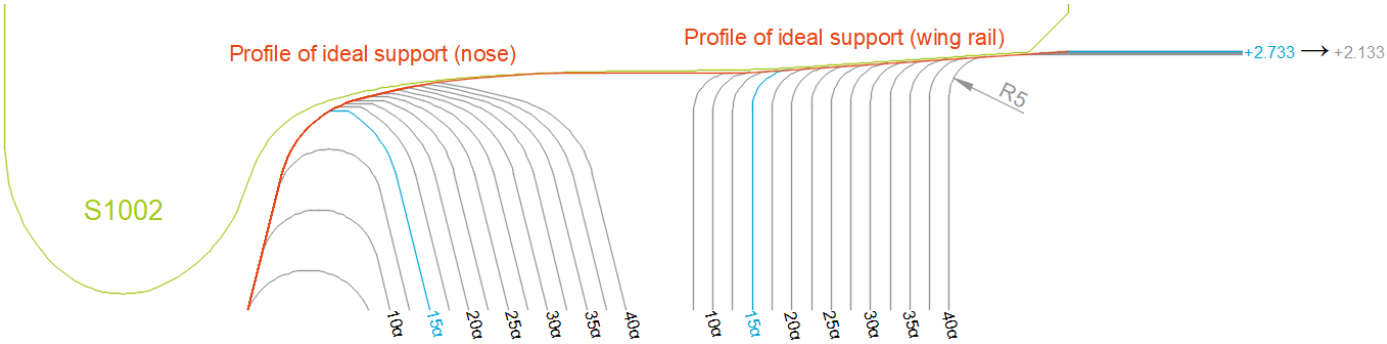

Figure 31 - Theory behind the Infrabel design

While it is not hard to derive the 3D shape from the Belgian standards, the drawings for the DB crossing however are more precise. This makes sense because these drawings were made by the designers themselves. The standards define the (lateral) cross section of a milling tool and accompany that with the position of that tool along the nose. Figure 32 shows this concept for the side view: not the nose height (blue) is defined in the standards, but the tool height is defined in the standards.

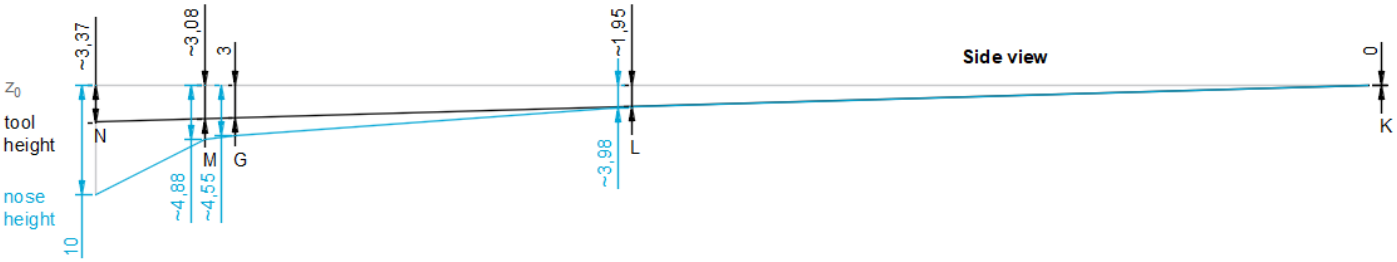

Figure 32 - Side view of the DB crossing: the tool height is in the standards, rather than the nose height

It can be concluded that ProRail and SBB leave it up to the manufacturer and that Infrabel and BWG constrain the design to a specific shape. It is up to these parties, whether they intended to make this choice.

3.2 Comparison of life cycle phases

This section will introduce the laser measurement rig, as shown at the start of this chapter in Figure 18. The rig allows the user to capture the shape of a crossing automatically in a convenient way. It does this parallel to the track centrelines that pass the crossing. For this reason, the setup is ideal for the modelling of the vehicle dynamics.

On the 24th of March 2018, the first measurement was carried out. The goal of this session was to capture the as-built state of the crossings. A total of four crossings has been measured. In this project only crossing 91A will be discussed, because this crossing has the correct running direction and is not influenced by vehicle dynamics from other crossings.

This section will show how the key features from the measured crossings were extracted from the measured point cloud. The next section will describe the same crossing after installation in the track.

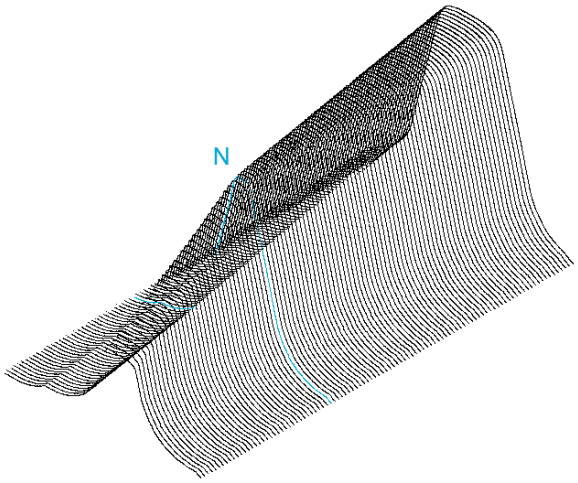

Figure 33 - Finding the first characteristic section

The scanning rig measures a cross-section every millimetre. The rig scans the crossing from two sides, per running direction (a total of 4 scans). Per scan, two laser scanners are used on different angles. This results in over a thousand data points per cross-section, for only the nose rail. A Matlab script has been written to import the scans in AutoCAD, to analyse them conveniently. To do this without asking too much of the PC, the number of cross-sections to work with in AutoCAD is limited to 100: 10 cm.

The longitudinal position of the scanning rig can vary freely, when attaching it to the crossing. For this reason, the characteristic points on the crossing do not appear in the same cross-section when comparing different crossings. These longitudinal variations are easily within the earlier mentioned 10 cm. Because of this, the characteristic cross-sections are found by generating their approximate locations. Within such a selection, the characteristic cross-sections are found by directions from the design drawings. A clear example of such an analysis is shown in Figure 33. From the height profile of the nose, one can quickly see that the blue cross-section is the characteristic one.

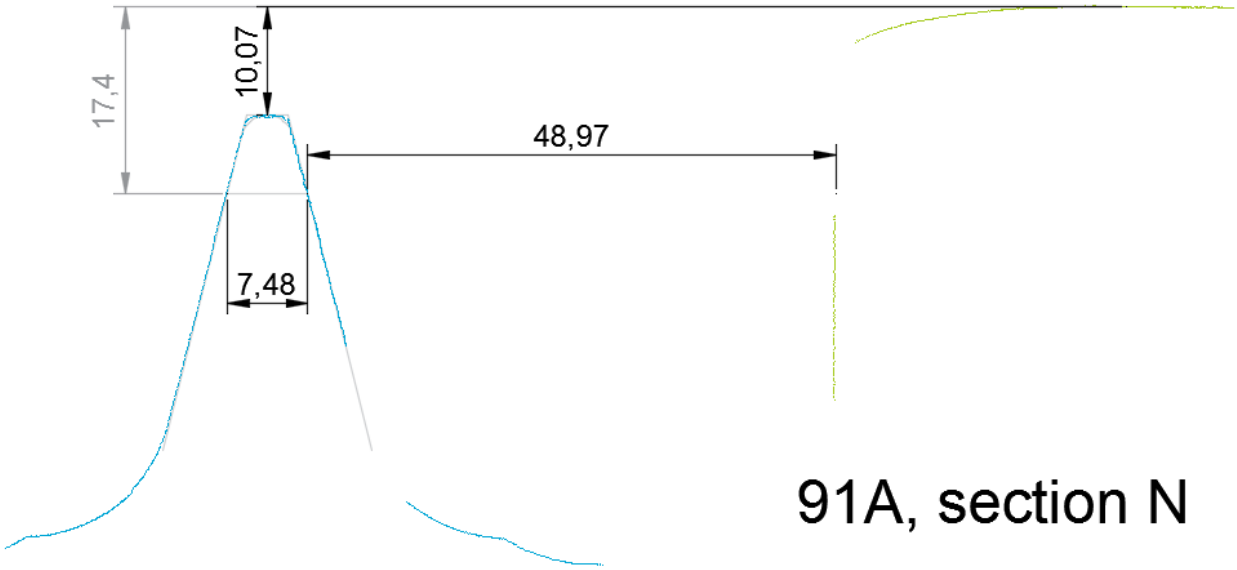

Figure 34 - Key features on the first characteristic section

After finding these characteristic profiles, they must be analysed for key features before comparing them with similar ones. In Figure 34, such an analysis is shown. The derived features are: nose rail depth, nose rail width and the distance to the wing rail. Due to noise in the signal, an error margin of +0.10 and -0.10 millimetre is assumed.

Problem IIIb: what are manageable factory tolerances?

The data from the measuring rig allows to compare delivered crossings with their design. Table 7 shows such a comparison for crossing number 91A, which is part of the current full-scale test.

	Nose depth		Nose width		Wing rail distance	
	Designed	Delivered	Designed	Delivered	Designed	Delivered
N	$10.00^{+1.00}_{-0.50}$	10.07	6.00 ± 0.50	7.48	48.75 ± 1.00	48.97
M	$4.50^{+0.50}_{-0.50}$	4.41	26.60 ± 0.50	26.69	44.00 ± 1.00	46.29
G	$3.90^{+0.30}_{-0.00}$	3.77	29.70 ± 0.50	30.90	44.00 ± 1.00	44.72
L	(2.00)		70.00 ± 0.50	69.76	44.00 ± 1.00	n.a.
K	(0.00)		145.00 ± 0.50	146.41	(47.18)	

Table 7 - DB crossing 91A (values in mm's)

The values in red show characteristics which were delivered outside the design tolerances. While it is out-of-scope to look further in to this subject, it is advisable to look further in to this matter. First, more crossings should be checked to see if the deviations are recurring. If this is the case, it would be wise to simulate the deviating situation and check for possible different performances. Based on that, decisions can be made to get to a solution (either widening the tolerances or changing the production process).

3.3 Conclusions on crossing comparisons

On the design drawings

From the previous sections it can be concluded that crossing drawings can be categorised in two categories: standards and designs. Standards are handed out by the asset owner (ProRail, SBB, Infrabel, DB Netze), while designs are discretisations within a standard. In other words, the standard is the solution space (black) and an appreciated design a solution within the solution space. As depicted in Figure 37, asset owners must choose their standards wisely.

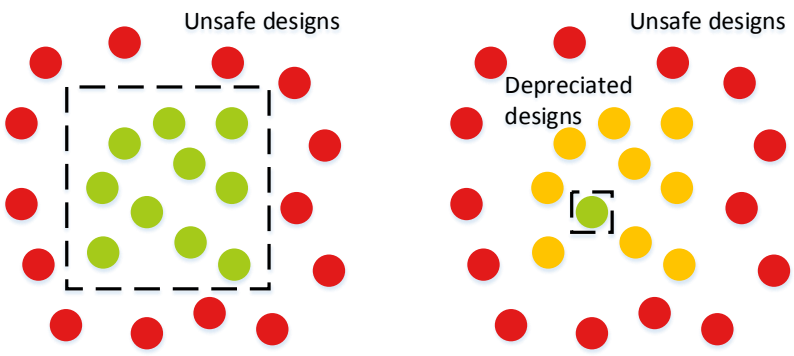

Figure 36 - Two extremes in the definition of standards

Currently, ProRail and SBB clearly focus their 1:9 crossing standards purely on ruling out the unsafe designs. Consequentially, the manufacturers have come up with a variety of designs with different properties. This is not necessarily a bad thing, as long as all safe designs are automatically appreciated. If however ProRail wishes to optimise the current practise, it is recommended to investigate the relation between more expensive designs and reliability. More expensive designs (cast and raised wing rail) might have a lower impact force, which helps to prevent cracking and thus raises the reliability of the crossing. This is extra relevant at locations where extra reliability is desired.

As soon as more reliable types of crossings have been found, the standards for important assets could be tightened. The search for crossings with less impact forces will be discussed in the next chapter.

On the life cycle comparison

The life cycle comparison has been carried out as a proof-of-concept. One comparison has shown that the manufacturer can fail to meet the tolerances of a design. This means that either the tolerances should be broader or that the production process should be more precise. The answer to this can be derived from additional simulations.

The same method can also be used for the comparison between manufactured crossings and worn crossings. This could help validating projects like [14] and could help with further optimising crossing designs. This however, is out of scope for this MSc thesis.

4 Simulation results

This chapter compares the output from VI-Rail with the output from the assessment tool. The comparison is made in order to check the pros and cons of both interfaces. The chapter will also discuss insights based on the simulation results; these are discussed in the last two sections.

4.1 Introduction

When running a VI-Rail simulation, one can choose to generate a contact animation. Frames like in Figure 37 are animated throughout the simulation. The animation frames consist of several parts:

- The wheels of the carriage, in blue
- Force vectors, also in blue
- The contact patches in red
- The rail profiles in black
- General data on the top (distance, time, speed)
- Data on the contact patches (longitudinal, lateral and vertical forces in kN)

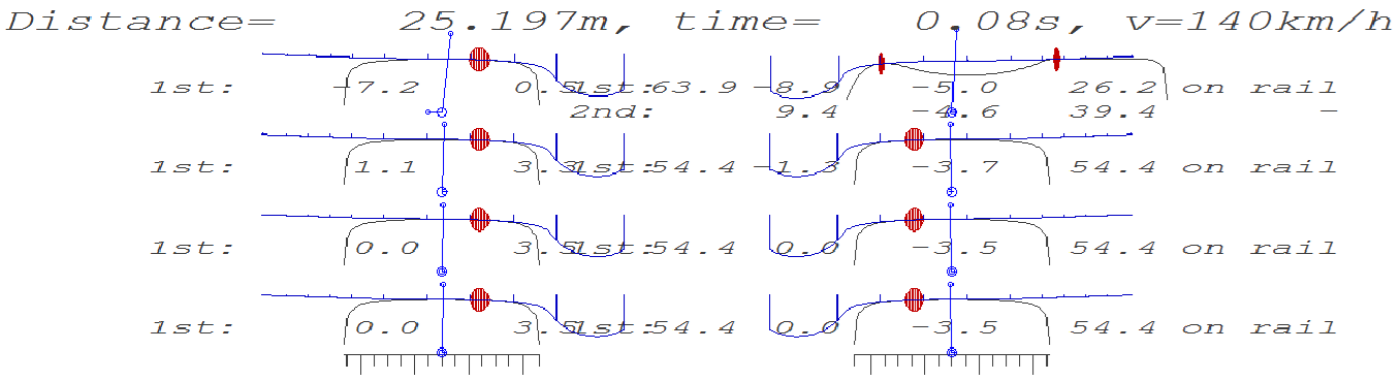

Figure 37 - Example of a contact animation

While the contact animation is very helpful when analysing the wheel-rail dynamics, it was sadly not possible to recreate it within the scope of this project. The frames use data which can only be accessed when a software extension is bought (like discussed in section 2.3). As an alternative, a contact indicator was developed for in the assessment tool. Figure 38 compares it with the contact animation of the same crossing (ProRail cast).

Because of the lack of data, the contact indicator is based on a simplification of the wheel-rail contact. It creates rows of pixels equal to the number of steps in a simulation. Each row contains a slice of contact patch, based on the lateral position, width and force. The force is distributed parabolically through the width of the contact patch, which is the most important simplification (due to the lack of contact data). For this

reason, the contact indicator should only be used as an indication. Despite this, the comparison in Figure 38 shows that important aspects from the wheel-rail contact can still be derived from the contact indicator.

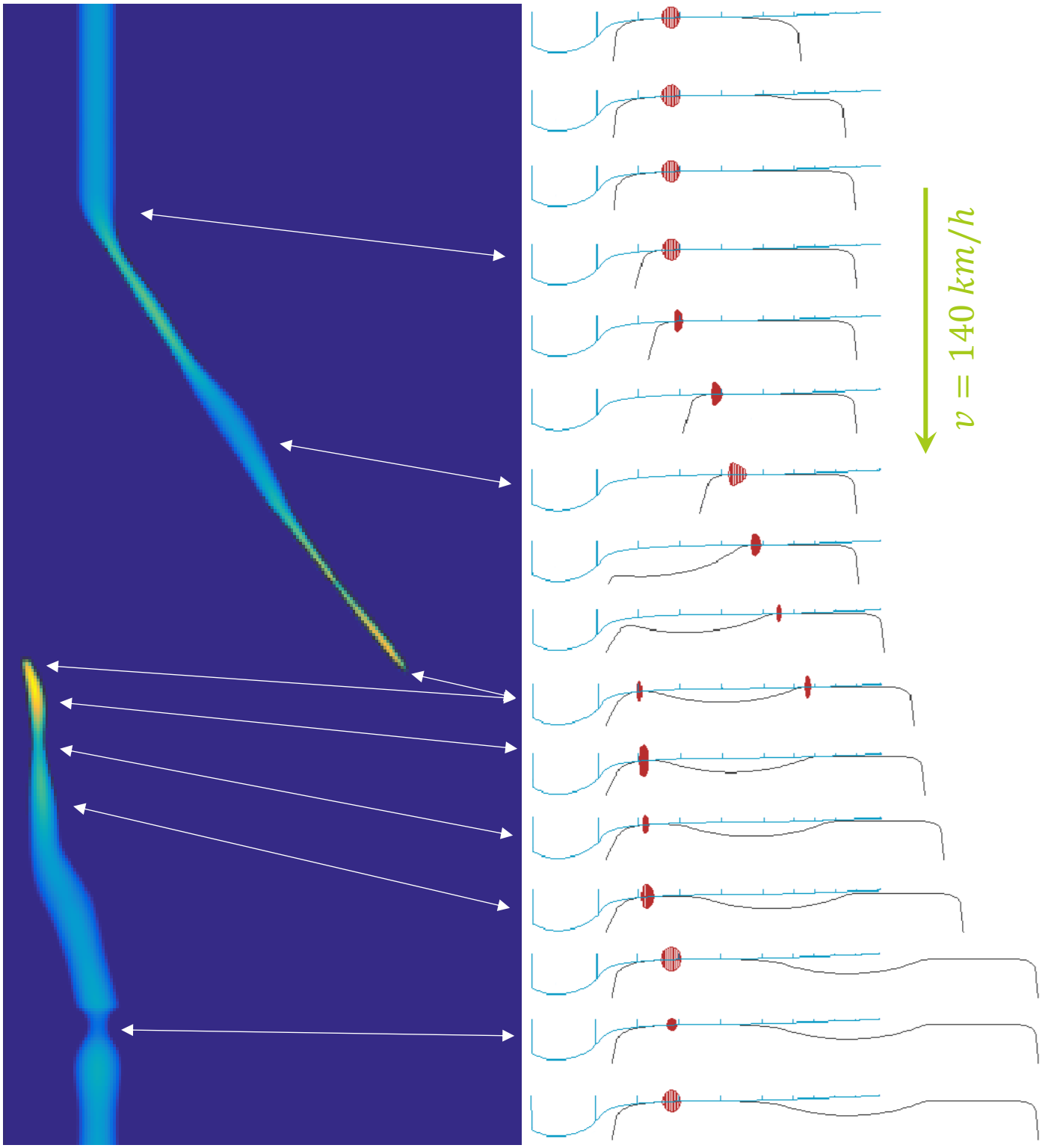

Figure 38 – The results from the ProRail cast crossing, in the assessment tool (left) VI-Rail (right)

VI-rail also gives the option of creating graphs from the simulation results, with a post-processing tool. These graphs can be used to display variables from the simulation. Figure 39 shows an example of such a graph. To create it, the VI-Rail user has to select a dataset, select an x-axis variable, select y-axis variables and apply style elements (like line types or a title). The problem with this is that it's impossible to use presets, which forcers the user to repeat these steps every time a new graph is made.

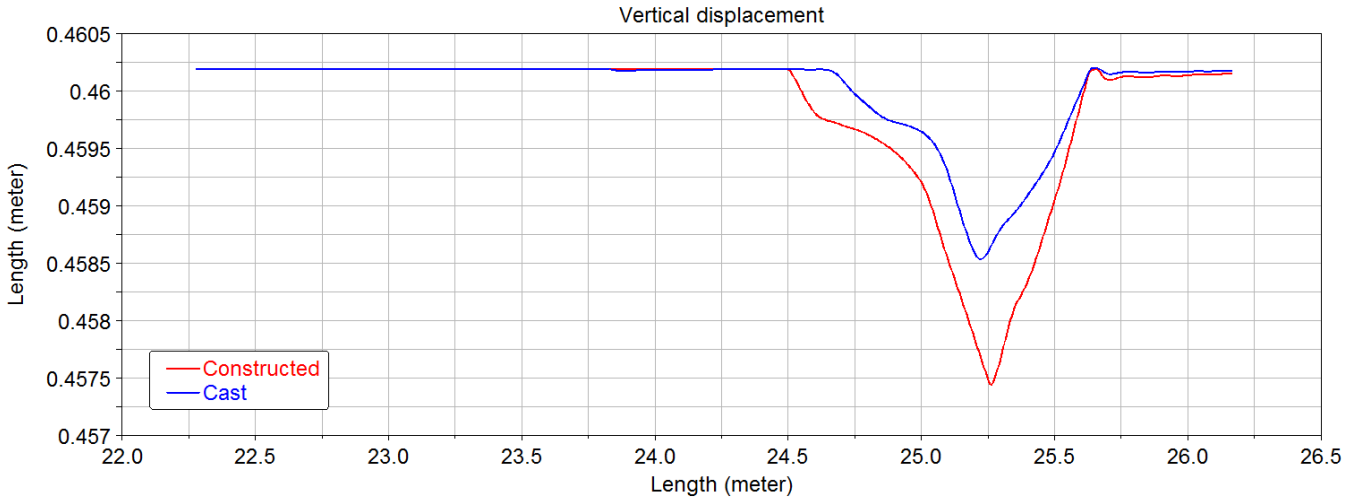

Figure 39 - Vertical displacement of the ProRail cast and ProRail constructed crossing

The alternative, which was developed for the assessment tool, has been discussed in section 2.3 and is shown in Figure 40. The results dashboard is an overview of the graphs that are most commonly used when comparing geometries. The displacements, forces and wear are aligned with a simplified version of the earlier mentioned contact indicator.

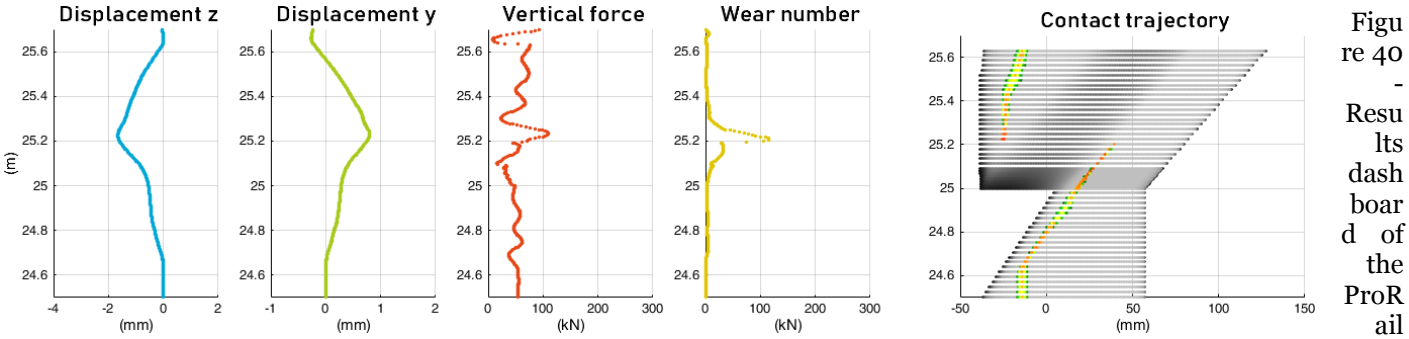

Figure 40 - Results dashboard of the ProRail cast crossing

The advantage of this approach is that the figures are generated automatically. The drawback is that the current version does not support the combination of multiple simulations in a single plot, like in VI-Rail. For now, this is mitigated by the wide shape of the dashboard; comparisons can be done by using the dashboards as rows in a matrix (as shown in section 4.3).

4.2 Comparison between geometry interpretations

As Figure 59 shows, ProRail's standards for cast crossings can be interpreted in four ways. Three of these interpretations have been simulated: the first (R300), the second (R80) and the fourth (Rvar). The third approach (R0) has not been simulated yet, because it violates the longitudinal height profile from the standards. Despite this, it is likely (based on their documents) that manufacturers use the third method.

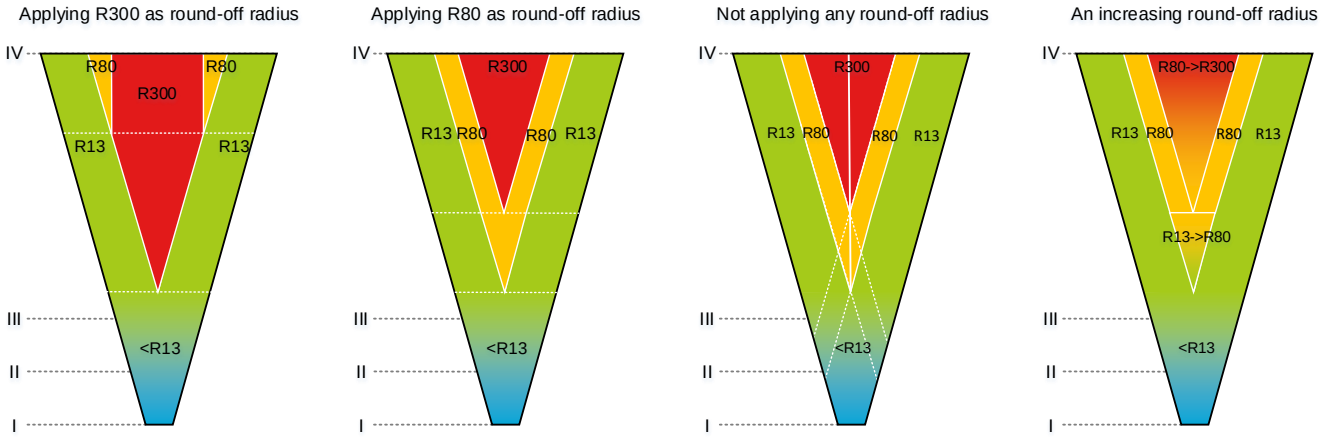

Figure 41 - Several ways of manufacturing a ProRail nose between cross-sections III and IV

The most visible difference was found between the results from the R80 and the R300 designs. While the top of the nose rises at a constant rate, the wheel doesn't. R80 has a discontinuity in the way up and R300 has the same discontinuity at the back of the nose. Rvar went through the middle, without a discontinuity.

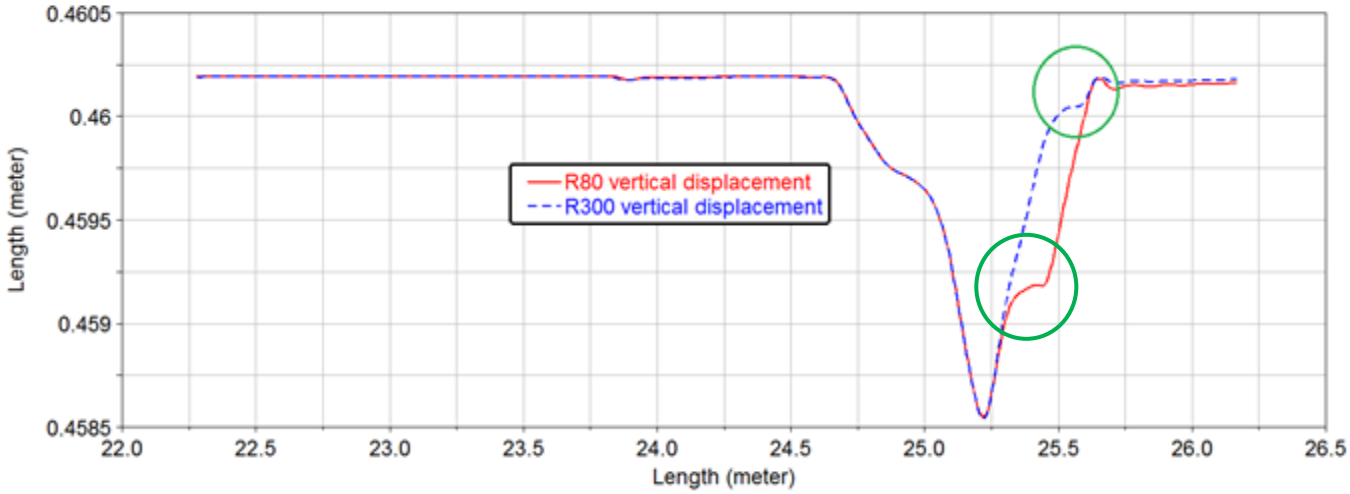

Figure 42 - Vertical displacement of the R80 and R300 design

Rvar involves a variable radius at the top of the rail, which is harder to manufacture than a constant round-off radius. However, the results have proven that a variable radius leads to a better performance than a fixed one. For this reason, ProRail's standards should be more specific between cross sections III and IV. As appendix B shows, the Belgian and German standards are less open to interpretation.

4.3 Comparison between crossings

Figure 43 shows the simulation results from three crossings: ProRail Constructed, ProRail Cast and Infrabel Cast. The results are primarily characterised by the displacements. The largest displacements can be found at ProRail Constructed. The deep (vertical) dip causes the largest vertical force and the largest wear number. ProRail Cast causes less wheelset displacement and thereby a better performance in terms of impact force.

The displacements at Infrabel Cast are from a different category. The characteristic wheelset-dip has been cut off by the elevated wing rail, which results in far less displacement. While the impact force is similar to that of ProRail Cast, the lack of displacement allows the dynamic components of the forces to be reduced quicker. It is recommended to investigate the latter further, with increased simulation time.

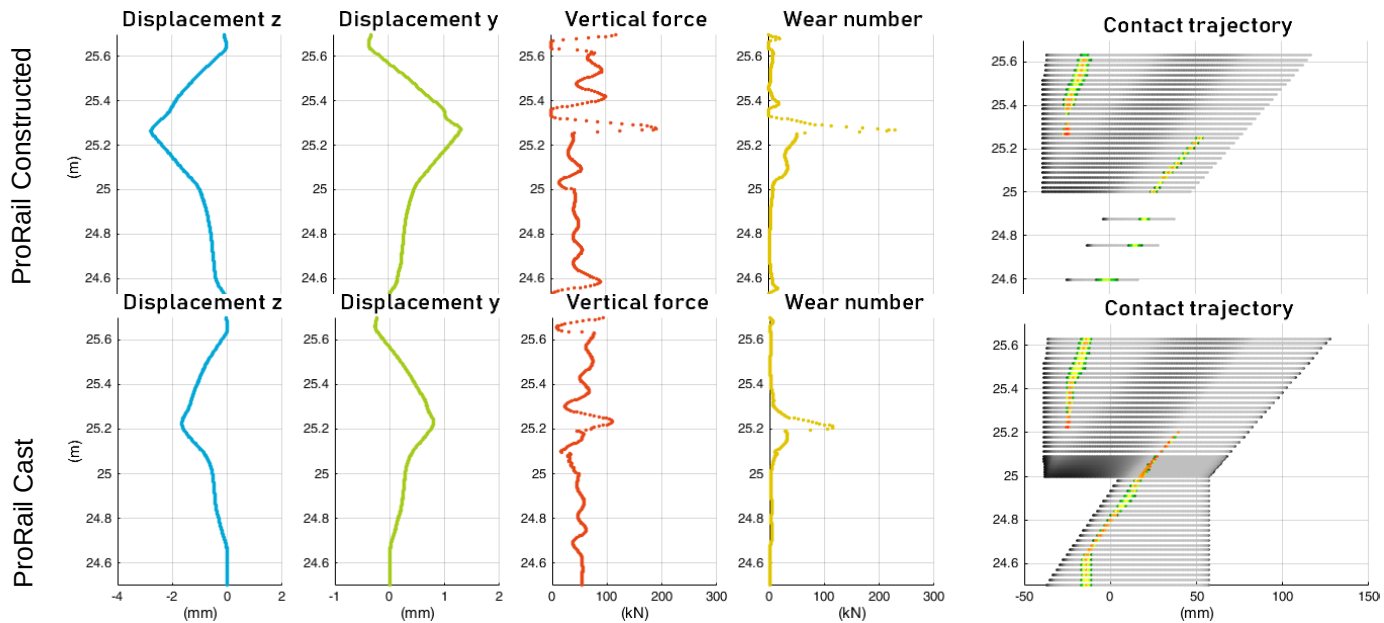

Figure 43 - Results dashboards from: ProRail constructed, ProRail cast and Infrabel cast

5 Conclusions and recommendations

In this chapter, the conclusions are discussed in three parts. These parts represent the three research goals:

- Providing an approach on the assessment of crossing geometry
- Finding geometry improvements by comparing different designs
- Providing insights in the relation between geometry and wheel-rail dynamics

After the conclusions and recommendations, the chapter finishes with a section on future work.

5.1 Conclusions

The first conclusions are general notions:

- Automated MBS simulations can provide useful insights in the consequences of design choices
- The same comparison can be made to validate factory tolerances
- Real stretches of track can be simulated, by importing geometry data from measuring trains

Based on the comparison of designs, the following propositions can be done:

- The standards from ProRail & SBB focus on defining the flangeways, rather than the transition zone
- ProRail's approach surfaces are optimised with respect to the S1002 flange
- ProRail's nose tip can be simplified, if the check rail flangeway is tightened
- Constructed crossings with elevated wing rails allow a larger variety of wing geometries
- Multiple interpretations of standards can be avoided, by defining the manufacturing process
- The slope of the side of the wing rail determines the contact location during flange back contact
- Longitudinal height profiles do not consist of straight lines and thus should not be depicted as such
- The choices between cast / constructed and elevated wing / level wing are most important

The following notions on wheel-rail dynamics were derived, based on the simulation results:

- Various interpretations of the nose geometry lead to different performances
- The throat is a sensitive part of the crossing, when not using an elevated wing rail
- Rounding between the side and top of the wing rail is beneficial at the throat of the crossing
- A constant profile of support, as discussed in Figure 31, minimises wheelset displacements
- Crossings with elevated wing rails may have two transition zones, instead of one
- The cross-section of the wing rails as a large influence on their ability to support passing wheels
- The impact force at the transition zone is determined by the impact angle (not by the displacement)

5.2 Recommendations

General recommendations:

- Make use of MBS simulations before conducting full-scale tests of new geometry
- Verify the MBS simulations with FEM modelling, if extra assurance is desired
- Promote the exchange of design experience between asset owners, by connecting specialists
- Work towards international standardisation of modern turnout designs
- Write down the theory behind a design, instead of only describing a design with drawings

Recommendations for the asset owners:

- The choice between freedom or constraints for the manufacturer should always be made conscious
- Make the higher nose profile of the cast crossing also the standard for constructed crossings
- Making raised wing rails the standard at high tonnages/speeds decreases the chances of sudden failures and thus increases the robustness

Recommendations for the manufacturers:

- Bend the throat of constructed crossings more gently, if they do not feature elevated wing rails
- Invest in a raised wing rail cast manganese crossing design

Recommendations for the contractors:

- Invest in raised wing rail crossings at turnouts with heavy tonnages / higher traffic speeds
- Simulate crossings with worn wing rails and determine a maximum for wing rail wear

5.3 Future work

This project has laid the focus on developing an easy comparison tool for crossing geometries. At the same time, the base has been laid for follow-up research:

- Testing variable geometry at different locations (i.e. switch panel, obtuse crossings, dilation joints, diamond crossings, movable frog crossings)
- Varying the angle of attack of the vehicle model, to test the safety of designs in extreme situations. To do so the Klingel motion phase of incoming vehicles should be altered by adding disturbances before the examined geometry
- Using geometry input from measuring trains, to gain insight in geometry degradation
- Making use of more VI-Rail output, like detailed contact patch calculations and additional variables like the wear number

Bibliography

[1] I. Shevtsov, „Rolling Contact Fatigue problems at railway turnouts – experience of ProRail,” 13 11 2013. [Online]. Available: http://www.sim-flanders.be/sites/default/files/events/Meeting_Materials_Nov2013/mm_13112013_ivan_shevtsov_prorail.pdf. [Geopend 27 10 2018].

[2] X. Liu, *Pictures of damaged crossings.*

[3] Nederlandsche Spoorwegen, Handboek voor spoorwegtechniek, Leiden: A.W. Sijthoff's uitgevers-maatschappij N.V., 1933.

[4] X. Liu, V. Markine en Y. Ma, „Dynamic behaviour of a railway crossing-comparison of the results of multi body system dynamic and explicit Finite Element Models,” in *The 5th Joint International Conference on Multibody System Dynamics*, Lisbon, 2018.

[5] C. Wan, „Optimisation of vehicle-track interaction at railway crossings | TU Delft Repositories,” 7 9 2016. [Online]. Available: https://repository.tudelft.nl/islandora/object/uuid%3A8dac8f02-fe9e-4baa-9503-e9b3d79dd1aa?collection=research. [Geopend 14 05 2018].

[6] ProRail, „Railmaps,” [Online]. Available: htpp://railmaps.prorail.nl/. [Geopend 27 2 2015].

[7] Nextsense, „Rail cross profile measurement | CALIPRI C4X - NEXTSENSE,” Nextsense, [Online]. Available: https://www.nextsense-worldwide.com/en/industries/railway/rail-cross-profile-measurement.html. [Geopend 22 09 2018].

[8] S. Iwnicki, The Manchester benchmarks for rail vehicle simulation, Abingdon: Routledge, 2017.

[9] VI-grade GmbH, VI-Rail 16.0 Documentation, Marburg: VI-grade GmbH, 2014.

[10] W. Kik en J. Pietrowski, „A Fast, Approximate Method to Calculate Normal Load at Contact between Wheel and Rail and Creep Forces During Rolling,” in *Proceedings of 2nd Mini Conference on Contact Mechanics*, Zabony, 1996.

[11] X. Ma, P. Wang, J. Xu, R. Chen en J. Wang, „Comparison of Wheel-Rail non-Hertzian Contact Models for Numerical Simulation of Rail Damages in Switch Panel of Railway Turnout,” in *11th International Conference on Contact Mechanics and Wear of Rail/Wheel Systems (CM2018)*, Delft, 2018.

[12] M. Sichani, R. Enblom en M. Berg, „A novel method to model wheel-rail normal contact in vehicle dynamics simulation,” *Vehicle System Dynamics,* vol. 52, nr. 12, pp. 1752-1764, 2014.

[13] M. Sichani, R. Enblom en M. Berg, „An alternative to FASTSIM for tangential solution of the wheel-rail contact,” *Vehicle System Dynamics,* vol. 54, nr. 6, pp. 748-764, 2016,.

[14] R. Skrypnyk, M. Ekh, J. C. Nielsen en B. Pålsson, „11th International conference on contact mechanics and wear of rail/wheel systems (CM2018),” in *Simulation of damage in railway crossings*

– *a comparison*, Delft, 2018.

[15] G. Brouwer, Interviewee, *ProRail.* [Interview]. 08 01 2018.

[16] C. Esveld, Modern Railway Track, Zaltbommel: MRT-Productions, 2001.

[17] Voestalpine BWG GmbH & Co KG, „FAKOP_KGO_E," 9 2008. [Online]. Available: http://www.voestalpine.com/bwg/static/sites/bwg/.downloads/en/products/FAKOP_en.pdf. [Geopend 7 10 2018].

[18] M. Steenbergen, „The mechanisms of squat formation on train rails," in *Euromech 514: new trends in contact mechanics*, Cargese, France, 2012.

[19] M. Steenbergen, E. De Jong en A. Zoeteman, „Dynamic Axle Loads as a Main Source of Railway Track Degradation," in *Geotechnical Risk and Safety V: 5th International Symposium on Geotechnical Safety and Risk*, Rotterdam, The Netherlands, 2015.

[20] B. Zuada Coelho, Dynamics of railway transition zones in soft soils, Delft: TU Delft Institutional Repository, 2011.

[21] J. P. Pascal en G. Sauvage, „New method for reducing the multicontact wheel/rail problem to one equivalent contact patch," *Vehicle System Dynamics; International Journal of Vehicle Mechanics and Mobility,* vol. 1992, nr. 20:sup1, pp. 75-489,, 1992.

[22] V. Markine en I. Shevtsov, „Experimental Analysis of the Dynamic Behaviour of Railway Turnouts," in *Proceedings of the Eleventh International Conference on Computational Structures Technology*, Stirlingshire, Scotland, 2012.

[23] Y. Ma, A. A. Mashal en V. L. Markine, „Modelling and experimental validation of dynamic impact in 1:9 railway crossing panel," *Tribology International,* vol. 118, pp. 206-226, 2018.

[24] WITT IndustrieElektronik GmbH, „ESAH-M-V2-Flyer-de.pdf," [Online]. Available: http://witt-solutions.de/assets/ESAH-M-V2-Flyer_de.pdf. [Geopend 25 08 2018].

[25] J. Swier, „Rail infrastructure life cycle costs and cost drivers," *Railway Gazette,* vol. I, p. 34, 2004.

[26] A. Mashal, „MSc thesis: Analysis and improvement of railway crossing Using explicit Finite Element simulations," TU Delft repository, Delft, 2016.

Appendices

A) Overview of the VI-Rail workflow

This appendix gives an overview of the VI-Rail simulation workflow. VI-Rail has either the option of using the so-called Moving Track model, or the Flextrack model. This section encompasses a simulation without Flextrack. For the latter, please continue to Appendix C.

Introduction

VI-Rail is basically an interface between the railway engineer and the MSC Adams package. Figure 44 shows how the Adams analysis is the key element in the Moving Track workflow; it bundles all input and leads to all output. While the input is quite extensive, VI-Rail simplifies generating this input by providing the user with a relatively simple interface. Moreover, the simulation time of Moving Track is relatively short (a matter of minutes). Still though, setting up a VI-Rail simulation may still be quite time-consuming.

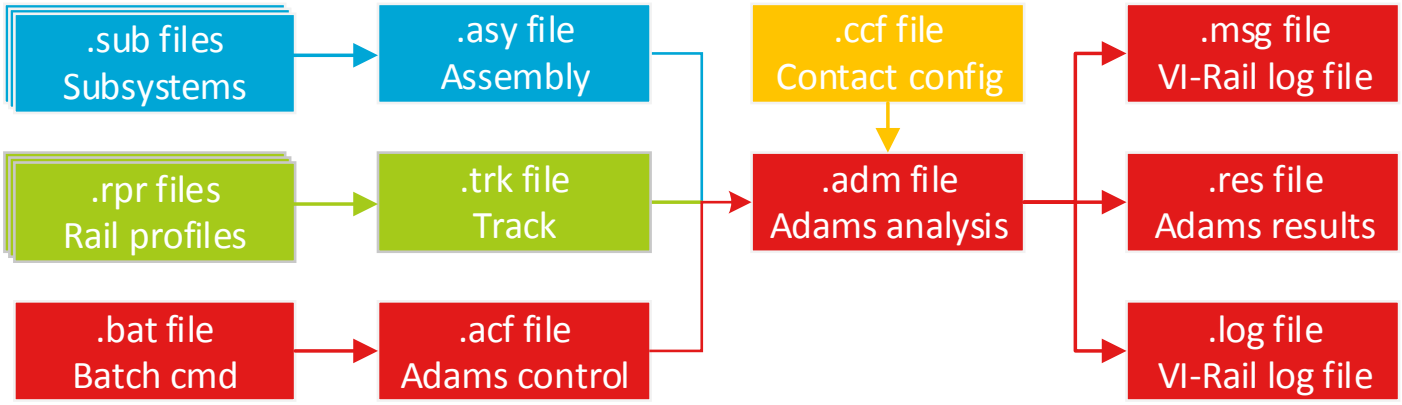

Figure 44 - Overview of the VI-Rail Moving Track workflow

In this thesis project however, the goal is to reduce the simulation setup time. This in order to simulate a lot of variable rail geometry profiles. This is done by taking the simulation out of the VI-Rail interface and in to a series of Matlab scripts, that are better tailored for variable geometry testing.

Subsystems (.sub)

Subsystem files are added to a model to represent physical objects and how the simulation should treat them. The only exceptions are properties that are specified through the track file. In most use cases, the only subsystems within a Moving Track model are vehicle parts.

Assembly (.asy)

Assemblies are simply a combination of subsystems. The .asy bundles the .sub files by containing their directories and connection properties. In this study, only one vehicle assembly will be used. A single carriage from a (Dutch) VIRM train set.

Rail profile files (.rpr)

Rail profile files describe a cross-section of the rail. To show what data is changed between the simulations, an example .rpr file is shown:

```
$--------------------------------------------------------------------MDI_HEADER
[MDI_HEADER]
 FILE_TYPE     =  'rpr'
 FILE_VERSION  =  1.0
 FILE_FORMAT   =  'ASCII'
$-----------------------------------------------------------------------UNITS
[UNITS]
LENGTH       = 'meter'
FORCE        = 'newton'
ANGLE        = 'radians'
MASS         = 'kg'
TIME         = 'second'
$-----------------------------------------------------------RAIL_PROFILE_DATA
[RAIL_PROFILE_DATA]
INCLINATION = 0.0
(PROFILE_PTS)
{       X_data                  Y_data          }
-5.00000000000000e-02 -3.00000000000000e-02
-4.89220075284921e-02 -3.00000000000000e-02
etc.
```

The most important part of the file is the description of the coordinates (red). These are used to make up the rail shape. However, one should be aware that these coordinates will not form the precise rail profile. VI-Rail turns the points of all profiles in to a Bézier surface (3D generalisation of the 2D Bézier spline). This will be discussed further, at the track file description.

Lastly, the amount of points is restricted to about 500 points per cross-section. This is automated by deleting points that are closest to others and/or far away from the wheel-rail contact.

Track file (.trk)

Track files determine the track geometry and alignment. The geometry comes from linked .rpr files and the alignment is defined within the .trk file itself. This results in the following file structure:

```
[MDI_HEADER]
[UNITS]
[MODEL]
[GLOBAL]
[IRREGULARITIES]
[HORIZONTAL_PATH]
[VERTICAL_PATH]
[CANT_ANGLE_PATH]
[RAILS_CONFIGURATION]
[RIGHT_RAIL_CONFIGURATION]
[RIGHT_RAIL_MATERIAL]
[LEFT_RAIL_CONFIGURATION]
[LEFT_RAIL_MATERIAL]
[RAIL_1_PROFILE]
[RAIL_2_PROFILE]
…
[RAIL_n_PROFILE]
```

As like in the .rpr file, the interchangeable settings are shown in red. First of all, the automated model setup currently projects all variable geometry on the right rail. For future purposes, it can easily be extended to also change the left rail. The configuration determines the location of the .rpr files. The last lines of the file contain the directory links to the .rpr files.

Batch file (.bat)

For Matlab to automate the VI-Rail simulation process, Matlab must send Adams a request to start a VI-Rail simulation. While Matlab can't start other programs including certain commands, batch files can. A typical VI-Rail request to Adams looks as follows:

```
call C:\MSC~1.SOF\ADAMS_~1\2013_2\\common\mdi.bat arail ru-solver Manchester_20km_dyn.acf
```

It can be derived that the line executes Adams, using VI-Rail's "ru-solver" environment, while opening the simulation "Manchester_20km_dyn". If the .acf file is in a different directory than the .bat file, the green part should be a full path/file combination.

Adams command file (.acf)

The simulation Manchester_20km_dyn is started by activating an Adams command file. It contains everything Adams needs to start the simulation. On top of the link to the .adm file, it contains very familiar settings from VI-Rail simulations, being: Velocity, EndTime and Dtout. The two blue numbers are also something to keep in mind. These are Adams IDs and they change every time you run a new sort simulation.

```
Manchester_20km_dyn.adm
Manchester_20km_dyn
preferences/solver=CXX
preferences/status=on
output/nosep
simulate/static
array/3, numbers = 2, 1, 5.555556, 5, 4, 5, 6
simulate/static
!--- Enable wheel rotation ----
control/routine=virailSOL::con301, &
 function=user(301,113)
!--- Set translational initial velocites ----
control/function=user(917,6,5.555556)
!--- Set wheel rotational initial velocites ----
control/routine=virailSOL::con300, &
 function=user(300,5.555556,112)
simulate/dynamic, end=1.0, dtout=1.0E-002
STOP
!
```

Contact configuration (.ccf)

The contact configuration file describes how VI-Rail should handle the wheel-rail interface. In this thesis, the element MDI Contact Gen will be used. This because it is the only commonly available configuration which can handle variable rail geometry.

Adams simulation settings (.adm)

The .adm files contain all parts of the MBS. All these definitions make .adm files very long. The upside though, is that only a few key parts must be changed to create custom simulations. These are:

- the location of the vehicle model
- the location of the wheel profiles and contact elements
- the location of the track model
- the location of the simulation's unique writing directory

The downside is that all the parts in the .adm file heavily depend on the vehicle model. Therefore, to ensure as much automation as possible, each vehicle model should have its own .adm file.

B) Disquisition of examined crossing designs

As pointed out earlier, crossing designs are most commonly distributed in PDF format. This however does not show the precise 3D shape. It has to be derived. At the different designs, the consequences of different interpretations are shown. First though, the most common ways of representing a crossing design are explained. When looking at a crossing design, one can distinguish three different drawing types. All three 3D planes are represented by: a side view overview, a top view overview and cross-sections. The side view shows the height of the rail-top along the crossing, like in Figure 45. Side views contain at least the height profile of the nose rail. When the design incorporates a raised wing rail, the wing rail ought to be in this overview as well. Last but not least, the locations of the cross-sections are shown. Cross-sections are often distinguished by name (E, F, G in Figure 45).

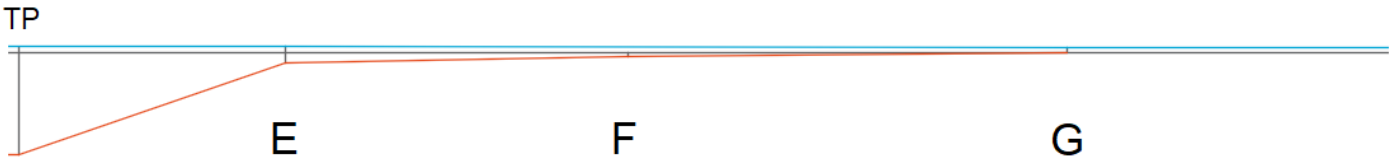

Figure 45 - Side view of the Belgian 1:14 UIC60 crossing (nose rail in red, wing rail in cyan)

The top view gives an overview of the crossing shape, by displaying a cross-section at 14 mm below the top of the rail. Both the inner sides of the wing rail and the sides of the nose rail are visible, like in Figure 46. Moreover, the theoretical lead lines (grey) and approach surfaces are displayed. The theoretical part of the lead lines shows where the theoretical point (TP) can be found. Approach surfaces are an addition at the tip of the nose, which makes the nose end before TP.

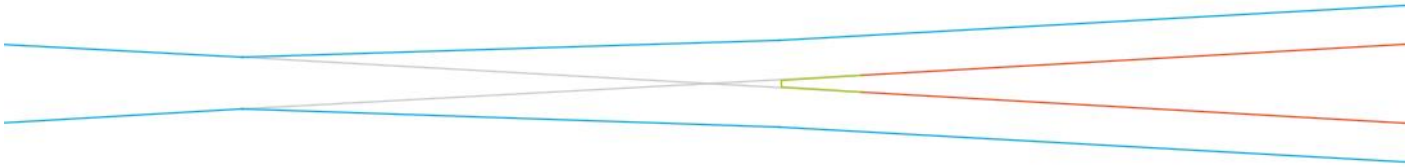

Figure 46 - Top view of the Swiss 1:9 SBB VI crossing (nose rail in red, wing rail in cyan, approach surface in green)

The cross-sections provide the reader with detailed information about the cross-sectional shape at various points. This information contains heights, inclinations and radii. Underlying theory is, in many cases, harder to derive. Designers attempt to incorporate them in the drawings, but in situations like the German example (Figure 47) this might be even harder.

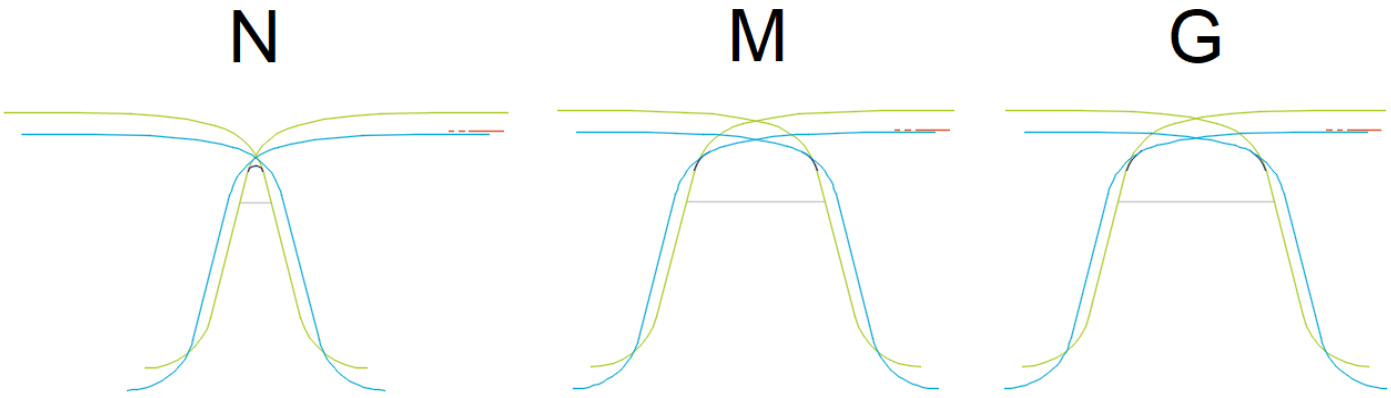

Figure 47 - A few cross-sections of the German constructed 1:9 crossing

Now that all three characteristics have been discussed, the designs will be shown in the same manner for each examined crossing. The last paragraph of this chapter will present a comparison.

Dutch constructed 1:9 NP38

The first crossing is derived from the Dutch Railways engineering handbook, from 1933 [4]. The design is a good place to start this chapter, because it provides insights in the development of crossing designs throughout the years. In the early days of railway engineering, most customs were derived from practise (trial and error). Calculations were definitely available to help in the search for more efficiency, but more advanced models for the wheel rail interface were simply not doable without computers. What's still the same though is how the nose design (Figure 48) shows the three earlier mentioned viewpoints: cross-sections, side view and top view respectively.

The cross-sections show how the crossing consists of an older rail profile than the current practise[3]. The older profiles were abbreviated as N.P., being Dutch Profile. These were available in NP34, NP38, NP42 and NP46 (by increasing cross-section area). Moreover, these profiles were also available as construction profile version. These incorporated the same rail head but a much thicker web. Such profiles were specified with a high C, like NP42^{C}. Characteristic for this profile, is that the head radii are not 300, 80 and 13 millimetres. These were 400 and 14. It must be noted though, that this was combined with a national wheel profile (simply referred to as the Dutch Railways wheel profile). When this is taken in to account, the difference in rail geometry is reasonable.

Another interesting part in the cross-sections of the nose design is the slope on the sides. This slope is 1:2.5, instead of the much more common 1:4 slope. The advantage of this is more stability of the nose, but it is simply incompatible with the S1002 wheel profile. This is because the S1002 wheel flange slope is approximately 1:2.8, while the Dutch Railways wheel profile had it at about 1:1.9. The rail side slope should always be steeper than the wheel flange slope, in order to avoid derailment.

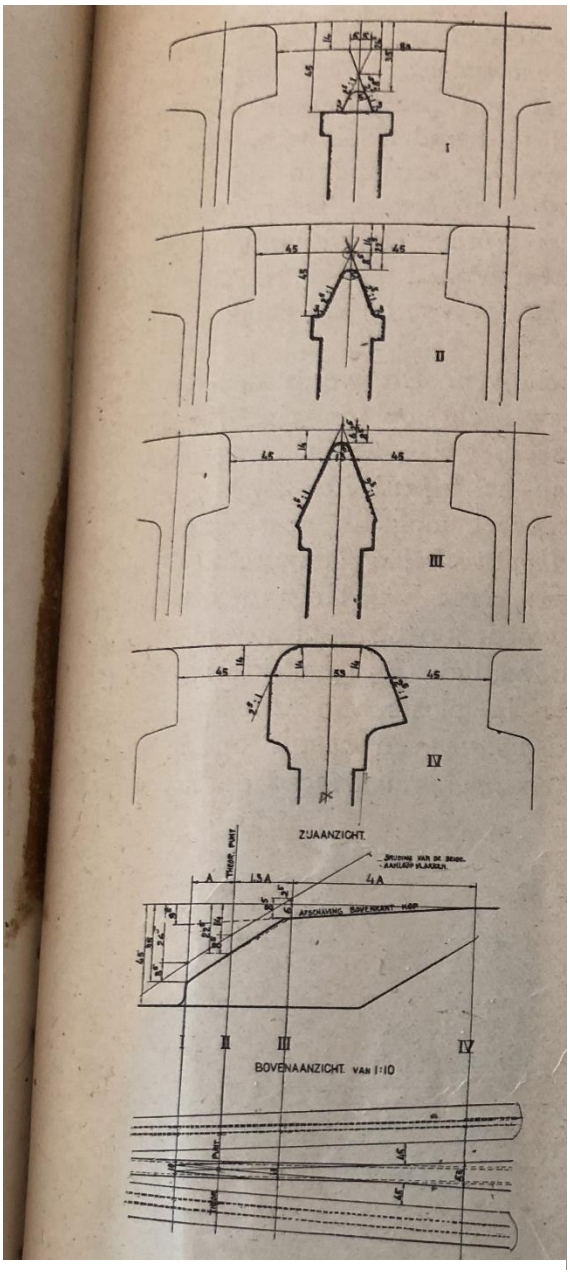

Figure 48 - NP nose profile [2]

On the side view, four profiles are depicted with Roman numerals. Between profile I and III, the handbook speaks of the 'approach surfaces' (in Dutch: "aanloopvlakken"). While it is special that this design has an actual word for the phenomenon, the approach surfaces are a common design feature. It actually is an extra treatment to blunt the tip of the nose. This is extra clear in the top view drawing. It protects the nose from wheel flanges that might hit it, when approaching with an unfavorable angle of attack. In chapter 4, dedicated simulations are discussed in order to prove this. After the approach surface (between III and IV) the design facilitates an area where the wheel transition takes place. By manipulating the height there, the transition zone is kept away from the tip of the nose. This is important because this part is vulnerable. The importance of this design feature will also be discussed in chapter 4.

[3] The currently used Dutch rail profiles are UIC54 or UIC60

Dutch constructed 1:9 UIC54 (ProRail, 2004)

The second crossing in this discussion is, to some extent, the successor of the previous design. For this reason, a part of the design comparison is expedited to this part of the chapter. Moreover, this design is the basis of this comparison. For this reason, this review will be more detailed than the others.

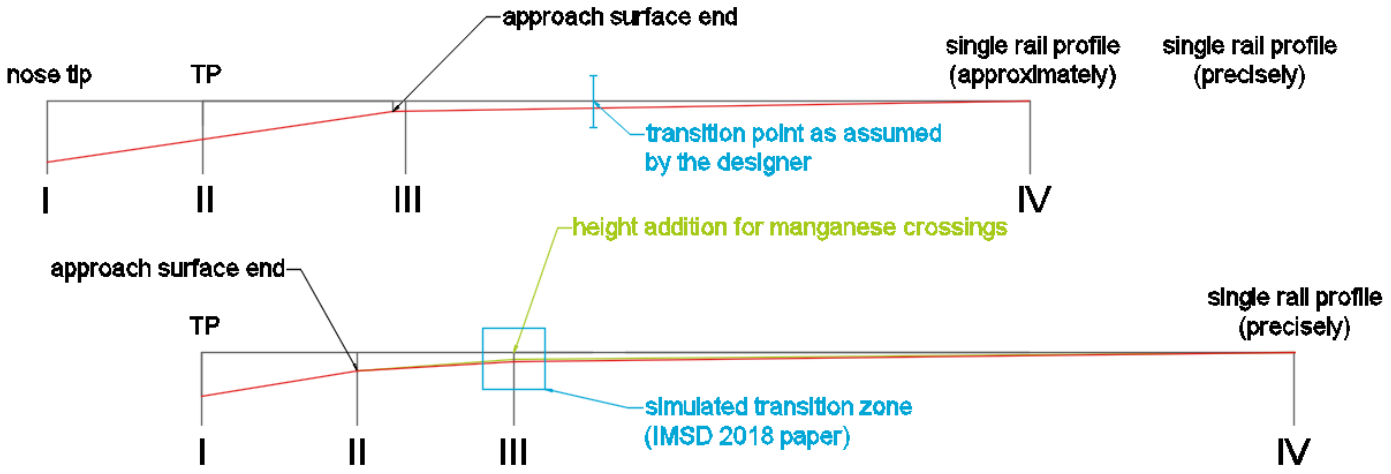

Figure 49 - Side view comparison between the former and current Dutch standards

One of the ways to see that this design is the evolution of the previous one, is through the cross-sections which are named in the same way. As shown in Figure 49, the location of the cross-sections has changed though. These are now at TP, TP+90 mm, TP+180 mm and TP+630 mm. The cross-section before TP was removed, which is very understandable because at this point the nose rail would be far too thin to support the forces from a passing wheel flange. The approach surfaces (the area between sections I and II) are steeper, but slightly lower than in the old design (Figure 50). This would point out that the tip of the nose is shorter and lower than it used to be. Changes at this location point towards a more conservative design, to avoid impact from the wheel flange at this location.

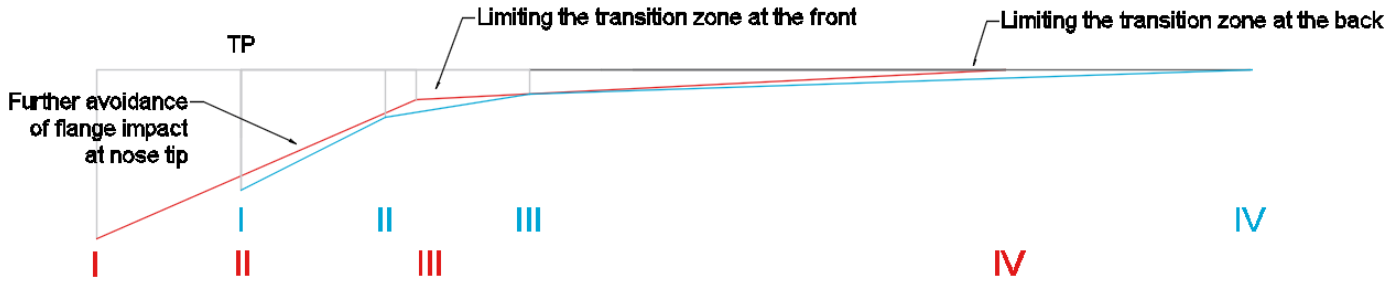

Figure 50 - Side view of the old (red) and new (blue) design

Further on at the nose, the old cross-section III is replaced by the new II and III. As depicted in Figure 50, the new cross-section III is exactly at the same height as the old profile. The only reason for the decreased height between the new II and new III is to further ensure the avoidance of a transition zone at the tip of the nose. This could be the consequence of bad experiences with the higher profile.

The last change in terms of the side view, is the location of cross-section IV. Because of the shift to the back, the back of the nose is lower. When running a train in the trailing direction (right to left in Figure 50) this would make the support by the nose decrease faster. When not changing the wing rail, this should cause the back of the transition zone to shift further away from the nose.

Overall, we can already derive three conjectures about the consequences of design differences. This shows how the comparison of existing designs can lead to a better understanding of crossing geometries. Conjectures like the above should always be put to the test however, as will be done in chapter 4.

Figure 51 shows the cross-sections from the standards. In contrast to the old standards from Figure 48, the emphasis of the new drawings is shifted from the approach surface to the original rail profile. This can be seen by looking at the two half rail profiles that are shown above the cross-sections. A similar phenomenon can be found at the old standards. In those drawings, the location of the approach surface is shown instead of the location of the rail profile.

Complementary to the original rail profile and the approach surface, the manufacturing process has a third step. In this last step, the nose is rounded off to the correct height. Moreover, it prevents a sharp edge at the top of the nose.

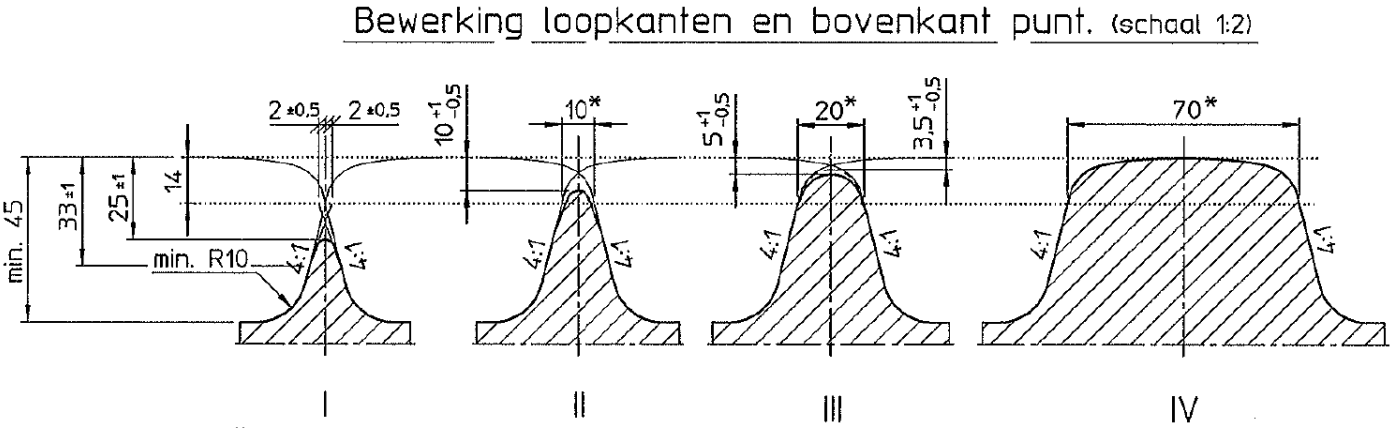

Figure 51 - The original definition of the ProRail nose cross-sections

It is important to understand the three steps of nose profiling. Figure 52 shows them for all cross-sections.

The curved red profiles show two halves of the original UIC54 rail profile, with the addition of a 1:4 slope at the sides. These profiles move outward with a ratio of 1:9, which is parallel to the track alignment.

The straight green profile shows the approach surfaces, which start at the inside of the red profile and move outwards up to the TP+225. After that point, the approach surface is not visible any more. The angle of the approach surface is determined at cross-section I, where the (in Figure 51 depicted) distance of 33 mm below the rail head is shown as the point where the approach surface intersects with the red profile. The top of the approach surface is anchored through the width of 2x -2 at the depth of 14 millimeters under the rail head. The angle, which originates from these two points, remains constant as the approach surfaces are fabricated along the nose.

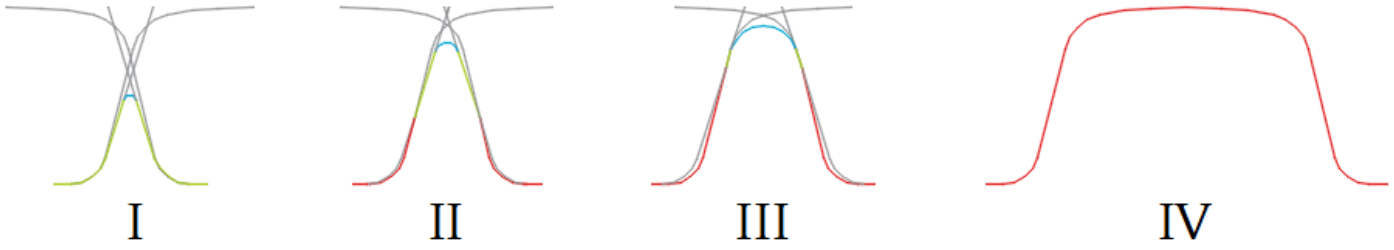

Figure 52 - Clarification of the ProRail cross-sections

The last part of the standards, the rounding at the top, is the part that raises questions. While it is very clear how the blue line rounds of the profiles I to III at the desired height, it is not clear how this is done between III and IV. As this section will show, this leaves room for interpretations by manufacturers.

Figure 53 shows the overviews from the top and side. The top view shows several characteristics of the crossing. Starting off with the approach surfaces, it is visible how the approach surface starts with a width of $2x - 2\,mm$ and ends at a length of $25 \cdot \alpha = 225\,mm$. Because the top view and side view are aligned, this can be seen in the side view as well. Notice the line below the top of the nose, starting at section I at -33 mm. The line, showing the border between approach surface and UIC profile, moves upwards and ends at 225 mm (behind cross-section III, as expected).

The top view also shows the reader something different: the way to tune the wing rail. At the left side of the drawing, the wing rail is bent at the so-called throat of the crossing. This causes a kink in the rail, where the rail cross-section starts shifting with respect to the wheel trajectory. At cross-section I, a second kink is applied to the wing rail, in order to align it with the other track centerline.

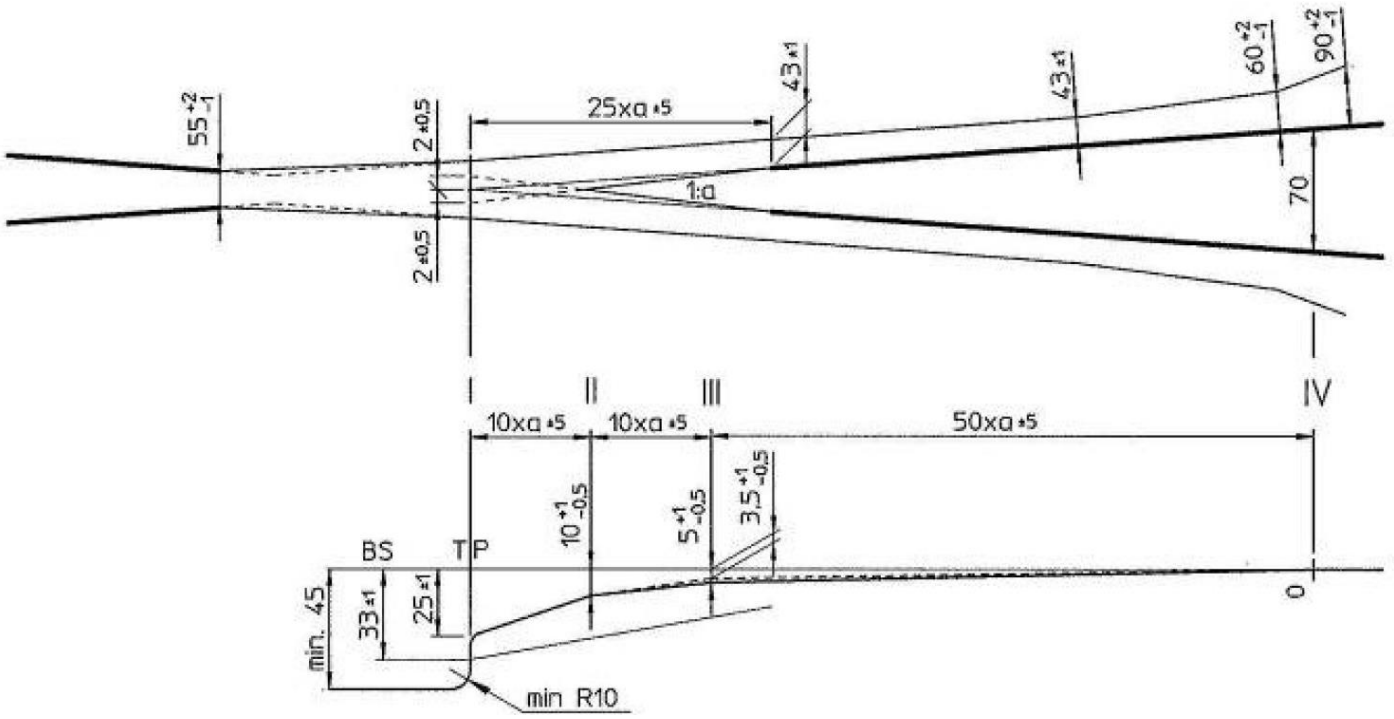

Figure 53 - The original ProRail top view and side view

The distance of 43 mm between nose and wing (measured at 14 mm below the rail head) partially achieved by altering the cross-section of the wing rail, like in Figure 54. At the regular wing profile, a 1:7 slope is applied at the side which faces the nose. The end of the wing rail has this 1:7 slope moving outwards, while a slope of 1:2.5 moves out faster. All of this results in the wing rail as depicted in the top view.

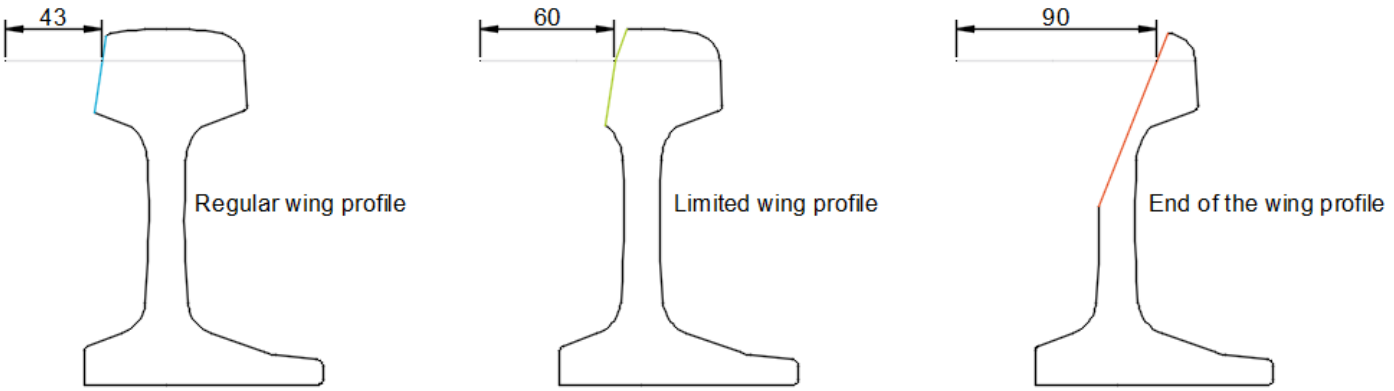

Figure 54 - Wing rail cross-sections

Dutch cast 1:9 UIC54

The ProRail standards for cast and constructed crossings are very much alike. They only differ at two aspects. The first difference can be found at cross-section III.

As shown in Figure 55 (in green), the nose has been made 1.5 millimetre higher (-3.5 instead of -5.0 mm). The reason behind this, is that the cast crossings are made from manganese steel. Manganese steel has the property that it deforms quite a bit. This was visualised very nicely in [10], where manganese steel was compared with R350HT steel. The deformation process is commonly regarded as a good property. The expectation is that the new geometry deforms to a more ideal form. For this reason, some extra height was added at cross-section III.

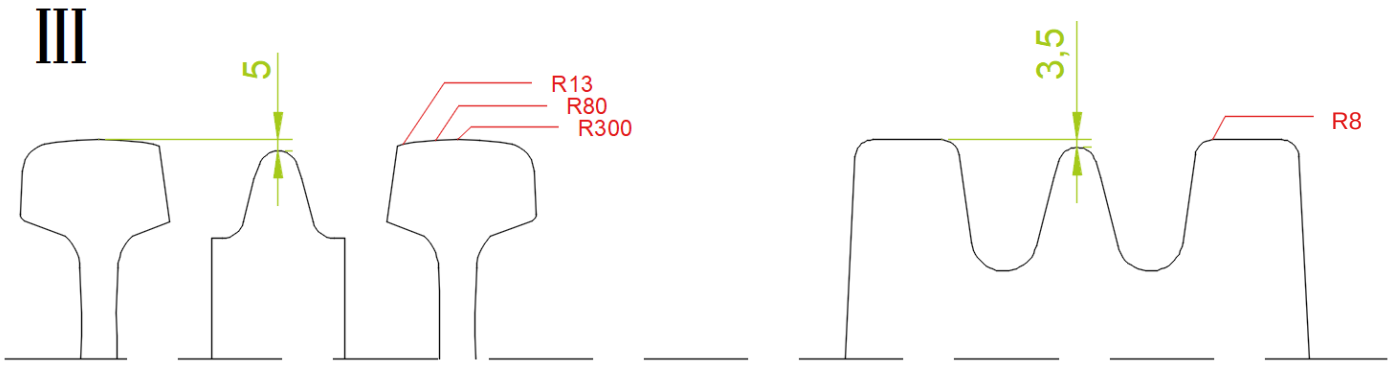

Figure 55 - Design differences between the constructed and cast crossing

The same phenomenon is visible at the wing rails. While the wing rails are not higher than usual, the radii are different (Figure 55, in red). As shown in Figure 56, the consequence of this is a bit more space for the manganese steel to deform in a more ideal shape. In this sense, the two differences with the standards for constructed crossings are complementing each other well.

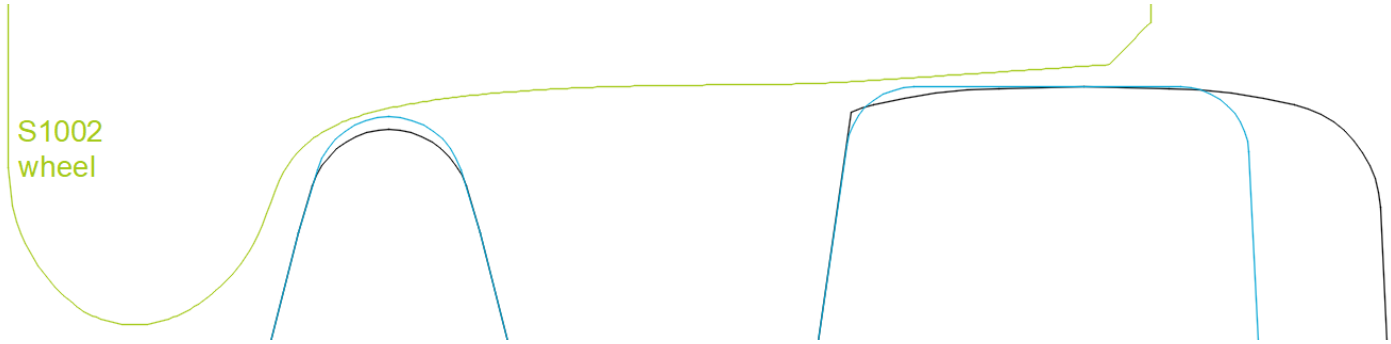

Figure 56 - A closer look on the differences: constructed in black, cast in blue

A third difference between the two standards is even less visible. It is the transition between the normal rail profile and the wing rail profile. This design aspect is hard to visualise, by only using a comparison of cross-sections. Therefore, the normal rail / wing rail transition will be discussed in chapter 4, at the simulation results. The output from the simulations will show the importance of a smooth transition between switch rail and wing rail.

Dutch constructed 1:9 UIC54 (BWG, 2003)

The design in this subsection is derived from a drawing which was provided as being one of the ProRail standards. This drawing originated from the German turnout manufacturer BWG in 2003, for a constructed Dutch crossing. It looks similar to the cross-sections from the earlier discussed constructed crossing but has one major difference. Cross-section IV has a width of 55 mm, instead of 70 millimetres (like in the normal UIC profile). This is compliant with the 1:9 crossing angle, because the location of cross-section IV is changed as well (Figure 57 orange).

The approach surface in this design is different as well. As marked down in green, it starts at 45 millimetres under the rail head, instead of the regular 33 millimetres. This changes the angle of the approach surface. In the top view, the approach surface ends at 200 mm from TP. While this plausible, it contradicts with the side view. In the side view, one would expect that the approach surface is denoted by the striped area. This area does not end at 200 mm from TP however.

It is somewhat unclear where both differences originated from. It is recommended to trace the history of the design, in order to understand this drawing better. While the drawing is much more recent than the 1933 design, it was made one year before the ProRail drawing from 2004 was made. A possible explanation is that the ProRail standards have changed since 2004. Another possible explanation is that BWG was asked to make a proposal for a profile change, which was not implemented.

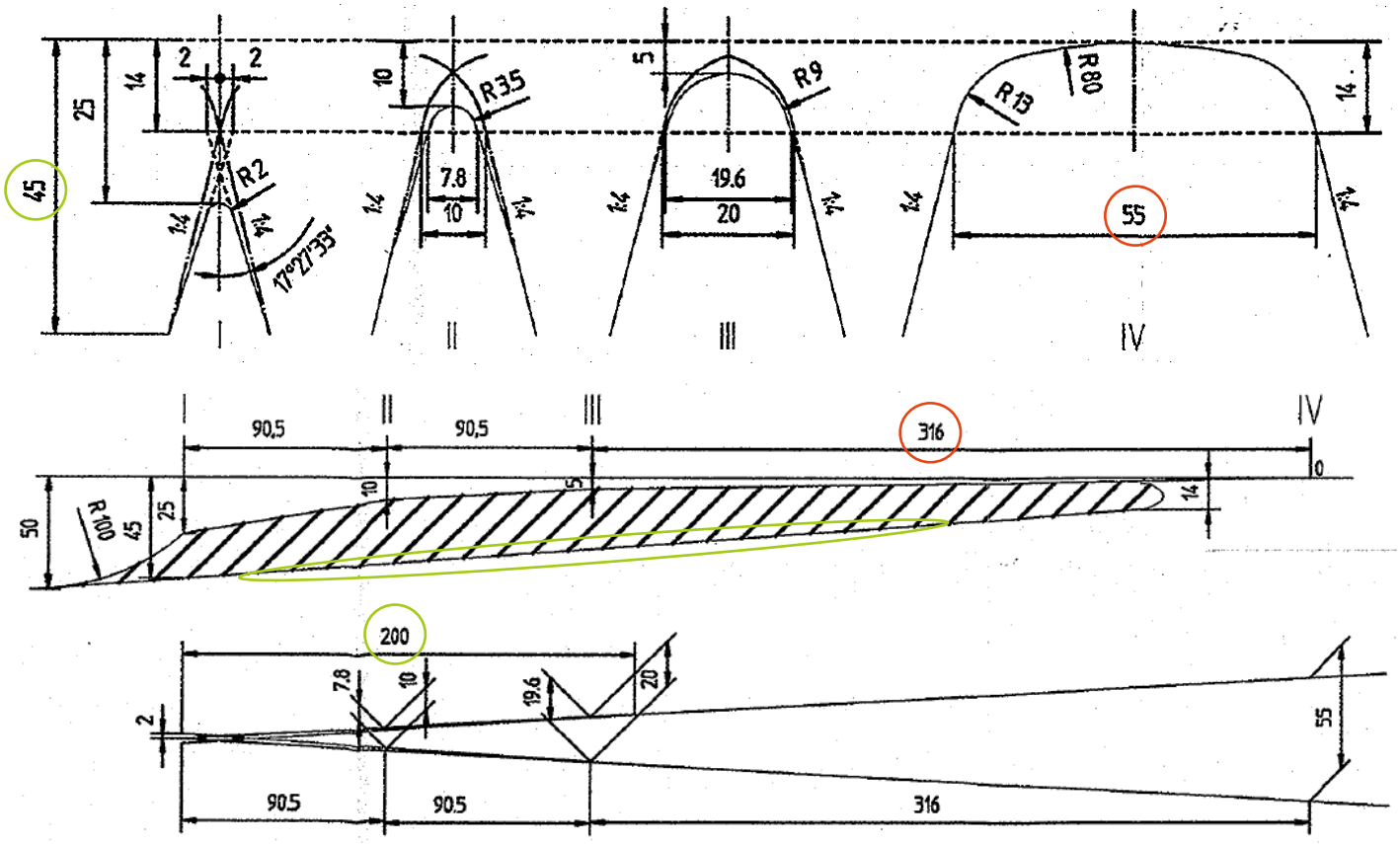

Figure 57 – Geometry from a BWG drawing from 2003

Dutch constructed 1:9 UIC54 (WBN, 2013)

The next geometry is from the Dutch turnout manufacturer WBN. It looks very much like the ProRail profile as described in the second subsection, but it solves the problem which was described there. As discussed before, it is not entirely clear what the manufacturer should do between cross-sections III and IV. In Figure 58, marked down in blue, the difference with the standards is depicted. The UIC54 profile starts below its normal position and moves upward along the nose. This makes it clearer what should be happening between III and IV.

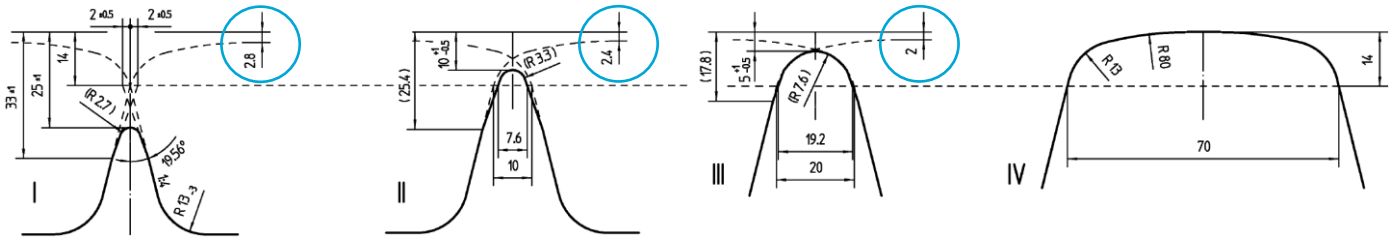

Figure 58 - Cross-sections from a WBN drawing from 2013

From the several possibilities in Figure 59, it is now completely clear that WBN chooses the third approach. The radii on the nose simply follow the track centerlines without additional rounding at the top of the nose. As a consequence, an edge is to be expected at the top of the nose. While this is the most easy/economic way of manufacturing, it is not fully clear what the consequences are. For this reason, all four ways of manufacturing were simulated. The results are compared in chapter 4.

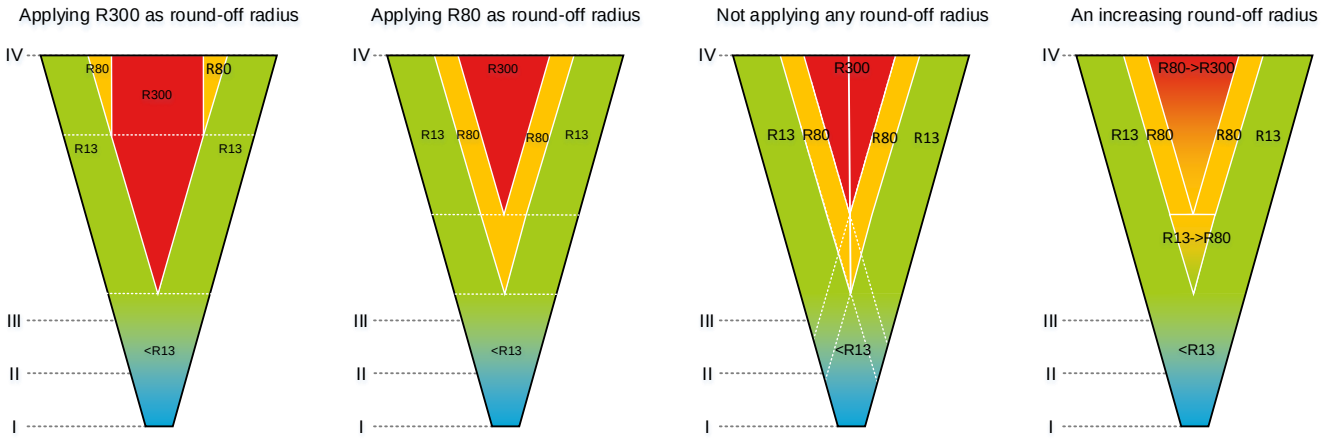

Figure 59 - Several ways of manufacturing a ProRail nose between cross-sections III and IV

Dutch constructed 1:9 UIC54 (Kloos, 2010)

The last Dutch geometry is the design by manufacturer Vossloh Cogifer Kloos BV. The Kloos crossings are known for several characteristics. One of them is its elevated wing rails. The wing rails are bent upwards, in order to overcome the problem which was mentioned at the cast crossing. More specifically, by moving the cross-section upward more space is created to customise the geometry on the wing. As shown in Figure 60, this space is utilized by grinding the wheel profile into the wing rail. By doing so, the wheel is supported much better by the wing rail. It is constantly supported without the need for a vertical displacement of the wheelset. This can be seen by comparing the support from the full wheel profile (Figure 60 in grey) and the support of the customised wing rail. The nose rail is building up from I to IV, while the wing rail keeps the wheel at the same position. By keeping the support of the wheel as constant as possible, a smoother transition should be ensured.

One short remark about the wing rail should be added. The ProRail standards apply the 1:7 slope without any smoothing at the top. Kloos however rounds it with a radius of 6 mm. As the comparison will show, this is a commonly applied design feature.

Figure 60 - Kloos crossing cross-section I: with the wheel profile (green), nose rail (orange) and wing rail (blue)

The side view in Figure 61 shows how the raised wing rail is built in to the design. The switch rail is bent upwards at one meter from TP. While the rail head of the wing rail would be raised to +5 mm, it is cut off at +3 mm in the way as depicted in Figure 60.

Another difference with the ProRail design is the number 495, in Figure 61. The distance is shorter than the expected 630 mm. It is however similar to the WBN design and BWG drawing. Further details on the cross-sections between I and IV is not publicly available. However, it is clear that Kloos uses a custom profile.

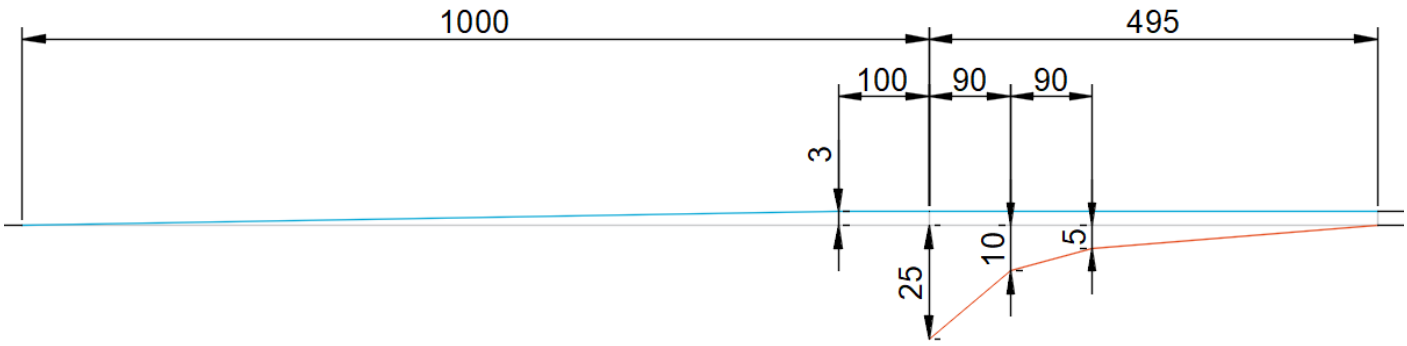

Figure 61 - Kloos crossing side view, wing (blue) and nose (orange)

Belgian cast 1:14 UIC60

The next design is the first geometry from outside the Netherlands. While the crossing angle (1:14) and the rail profile (UIC60) are deviating from all other designs in this chapter, it remains a very nice addition to the discussion. This because Infrabel (the Belgian colleague of ProRail) changed its geometry standards recently, in order to gain a performance increase. This was done by asking some of their best welders to provide suggestions and as a result the performance of the crossings was successfully increased [3]. In order to look in to this case, Infrabel was contacted to ask for cooperation. To help this thesis project, they provided the drawing from a UIC60 1:14 cast manganese crossing. Before starting the discussion on that, please recall the following earlier discussed crossings: ProRail cast manganese and Kloos constructed. As this subsection will show, the Belgian design has characteristics from both of those crossings.

Perhaps the most interesting part of this design is the care for interaction between wheel, switch rail, wing rail and nose. When projecting a S1002 wheel profile on any cross-section like in Figure 62, it is immediately clear why each cross-section has its distinctive shape. Similarly to the Kloos design, the wings of the Belgian crossing are elevated to provide optimal support to passing wheelsets.

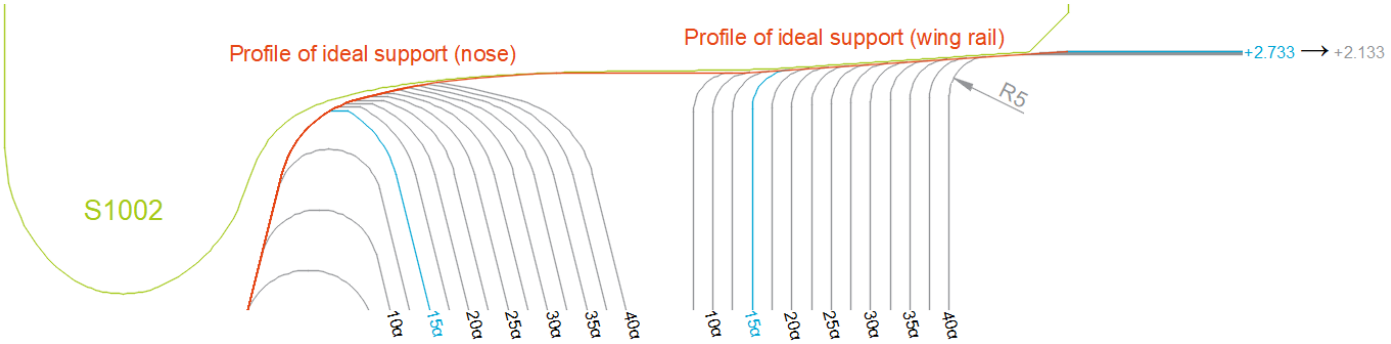

Figure 62 – Cross-sections of Infrabel's design, projected along the left track centerline, with S1002 in neutral position

While both designs make use of elevated wing rails, differences between the wing from Kloos and Infrabel do exist. In example, the wing rail profile (red in Figure 62) is simply a 1:15 slope at Infrabel's design while Kloos claims to manufacture the S1002 profile directly into the rail. Another difference is the round-off radius at the wing rail, which is 5 mm at Infrabel and 6 mm at Kloos. While technically this is a difference, it may be considered as a similarity when taking in to account that Kloos has to keep the original ProRail standards in mind. The ProRail standards do not require to round off the wing rails. Kloos did do that, while doing so should cost them extra time (money). It would be recommended to look in to the value of this.

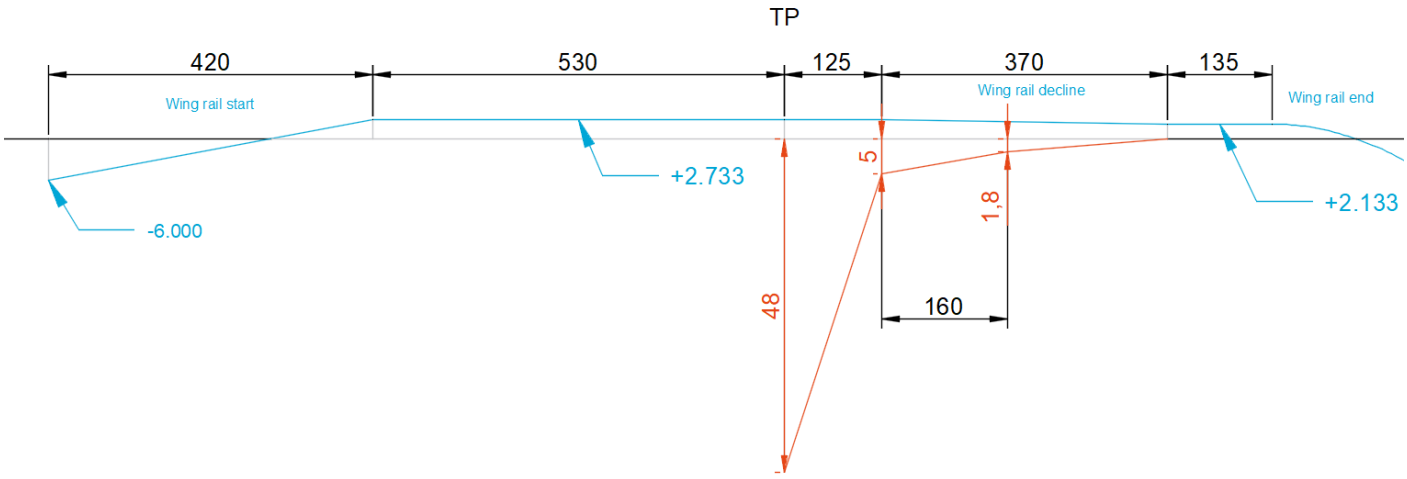

Figure 63 - Side view of the Infrabel design (please note: it has been scaled from 1:14 to 1:9)

An insurmountable property of the crossing is that the Profile of Ideal Support (ideal profile) can never be fully maintained throughout the crossing. Wheel flanges from both directions must be able to pass safely through the crossing. This requires room for these flanges; room where the wheel cannot be supported. When not solving this issue, wheelsets dip in to the gap. To illustrate this, we borrow Figure 64 from the results chapter. It shows such a dip for the ProRail cast and constructed crossing (vertical displacement of a passing S1002 wheel, moving in the facing direction).

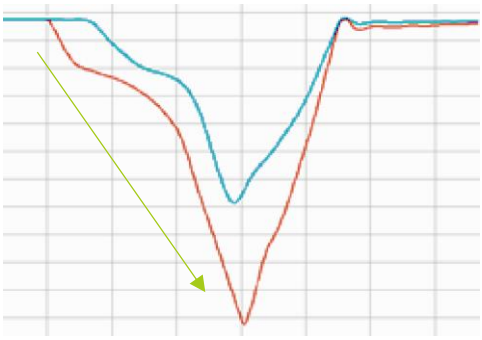

Figure 64 – Wheelset dip: the consequence of insufficient wing support

To prevent such dips, the ideal profile should be approached at each cross-section. When comparing Kloos and Infrabel with all other designs, this is a new way of looking at crossing designs.

To do this in the proper way, Figure 63 shows the side view of the crossing with both the wing profile and nose profile (in the same way as at the Kloos design). When examining the side view, three stages of wheel support can be distinguished. Moving from left to right the wheel is carried by the switch rail, elevated wing and nose. While the transition between elevated wing and nose has been illustrated at Figure 62, the transition between switch rail and elevated wing rail is shown in Figure 65. The blue part of the cross-section starts lowered and moves upward along the crossing. This happens faster than at Kloos' design, but starts at roughly the same distance from TP.

Figure 65 - Infrabel's transition between switch rail and wing rail

The last part of this discussion is the top view. While it shows nicely how the ideal profile is maintained in the proper directions (parallel to the track centerline), it also shows how the wing rail is ended. The design incorporates a curve of R13500 in to the wing rail, which starts as soon as the nose rail reaches the width of a regular rail. The wing ends at 75 mm from the nose. This is earlier than the discussed ProRail designs, but it is not entirely comparable because of the different cross-sections. ProRail cuts the cross-section, instead of bending it.

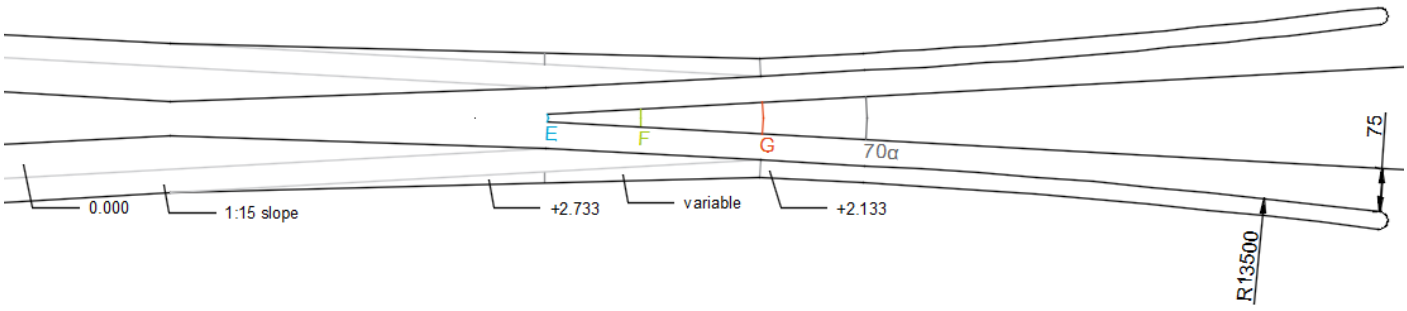

Figure 66 - Top view of the Infrabel design

German constructed 1:9 UIC54 (standard design)

To understand the original German design, recall the subsection which discussed the Dutch constructed 1:9 UIC54 (WBN, 2013). Notable is that WBN is affiliated with the German BWG, which might explain the similarities that this subsection will discuss.

Starting with the top view in Figure 67, the approach surfaces start quite far from TP (cross-section O in Germany). While the Dutch design extends all the way up to TP, the German design starts even further in the back than the Belgian design (140 mm versus 125 mm).

With Figure 67, not the entire nose is covered. To do so, Figure 68 presents the full view of the side and the top. It immediately shows that the German design is much longer than the others. The nose width extends to two rail profile widths (2 times 70 mm). This is twice as long as the Dutch nose and more than twice as long than the Belgian nose. This is caused mainly by the much gentler slope in the back of the nose. The cross-section names run alphabetically from K to O, with one odd one out. The cross-sections K to O are used to inspect the German crossing. Cross-section C is a special cross-section, which serves a different purpose. The cross-section seems to solely exists because this is the theoretical point where a new S1002 wheel should transfer from nose to wing and vice versa. While it is not used for inspection, the cross-section helps the reader to understand the reasoning behind the design. ProRail has such a cross-section at TP+225 mm but doesn't depict it as such.

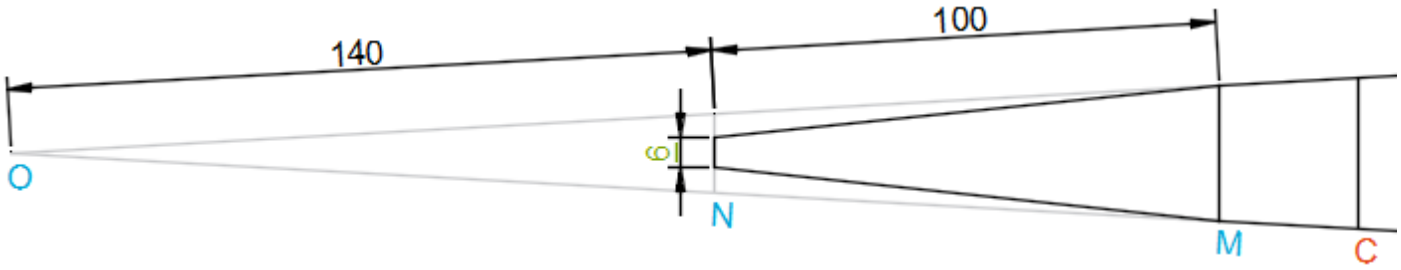

Figure 67 - The German approach surfaces

When looking at the side view however, cross-section C does serve a purpose for the manufacturer. The side view in Figure 68 shows a green line. This is the height of the German manufacturing tool (Figure 70 left). In cross-section K, the tool is applied to the unfinished nose at neutral height. The manufacturer should move the tool along the track centreline, while declining its height linearly towards the nose tip. Most importantly, the tool should be at -3 mm at the theoretical transition point. This even continues at the approach surface, with the only difference that the tool stops following the track centreline; it moves horizontally in accordance with Figure 67.

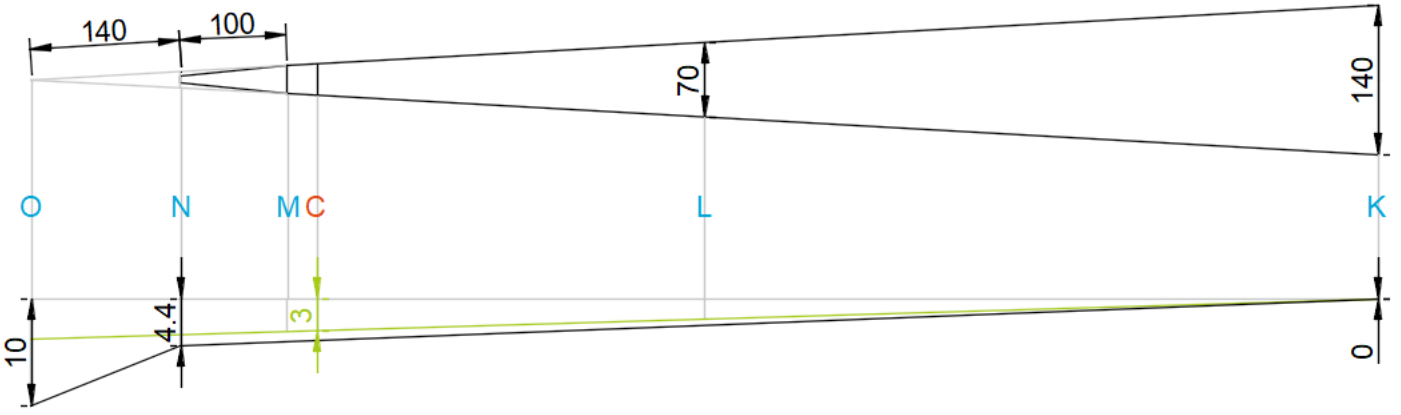

Figure 68 - The full top view and side view of the German design

While all other designs fully focus on showing the nose height in the side view, the German design clearly focuses on the manufacturing instruction. Moreover, it should be noted that the nose height (in black) in the

side view is only an indication[4]. The real height profile results from tool cross-sections moving through each other. As these tools consists of circle sections, a correct nose height profile should consist of semi ellipses. Such a profile can be reconstructed in AutoCAD, like in Figure 69. While this shows nicely how the nose shape is dependent on the manufacturing method, something else should draw attention as well.

Figure 69 - German nose profile, consisting of semi ellipses

Notice how the top of the nose reaches 0 before section K. This can be explained by taking a look at the cross-sections. The right side of Figure 70 shows how the factory equipment leads to the characteristic cross-sections. This discloses how K marks the start of the nose not at the top, but at the side. As the milling tool intersects further in to the UIC54 profile, the top of the nose starts lowering as well.

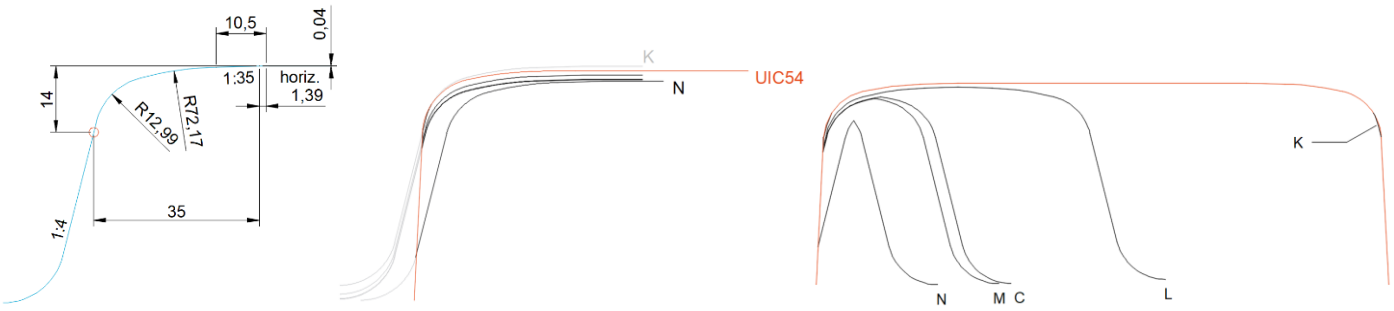

Figure 70 - German cross-sections: the factory equipment, equipment positions and resulting cross-sections

All in all, it was interesting how the German design deviates by defining the crossing through the manufacturing process. This is a different approach than the other designs, where standards are defined by only showing certain characteristic cross-sections. Defining the manufacturing process leaves no room for interpretation. This ensures that the customer (DB Netze) exactly receives what they want.

[4] Note: this has not been acknowledged by Arcadis' concept drawing 420868, version 21-12-2017.

German constructed 1:9 UIC54 (improved design)

Voestalpine BWG GmbH, turnout manufacturer in Germany and colleague of WBN, claims to have improved the German design. This has been done by the concept of Delta Kappa Profilierung, or $\Delta\kappa$ profiling.

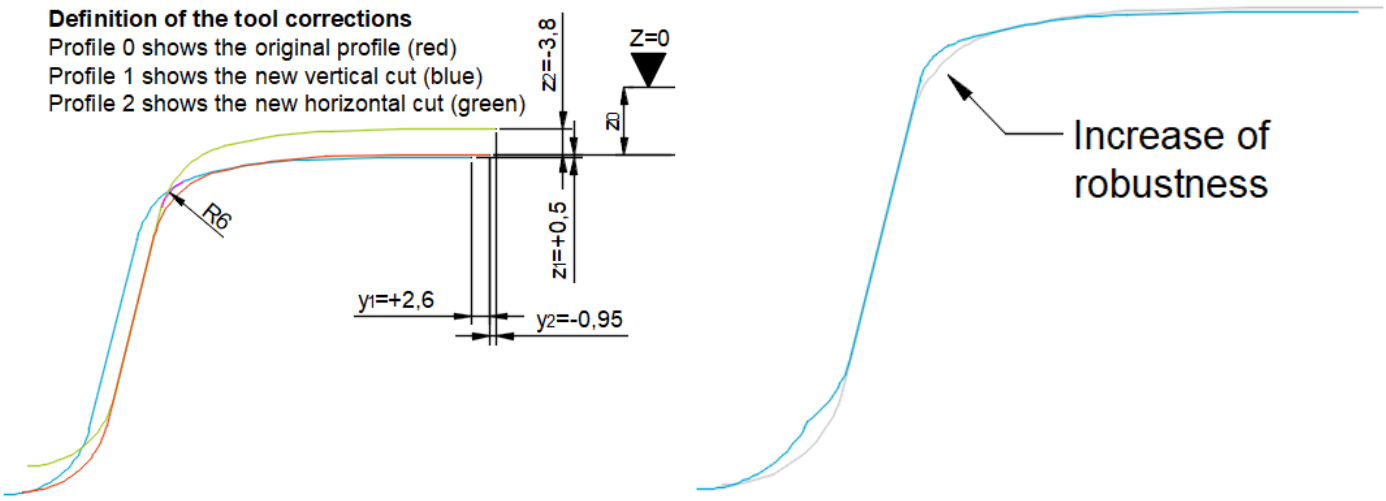

Figure 71 - Explanation of the $\Delta\kappa$ profiling

Figure 71 shows how BWG applies the standard milling tool twice, in order to alter its profile. The profile is altered to decrease the radius of the at the side of the nose. These corrections are applied only between sections N and C and should increase the robustness of the nose tip. After the wheel transition, the nose is assumed to have enough robustness. Between C and L, the correction is removed gradually.

The name of the concept suggests a link with the concept of rolling radius difference. This concept is often denoted as ΔR, while the definition of roundness is $\kappa = 1/R$. "Delta Kappa" might be the German equivalent of rolling radius difference. Sadly, this cannot be confirmed yet. WBN was asked whether they knew more about the theory from their German colleagues, but the answer was that they don't. This is interesting, because they are about to sell these crossings to ProRail.

No information was obtained from the supplier, but [15] may provide guidance in this situation. The concept of rolling radius difference is discussed as a key factor influencing the wheel-rail dynamics. The rolling radius difference is the difference of rolling radius, between the contact locations on the right and left wheel of a wheelset. The combination of a wheelset and two rail profiles leads to a set of possible pairs of contact locations. Figure 72 shows them for two S1002 wheels and two UIC54 rails. Such a plot changes when one of the UIC54 cross-sections is replaced by a cross-section from a crossing. The goal of the BWG design team could have been to decrease the change of the $\Delta\kappa$ profile. This surmise is fed by the fact that BWG did the same trick with the concept of Kinematic Gauge Optimization [16] (also known as FAKOP). This project alters the $\Delta\kappa$ profile in the switch panel to better match the $\Delta\kappa$ profile from outside the switch panel. This to decrease the wear at that location. The concept is commonly applied in high-speed turnouts (also at HSL-Zuid in the Netherlands.

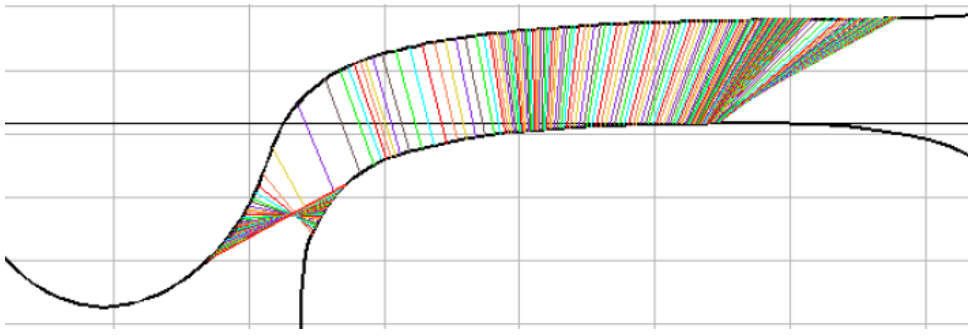

Figure 72 - Possible contact points between S1002 and UIC54 (VI-Rail)

Swiss constructed 1:9 SBBIV

The last two existing designs are from Switzerland. SBB provided the drawings for the purpose of this research. The designs provide a comparison within the same operator, but between different rail profiles. This subsection discusses a crossing with the SBBIV (UIC54E2) rail profile, while the next design is the same turnout with the SBBVI (UIC60) rail profile. The comparison should provide insights in the design aspects that are dependent on the rail profile.

Figure 73 shows the height of the nose from the side. The fact that a wing rail profile is missing here, shows that the wing rail stays at the neutral level. The nose standards however do show the definition of the approach surfaces. These are defined by a nose width at cross-section C and distance from the normal profile in cross-section D. The approach surfaces end at TP+262.85.

The cross-sections of the approach surfaces (Figure 74) are quite similar to ProRail's sections II and III. The sides are formed by 1:4 slopes and the top is rounded off based on the desired height profile.

The wing rails are also similar to the Dutch design. The Swiss cut out a slope from the side of the wing rails, but contrary to the Dutch they round it off with a radius of ten millimeters. This radius is the largest round-off radius throughout all designs. Another difference is that the slope of the wing is less steep than the Dutch 1:7 slope.

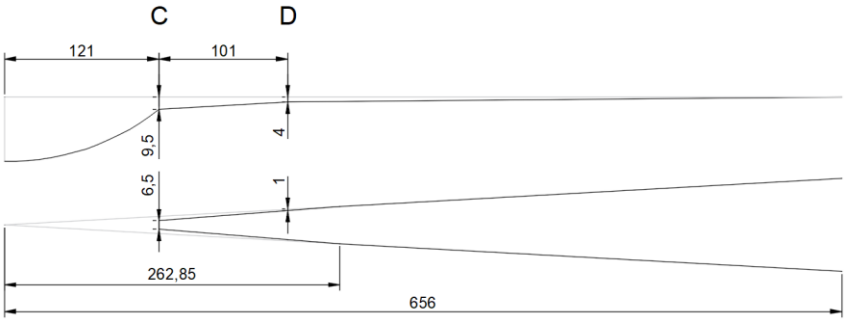

Figure 73 - Side view and top view for SBBIV

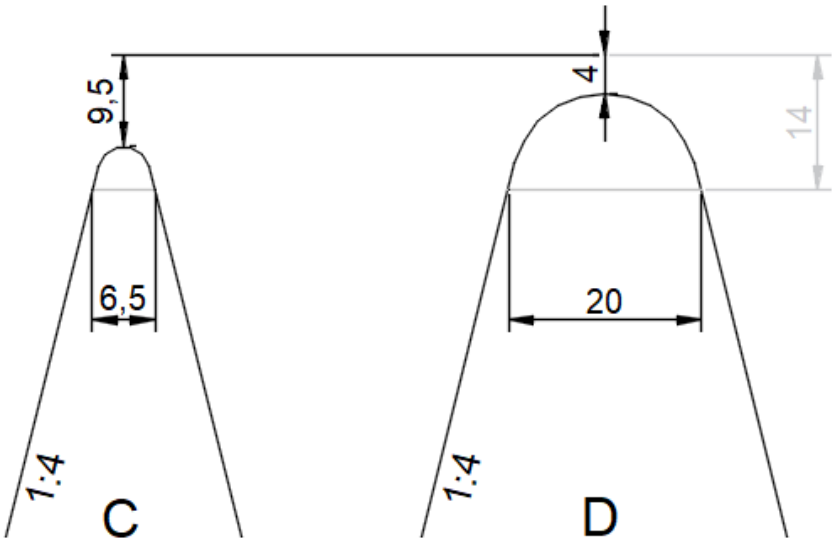

Figure 74 - Cross-sections for SBBIV

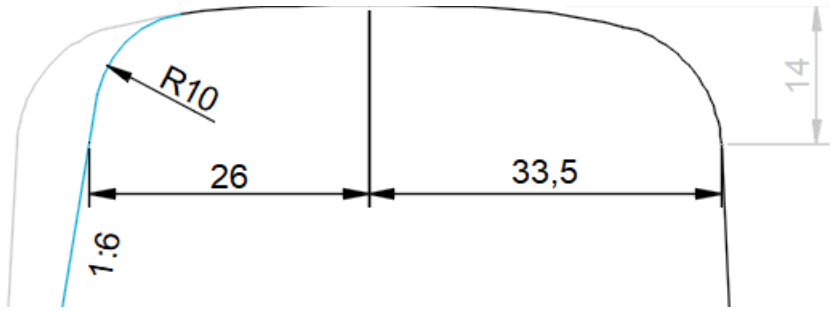

Figure 75 - The Swiss SBBIV wing rail profile

Swiss constructed 1:9 SBBVI (UIC60)

The second Swiss design features the SBBVI (UIC60) rail profile. The profile has a nominal width of 72 instead of 67 millimetres. The consequence is that the profile takes more length to build up, when using the same slope. The SBBVI design is even less steep behind D though, which also contributes to the longer nose length (725 mm instead of 656 mm).

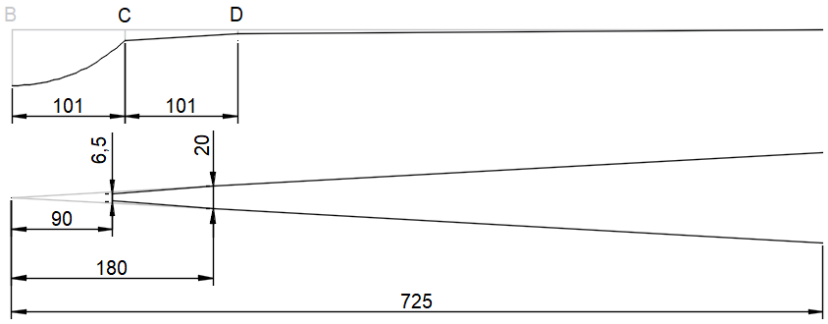

Figure 76 - Side view of the SBBVI crossing

The approach surfaces seem a bit different, but their shapes and sizes at the top are the same. The only difference is the location of the cross sections: TP + 90 and 180 mm, instead of TP + 121 and 222 mm. After cross section D, the nose is slightly different as well. It builds up with a 1:12 slope at the top and an R ≈ 9.6 mm side. This difference has similarities to the 'improvement' of the German profile, from BWG.

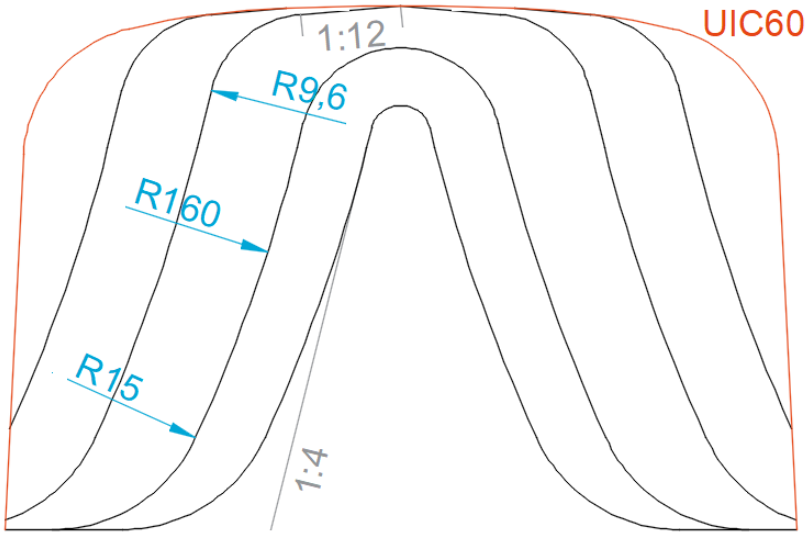

Figure 77 - Cross sections of the SBBVI nose

In terms of the entire nose, the sides are not 1:4 anymore. At a certain height, these are rounded off gradually. The blue radii in Figure 77 show estimates of the nose sides, based on the original drawings. The R160 makes the nose wider at the bottom, without influencing part of the nose where wheel-rail contact is possible. Therefore, it should have something to do with the strength of the nose. Figure 78 shows a possible explanation. This 'constructed' crossing actually contains a custom cast hollow nose. When looking at the cross section from the drawing, it makes sense why the designers would appreciate extra width at this part of the crossing.

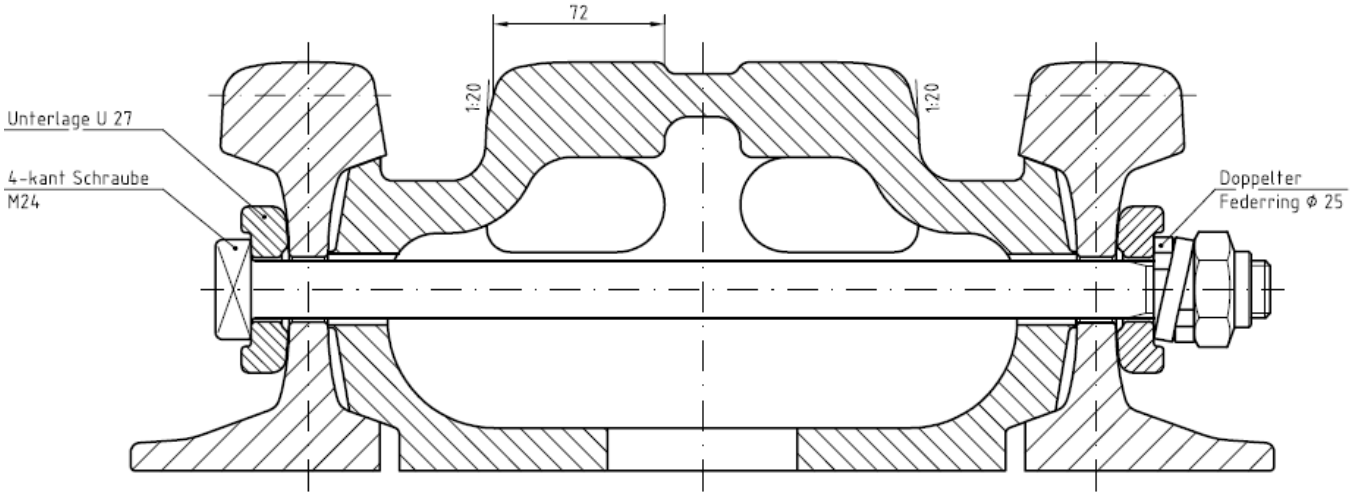

Figure 78 - A cross section from SBB drawing no. 6430

Proposed 1:15 UIC54 design from numerical optimisation

In [11], a method is proposed to improve the Dutch 1:15 crossing design by using numerical optimisation. The optimisation takes in to account two criteria: wear number and maximum contact pressure. The benefits of such an optimisation have been quantified in Figure 79. On the vertical axis, the maximal contact pressure of the new design $\bar{S}(x)$ is compared with the maximal pressure of the existing design $\bar{S}^*(x)$. At the horizontal axis, the same is done for the wear index. Lastly, the importance (weight) of the two criteria is shown at each design.

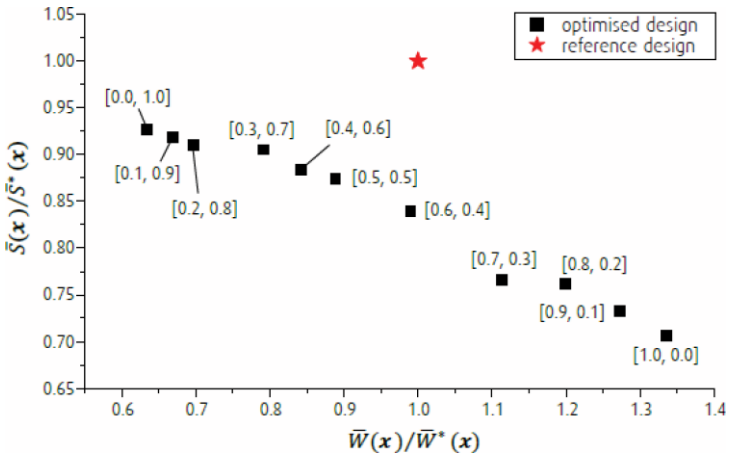

Figure 79 - Optimisation results (image from [11])

This suggests that the reference design is sub-optimal. Without altering the wear index, it should be possible to achieve less contact pressure. Moreover, less wear or contact pressure can be achieved if an increase of the other is accepted. This by only changing the shape of the crossing nose. As a last part, further on in [11], more uncertainty factors are taken into account (mentioned as robust optimisation). In Figure 80 an overview is depicted, showing the nose height from the three optimisation problems.

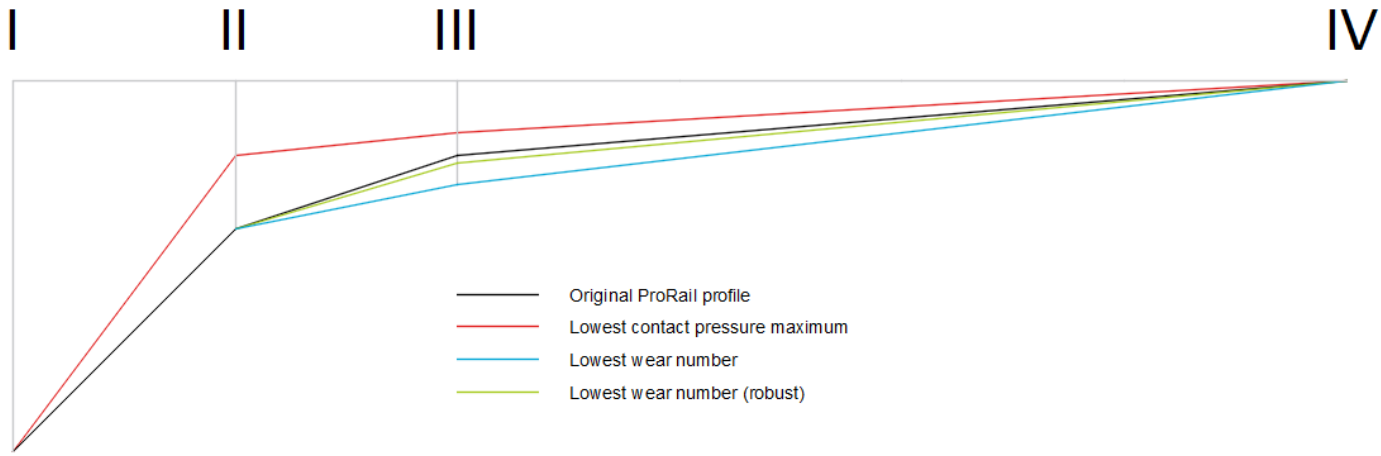

Figure 80 - Side view at the nose rail height, for the three optimisation problems

Regarding the cross-sections, two methods have been used to alter them. The semi ellipse method (Figure 81 left) varies both the gauge and nose height. The B-spline method (Figure 81 right) keeps a constant gauge, varies diagonally and varies the nose height. Overall, we can conclude that the optimisations tend to a wider nose, while the nose height seems to be a trade-off between wear and contact pressure.

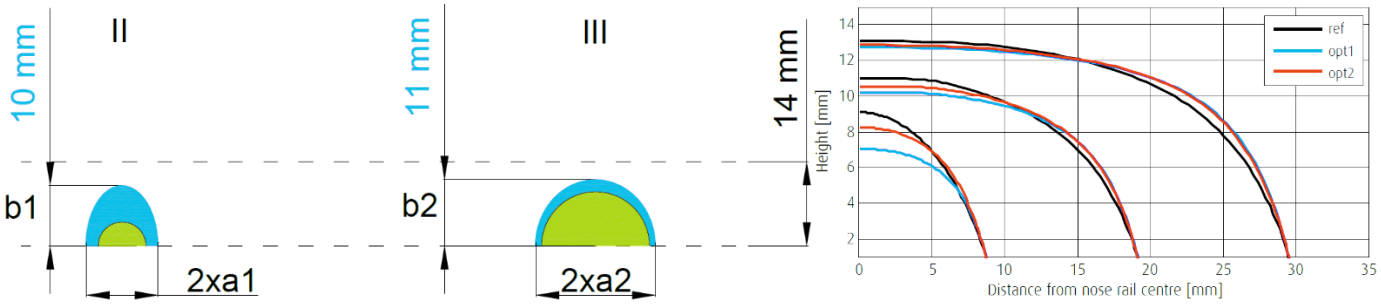

Figure 81 - Optimised cross-sections in blue and red (left semi-ellipse method, right B-spline method) [11]

C) Full list of model settings

The VI-Rail model settings are specified in various files. This appendix will show the most important contents, so that the simulations can be reproduced at will.

Overview

Figure 82 shows the files needed for a Moving Track model and the files needed for a Flextrack model.

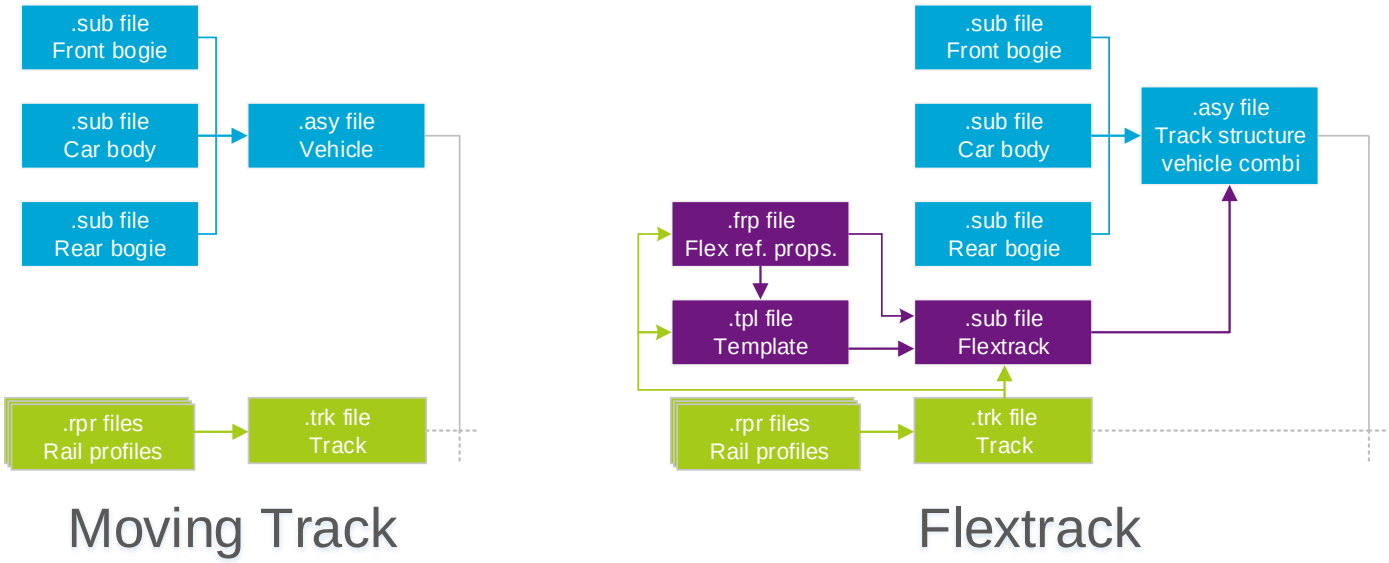

Figure 82 – Differences between the Moving Track and Flextrack workflow

Flextrack reference properties (.frp)

As derived from [3]:

Rail mass:	$54{,}77\ kg/m$
Ballast, lateral stiffness:	$45 \cdot 10^9$
Ballast, lateral damping:	$32 \cdot 10^3$
Ballast, vertical stiffness:	$45 \cdot 10^9$
Ballast, vertical damping:	$32 \cdot 10^3$
Ballast, rolling stiffness:	$10 \cdot 10^6$
Ballast, rolling damping:	$10 \cdot 10^3$
Rail pad, lateral stiffness:	$280 \cdot 10^6$
Rail pad, lateral damping:	$58 \cdot 10^3$
Rail pad, verical stiffness:	$1300 \cdot 10^6$
Rail pad, vertical damping:	$45 \cdot 10^3$
Rail pad, rolling stiffness:	$360 \cdot 10^6$
Rail pad, rolling damping:	$360 \cdot 10^3$

Template (.tpl)

Flexible section initiation: $30\ m$

Flexible section end: $36\ m$

End of track: $150\ m$

Sleeper distance: $0{,}6\ m$

Sleeper height: $0{,}2\ m$

Sleeper width: $0{,}3\ m$

Rail height: $0{,}159\ m$

Rail I_{xx}: $1{,}850 \cdot 10^{-5}\ m^4$

Rail I_{yy}: $2{,}338 \cdot 10^{-5}\ m^4$

Rail I_{zz}: $2{,}787 \cdot 10^{-6}\ m^4$ per meter track

Rail area (cross-section): $6{,}977 \cdot 10^{-3}\ m^2$

Young's modulus: $2{,}1 \cdot 10^{11}$

Rail damping ratio: $1{,}0 \cdot 10^{-4}$

Sleepers 51 to 61 were activated, in order to request output in the flexible track section.

Variable track (geometry) model

```
$-------------------------------------------------------------------MDI_HEADER
[MDI_HEADER]
 FILE_TYPE     =  'trk'
 FILE_VERSION  =   5.0
 FILE_FORMAT   =  'ASCII'
$-----------------------------------------------------------------------UNITS
[UNITS]
 LENGTH       = 'meter'
 ANGLE        = 'radians'
 FORCE        = 'newton'
 MASS         = 'kg'
 TIME         = 'second'
$-----------------------------------------------------------------------MODEL
[MODEL]
 TYPE  =  'ANALYTIC'
 FORMAT  =  'TRK_4'
$-----------------------------------------------------------------------GLOBAL
[GLOBAL]
 TOTAL_LENGTH  = 150
 CANT_MODE  =  'CENTER'
 IRREGULARITIES  =  'no'
 SWITCH_OFFSET   = 0.0
$-----------------------------------------------------------IRREGULARITIES
[IRREGULARITIES]
 TYPE  =  'ANALYTIC_SINUS'
 FORMAT  = 'ANA_1'
 DIRECTION  =  'VERTICAL'
 RAIL_SIDE  =  'RIGHT'
 STARTING_S  =  0
 AMPLITUDE = 0
 WAVE_LENGTH = 0
 CYCLES = 0
 SHIFT = 0
```

```
$-------------------------------------------------------------HORIZONTAL_PATH
[HORIZONTAL_PATH]
{horizontal_s   curvature   kink}
0 0 0
150 0 0
$-------------------------------------------------------------VERTICAL_PATH
[VERTICAL_PATH]
{vertical_s  coordinate}
0 0
150 0
$-------------------------------------------------------------CANT_ANGLE_PATH
[CANT_ANGLE_PATH]
{cant_angle_s   angle}
0 0
150 0
$-------------------------------------------------------------RAILS_CONFIGURATION
[RAILS_CONFIGURATION]
{track_s gauge   vdg}
0.0 1.435 0.014
150 1.435 0.014
$-------------------------------------------------------RIGHT_RAIL_CONFIGURATION
[RIGHT_RAIL_CONFIGURATION]
{track_s  inc  rail_id  guiding_rail_id}
0.0000 0 1 0
150.0000 0 1 0
$-------------------------------------------------------------RIGHT_RAIL_MATERIAL
[RIGHT_RAIL_MATERIAL]
 Y_MODULUS  =  210000000000.0
 P_RATIO  =  0.27
$-------------------------------------------------------LEFT_RAIL_CONFIGURATION
[LEFT_RAIL_CONFIGURATION]
{track_s  inc  rail_id  guiding_rail_id}
0.0000 0 1 0
150.0000 0 1 0
$-------------------------------------------------------------LEFT_RAIL_MATERIAL
[LEFT_RAIL_MATERIAL]
 Y_MODULUS  =  210000000000.0
 P_RATIO  =  0.27
$-------------------------------------------------------------RAIL_1_PROFILE
[RAIL_1_PROFILE]
PROFILE_FILE  =  'D:\jwegdam\Desktop\Google Drive\Thesis\VI-
Rail\AutomaticTestingDatabase.cdb\wheel_rail_profiles.tbl\rprNS32494.rpr'
```